


12-2011

CONFORMATIONAL CHANGES IN THE EXTRACELLULAR DOMAIN OF GLUTAMATE RECEPTORS

Anu Rambhadran

Follow this and additional works at: https://digitalcommons.library.tmc.edu/utgsbs_dissertations

 Part of the [Biochemistry Commons](#), [Biophysics Commons](#), [Medicine and Health Sciences Commons](#), [Molecular and Cellular Neuroscience Commons](#), [Molecular Biology Commons](#), and the [Structural Biology Commons](#)

Recommended Citation

Rambhadran, Anu, "CONFORMATIONAL CHANGES IN THE EXTRACELLULAR DOMAIN OF GLUTAMATE RECEPTORS" (2011). *The University of Texas MD Anderson Cancer Center UTHealth Graduate School of Biomedical Sciences Dissertations and Theses (Open Access)*. 196.
https://digitalcommons.library.tmc.edu/utgsbs_dissertations/196

This Dissertation (PhD) is brought to you for free and open access by the The University of Texas MD Anderson Cancer Center UTHealth Graduate School of Biomedical Sciences at DigitalCommons@TMC. It has been accepted for inclusion in The University of Texas MD Anderson Cancer Center UTHealth Graduate School of Biomedical Sciences Dissertations and Theses (Open Access) by an authorized administrator of DigitalCommons@TMC. For more information, please contact digitalcommons@library.tmc.edu.

CONFORMATIONAL CHANGES IN THE EXTRA-CELLULAR
DOMAIN OF GLUTAMATE RECEPTORS

by

Anu Rambhadran, M.S.

APPROVED:

[Advisor, Vasanthi Jayaraman, Ph.D.]

[Michael R. Blackburn, Ph.D.]

[Jianping Jin, Ph.D.]

[Jeffrey A. Frost, Ph.D.]

[John L. Spudich, Ph.D.]

APPROVED:

Dean, The University of Texas
Graduate School of Biomedical Sciences at Houston

CONFORMATIONAL CHANGES IN THE EXTRA-CELLULAR
DOMAIN OF GLUTAMATE RECEPTORS

A

DISSERTATION

Presented to the Faculty of
The University of Texas
Health Science Center at Houston
and
The University of Texas
M. D. Anderson Cancer Center
Graduate School of Biomedical Sciences
in Partial Fulfillment

of the Requirements

for the Degree of

DOCTOR OF PHILOSOPHY

by

Anu Rambhadran, M.S.
Houston, Texas

December 2011

Dedication

To my husband , the rock in my life, Joshua Ramaiah, for being there for me when I need him the most and for being a constant source of wisdom and encouragement. To my precious son, Jonah Ramaiah, for making my life meaningful and for providing the impetus I much needed to succeed and aim higher in life. Furthermore, to my doting parents, Rambhadran and Vanaja for their unparalleled love and support...!!!

Acknowledgments

My special thanks to Dr. Vasanthi Jayaraman for being the ultimate mentor. I could not have finished this dissertation without her!! Thanks for believing in me and encouraging me to do my very best. I will always cherish and respect the time I spent with you.

I would like to express my deepest gratitude to the members of my advisory and supervisory committees, Dr. Renhao Li, Dr. John Spudich, Dr. Mike Blackburn, Dr. Jianping Jin and Dr. Jeff Frost for their dedication and invaluable feedback.

Thanks to the past and current members of the Jayaraman lab. A special thanks to Dr. Jennifer Gonzalez, in whom I found a great friend and confidant!! Jen, I really enjoyed our days in the lab together and our 'chats' during lunch time. Thanks to Kim, Suba and Rita for their great camaraderie.

CONFORMATIONAL CHANGES IN THE EXTRACELLULAR DOMAIN OF GLUTAMATE RECEPTORS

Publication No. _____

Anu Rambhadran, Ph.D

Advisor: Vasanthi Jayaraman, Ph.D.

The family of membrane protein called glutamate receptors play an important role in the central nervous system in mediating signaling between neurons. Glutamate receptors are involved in the elaborate game that nerve cells play with each other in order to control movement, memory, and learning.

Neurons achieve this communication by rapidly converting electrical signals into chemical signals and then converting them back into electrical signals. To propagate an electrical impulse, neurons in the brain launch bursts of neurotransmitter molecules like glutamate at the junction between neurons, called the synapse. Glutamate receptors are found lodged in the membranes of the post-synaptic neuron. They receive the burst of neurotransmitters and respond by fielding the neurotransmitters and opening ion channels.

Glutamate receptors have been implicated in a number of neuropathologies like ischemia, stroke and amyotrophic lateral sclerosis. Specifically, the NMDA subtype of glutamate receptors has been linked to the onset of Alzheimer's disease and the subsequent degeneration of neuronal cells. While crystal structures of AMPA and kainate subtypes of glutamate receptors have provided valuable information regarding the assembly and mechanism of activation; little is known about the NMDA receptors. Even the basic question of receptor assembly still remains unanswered. Therefore, to

gain a clear understanding of how the receptors are assembled and how agonist binding gets translated to channel opening, I have used a technique called Luminescence Resonance Energy Transfer (LRET). LRET offers the unique advantage of tracking large scale conformational changes associated with receptor activation and desensitization. In this dissertation, LRET, in combination with biochemical and electrophysiological studies, were performed on the NMDA receptors to draw a correlation between structure and function. NMDA receptor subtypes GluN1 and GluN2A were modified such that fluorophores could be introduced at specific sites to determine their pattern of assembly. The results indicated that the GluN1 subunits assembled across each other in a diagonal manner to form a functional receptor. Once the subunit arrangement was established, this was used as a model to further examine the mechanism of activation in this subtype of glutamate receptor. Using LRET, the correlation between cleft closure and activation was tested for both the GluN1 and GluN2A subunit of the NMDA receptor in response to agonists of varying efficacies. These investigations revealed that cleft closure plays a major role in the mechanism of activation in the NMDA receptor, similar to the AMPA and kainate subtypes. Therefore, suggesting that the mechanism of activation is conserved across the different subtypes of glutamate receptors.

Table of Contents

Approval Sheet	i
Title page	ii
Dedication	iii
Acknowledgements	iv
Abstract	v
Table of Contents	vii
List of Illustrations	xi
List of Tables	xiv
Abbreviations	xv
Chapter 1—Introduction to Ionotropic Glutamate Receptors	1
I. Ion channels: Glutamate Receptors.....	2
II. Glutamate receptor subtypes.....	3
III. Molecular Properties of N- Methyl- D- Aspartate (NMDA) receptor.....	6
a. Splice variants and subunit composition.....	7
b. Expression pattern of different subunits.....	7
c. NMDA receptor modulation.....	7
d. NMDA receptor subunit topology.....	8
e. Crystal structure of isolated ABD of NMDA receptor.....	8
f. Significance.....	14
Chapter 2—Fluorescence Resonance Energy Transfer (FRET)	17
I. FRET.....	18
II. Luminescent Resonance Energy Transfer (LRET)	21

III. LRET Instrumentation.....	25
Chapter 3—Two Electrode Voltage Clamp (TEVC).....	28
I. Expression system - <i>Xenopus laevis</i>	29
II. The Two-Electrode Voltage Clamp.....	30
Chapter 4—LRET Part I: LRET investigations to determine subunit arrangement in NMDA receptors	34
I. Architecture of NMDA receptors.....	35
II. Establishing the subunit arrangement of NMDA receptor	38
III. Mechanism of desensitization of NMDA receptor based on distance within the dimer interface.....	58
IV. Results and Discussion.....	62
a. Receptor characterization by electrophysiology	65
b. Validation of the results based on comparison to full length AMPA structure and cross linking investigations	73
V. Future experiments.....	73
Chapter 5—LRET Part II: Probing the conformational changes in the agonist binding domain that controls receptor activation in NMDA receptors.....	77
I. Testing the Activation Hypothesis.....	78
II. LRET to measure the extent of cleft closure at the ABD of GluN2A subunit of the NMDA receptor.....	79
III. LRET to measure the extent of cleft closure at the ABD of GluN1 subunit of the NMDA receptor.....	86

IV. Results and Discussion.....	91
a. Modifications introduced to the full length NMDA receptor for LRET studies	91
b. Mechanism of activation at GluN2A subunit of NMDA receptor.....	91
c. Mechanism of activation at GluN1 subunit of NMDA receptor.....	92
d. Statistical evidence regarding significance of differences in the calculated LRET distances.....	95
V. Future experiments.....	95
Chapter 6—LRET Part III: Examining the conformations explored by the agonist binding domain of AMPA (α-amino-3-hydroxy-5-methyl-4-isoxazole propionate) subtype of glutamate receptors.....	97
I. Mechanism of activation in AMPA receptors.....	98
II. Experimental set- up for the smFRET experiments	102
III. Structural landscape of the GluA2- glutamate bound form.....	108
IV. Structural landscape of the GluA2- Apo form	112
V. Structural landscape of the GluA2- T686S mutant protein.....	115
VI. Results and Discussion.....	118
VII. Future Experiments.....	122
Chapter 7—Overall Conclusions.....	123
Appendix.....	126
I. Molecular Biology.....	127
a. ΔN^* -NMDA receptors.....	127

b GluN1*: GluN2A* Receptor	127
c. RNA synthesis for oocyte injection	127
II. <i>Xenopus</i> Oocyte extraction and preparation.....	129
III. Pre-blocking and Expression.....	132
IV. Labeling oocytes (cells).....	133
V. Membrane Preparation.....	134
VI. Electrophysiology.....	135
VII. Radioactive Ligand Binding.....	136
VIII. Expression of the isolated ABD of GluA2.....	136
IX. Sample preparation for smFRET experiments	137
Bibliography	138
Vitae	150

List of Illustrations

Figure 1 Subtypes of the eukaryotic ionotropic glutamate receptors	4
Figure 2 Crystal structures of GluN1 ABD and GluN1-GluN2A ABD dimer.....	10
Figure 3 Cleft closure Vs activation in AMPA receptors	12
Figure 4 NMDA receptor significance.....	15
Figure 5 FRET overlap spectrum	19
Figure 6 Jablonski diagram	22
Figure 7 Terbium chelate excitation and emission spectrum	26
Figure 8 Schematic of the expression system in oocytes used for LRET experiments in the NMDA receptors	31
Figure 9 Schematic of NMDA receptor topology	36
Figure 10 Possible subunit arrangements in the NMDA receptor.....	39
Figure 11 Sites used for LRET investigations to determine subunit arrangement in NMDA receptors.....	42
Figure 12 Strategy for control experiments in LRET studies.....	45
Figure 13 FRET efficiency Vs distance plot for Terbium chelate: Ni-(NTA) ₂ -Cy3	47
Figure 14 LRET lifetime and residuals.....	49
Figure 15 Sites tagged for LRET measurements within NR1-NR2A dimer	52
Figure 16 LRET lifetime and residuals for NR1-NR2A dimer	54
Figure 17 LRET lifetime and residuals for measurements within NR1 subunit of NR1-NR2A receptor.....	66
Figure 18 Single channel recordings from NR1-NR2A membrane bilayers.....	69
Figure 19 Dose response curve for NMDA wild type and mutant receptors.....	71

Figure 20 Full length crystal structure of GluA2 subunit.....	75
Figure 21 Sites tagged in the GluN1* and GluN2A* subunit to probe for cleft closure conformational changes using LRET measurements	80
Figure 22 Dose response curves for GluN1*: GluN2A* and mutant NMDA receptors.....	82
Figure 23 Cleft closure in the ABD of GluN2A* subunit	84
Figure 24 Cleft closure in the ABD of GluN1* subunit	87
Figure 25 Dependence of cleft closure versus extent of activation for the ABD of GluN1*and GluN2A* subunit.....	93
Figure 26 Extent of cleft closure in the ABD of glutamate receptor plotted as a function of activation	100
Figure 27 Set- up for immobilization of labeled GluA2-ABD for smFRET experiment.....	103
Figure 28 Scanning confocal smFRET instrument set- up	106
Figure 29 Denoised histogram for the glutamate bound GluA2-Wild type protein.....	109
Figure 30 Denoised histogram for the Apo GluA2-Wild type protein	113
Figure 31 Denoised histogram for the T686S mutant GluA2- protein	116
Figure 32 Mechanism of inhibition in NMDA receptors	126

List of Tables

Table 1 Fluorescence lifetimes and distances for $\Delta NR1^*:\Delta NR2A^*$ receptors	57
Table 2 Comparison of distances between desensitized state LRET measurements to antagonist bound crystal structure of AMPA receptor and the other possible configurations	60
Table 3 Comparison of changes in distances between desensitized state and open channel state of NMDA and AMPA receptors	63
Table 4 The Fluorescence Lifetimes and Distances for GluN1*:GluN2A* Receptors....	89
Table 5 Shows a comparison of distances obtained via the smFRET experiments, traditional ensemble FRET investigations and X-ray structures.....	119

Abbreviations

AMPA receptors - α -amino-5-methyl-3-hydroxy-4-isoxazolepropionate receptors,

NMDA receptors - *N*-methyl-D-aspartate receptors

ABD - Agonist Binding Domain

D1 - domain 1

D2 - domain 2

GluA2_{cryst} - Glutamate receptor, AMPA subtype 2, crystal structure

NMR - Nuclear Magnetic Resonance

FTIR - Fourier Transform Infrared Spectroscopy

HEK-293 cells- Human Embryonic Kidney-293 cells

Th - Thrombin

NR1/ GluN1, N-methyl-D-aspartic acid Receptor subunit 1

NR2A/ GluN2A, N-methyl-D-aspartic acid Receptor subunit 2A

DCS - D-cyclo serine

ACPC - 1-aminocyclopropane-1-carboxylic acid.

PEG – polyethylene glycol

SA – streptavidin

PBS – Phosphate buffered saline

FRET - Fluorescence Resonance Energy Transfer

SmFRET - single molecule Fluorescence Resonance Energy Transfer

LRET - Luminescence Resonance Energy Transfer

(Ni-NTA)₂Cy3 - Cy3 derivative of nitrilotriacetic acid chelate of nickel

SDS-PAGE- sodium dodecyl sulfate polyacrylamide gel electrophoresis

AD- Alzheimer's disease

IGluRs - Ionotropic glutamate receptors

MGluRs - metabotropic glutamate receptors

Chapter 1—Introduction: Ionotropic Glutamate Receptors

I. Ion Channels- Glutamate Receptors

The complexity of glutamate as a signaling molecule and as an excitatory neurotransmitter has been a major subject of study for more than 50 years (1). Glutamate released in synaptic pockets induces its effect by interacting with specialized membrane proteins embedded in the post synaptic membrane called glutamate receptors (2). Glutamate receptors are subdivided into two major subtypes: Ionotropic glutamate receptors (iGluRs) form integral ligand - gated ion channels and metabotropic glutamate receptors (mGluRs) that activate G- proteins via a secondary messenger system (3, 4). This thesis will focus on iGluRs.

iGluRs are major mediators of excitatory signal transmission in the mammalian central nervous system (5). Glutamate, upon binding to the receptor induces formation of ion channels and thereby enables cations like sodium, potassium and sometimes calcium to flow through the membrane (1, 6). Based on their pharmacological properties; iGluRs are divided into three major receptor families: α -amino-5-methyl-3-hydroxy-4-isoxazole propionate (AMPA) receptors, *N*-methyl-D-aspartate (NMDA) and Kainate receptors (3). Although the three receptor subtypes share a similar subunit topology, their overall structure, function and ligand affinity differ across each subtype (7-9).

In 1998, Roderick Mackinnon solved the first structure of the voltage gated K^+ channel that described the mechanism of ion channel selectivity by the pore region of the receptor (10). This discovery has paved the way for the identification of numerous ion channel crystal structures in the last decade. In 2009, Eric Gouaux and co- workers solved the first crystal structure of the full length AMPA receptor subunit (GluA2) and revealed the intricate architecture of the glutamate receptor family (11). This structure

along with the multitude of soluble ABD structures has helped delineate the mechanism of activation of the AMPA subtype of glutamate receptors. However such information for the NMDA subtype of glutamate receptors is still largely amiss, and with just a handful of structures available on the ABD of GluN1 and just one for the GluN2A subunit, these receptors still remain an enigma in the ion channel field (12-14). Given their role in the modulation of numerous physiological processes there is a tremendous need to understand the molecular mechanism of the NMDA receptor activation. Even the basic question of subunit assembly is unknown for this receptor. In my dissertation, I am presenting the use of LRET as a molecular ruler to determine the specific subunit arrangement of a functional NMDA receptor and established the mechanism of activation in this receptor family.

II. Ionotropic Glutamate receptors subtypes:

iGluRs, based on their pharmacology are subdivided into three major types of receptors, AMPA, NMDA and Kainate(3). While AMPA receptors bind to AMPA (a synthetic ligand) as a full agonist, NMDA receptors bind to NMDA (another synthetic ligand) as a full agonist, lastly Kainate receptors bind to Kainate (a natural toxin present in sea weed) as a full agonist (15). There is a unique role for each of the receptors in this family. AMPA receptors play a vital role in mediating rapid excitatory synaptic current in the brain (16). NMDA receptors act as coincidence detectors, monitoring changes in glutamate concentrations in the synaptic cleft and variations in membrane potential (17). Kainate receptors play a modulatory role both at presynaptic and synaptic cleft (18). The receptors are further subdivided into different subunits (Figure 1). While AMPA receptors are composed of subunits GluA1-4 (3, 4, 8, 19, 20), and Kainate receptor

Figure 1 Subtypes of the eukaryotic ionotropic glutamate receptors based on their pharmacology.

Ionotropic Glutamate
Receptors

α -amino 3-hydroxy 5-methyl
4-isoxazolepropionic
acid (AMPA)

N-methyl-D-Aspartate
(NMDA)

Kainate

GluA1, GluA2,
GluA3, GluA4

GluN1, GluN2, GluN3

GluK5, GluK6,
GluK7, and KA1,
KA2

GluA5-7 (19, 20), KA1-2 are capable of forming homo or hetero - tetramers, the NMDA receptors are primarily composed of subunits GluN1, GluN2A-D and GluN3 subunits (21-24). They are obligate hetero tetramers. In addition, while non NMDA receptors can be activated solely by glutamate, NMDA receptors require both glycine and glutamate for full activation (23, 25, 26). Other than their importance in mediating excitatory synaptic transmission in the CNS, these receptors are also involved in neuronal development, synaptogenesis and neuronal viability (27, 28). Excitotoxicity or excessive activation of these receptors results in neuronal damage, which in turn is linked to various neuropathologies like ischemia, stroke, Alzheimer's, Parkinson's and seizures etc (29, 30). In addition to their involvement in the CNS, these receptors are further found expressed in several other tissues: insulin secretion in pancreatic islet cells express glutamate receptor, bone re absorption in osteoblasts, cardiac pacemaking in cardiac ganglia cells, and nerve terminals in skin where glutamate receptors participate in pain perception and tactile sensation (31, 32). Their broad distribution among different cell types thus makes them an ideal candidate for drug investigations.

III. Subtype of Glutamate Receptors: Molecular properties of NMDA Receptors

NMDA receptors, a major subtype of iGluRs have been studied extensively for the last two decades since their discovery in the 1980's (23). They are widely distributed throughout the CNS and play a vital role in establishing neuronal connection early during development. While in adults, NMDA receptors are involved in the modulation of synaptic strength and learning and memory (23). Therefore, regulation of these receptors is vital.

a. Splice variants and subunit composition

Three subunits of the NMDA receptor have been identified, GluN1, GluN2 and GluN3 (24, 25, 33). The glycine binding GluN1 subunit has one gene product with eight splice variants, while the glutamate binding GluN2 subunit has four gene products, GluN2A-D (25, 34). The GluN3 subunit of the NMDA receptor consists of two gene products GluN3A-B and can form functional receptor in combination with GluN1. A functional receptor is formed by a combination of GluN1 subunits with any of the glutamate binding GluN2 subunits (24, 35, 36). Each subunit is characterized by unique activation and desensitization kinetics. The open channel probability of the subunits differs markedly with GluN2A containing receptors having the maximum channel open probability (37, 38).

b. Expression pattern of subunits

There is a general shift in the trend of subunit expression from GluN2B and GluN2D to GluN2A and GluN2C receptor predominance during development. GluN2B and GluN2D subunit expression is found as early as in the embryonic stage while the pattern of expression upon maturity in the adult brain is typically GluN2A containing receptors, except in the forebrain region (39). While GluN2A expression is not limited, GluN2C expression is limited to the cerebellum during adulthood.

c. NMDA receptor modulation

The NMDA receptors are modulated by various substances including sulfhydryl reagents, polyamines, histamine, protons, ethanol, protein kinases, arachidonic acid, cations and numerous organic compound (23). More importantly, channels, irrespective of their subunit composition, are inhibited by a voltage dependant Mg^{2+} block. GluN2A containing receptors are modulated and inhibited by Zn^{2+} ions while GluN2B receptors

are allosterically inhibited by phenoethanolamine derivatives like ifenprodil (40-43). The allosteric modulators typically bind to the amino terminal region of the receptors (44).

d. NMDA receptor subunit topology

The different subunits of NMDA receptors share a similar topology to the other non-NMDA receptors. Each subunit is composed of anywhere from 900- 1500 amino acids and is a single gene product. The domain organization of the single subunit is shown in Figure 9. The extracellular region is composed of an Amino Terminal Domain (ATD) (where allosteric modulators bind) and an Agonist binding domain (ABD) (glycine and glutamate binding modules) (12, 13). The 350 amino acid ATD bears resemblance to the bacterial LIVBP (Leucine/ Iso-leucine/ Valine binding protein) and also the mGluR1 (metabotropic Glutamate receptor) glutamate binding subunit (45). The ATD is primarily involved in organization and also has modulatory effects on the channel (46). However, NMDA receptors lacking the ATD express have been shown to be functional similarly to the wild type (43, 47). Below the ATD lies the 280 amino acid ABD where the agonist glutamate binds in the GluN2 subunit and glycine in the GluN1 subunit. The ATD and ABD both have clamshell like bi-lobed domains. The ion channel pore consists of three transmembrane regions M1, M2, M3 and a re-entrant loop M2 which is similar to the P-loop of the voltage gated channels (11). The pore region confers selectivity to the ion channel and below the channel segments lays the variable length intracellular C-Terminal tail. Calmodulin and other proteins have been shown to bind to this region.

e. Crystal structures of the isolated ABD of NMDA receptor

Crystal structures of the ABD of NMDA receptor GluN1 subunit was solved in 2003 by Eric Gouaux and co-workers (12) (Figure 2). Similar to the other non-NMDA receptors,

the NMDA receptor subunit is also modular and the ABD has been excised, expressed as a soluble bacterial protein and crystallized in complex with various ligands (13). The crystal structures of the isolated ABD of the three subtypes of ionotropic glutamate receptors have provided a first glimpse into the conformational changes accompanying agonist binding and have given a rudimentary understanding into the mechanism by which agonists could control activation and eventually the desensitization of ion channels (48-50). There are more than sixty structures of the AMPA subtype in complex with a variety of ligands of differing efficacies (7, 51). Based on these structures, a graded cleft closure hypothesis was developed for activation of the AMPA subtype where the cleft closure correlated to the extent to of activation or in other words efficacy of the agonist (52-54). Hence it has been proposed that this is the coupling mechanism by which the agonist controls the gate (Figure 3). However for the NMDA subtype, the least studied among the GluR subtypes, such a wealth of crystallographic data is not available. The structures of the ABD of the GluN1 subunit bound to full agonist glycine and partial agonists such as D-cycloserine and ACPC showed no significant differences in the extent of cleft closure (Figure 2) (12, 13). Based on these structures it has been hypothesized that the NMDA receptors could follow a two state model, where the cleft exists in either an open or closed form. In addition, at present there is only one structure available for the isolated ABD of the GluN2A subunit, it is of a dimer of GluN1-GluN2A bound to their respective agonists- glycine and glutamate (13) (Figure 2). The glutamate bound GluN2A subunit cleft is closed. Therefore, it is still not known if the GluN2 subunit exhibits a graded cleft closure as seen for the AMPA and kainate subtypes.

Figure 2 Crystal structures of GluN1 ABD in complex with Glycine and D-cyclo serine (DCS) (12, 14). Glycine and glutamate bound crystal structure of GluN1-GluN2A ABD dimer (13).

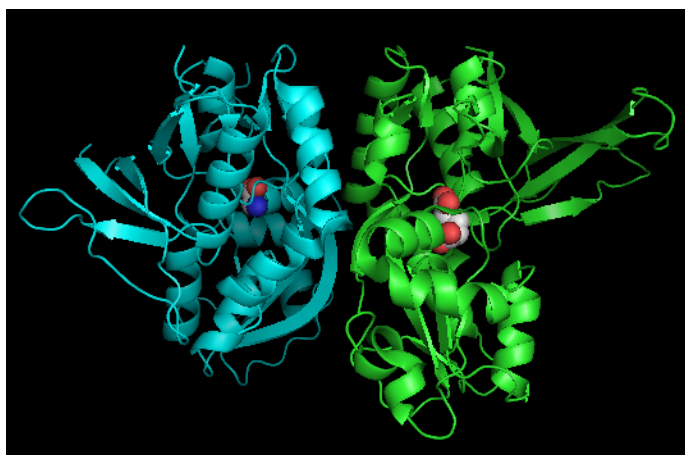
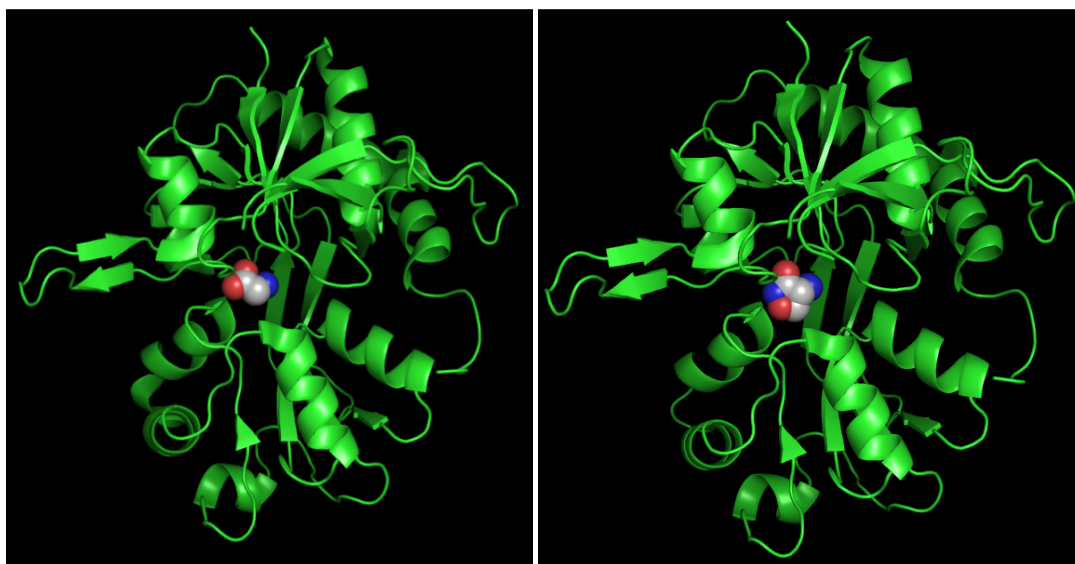
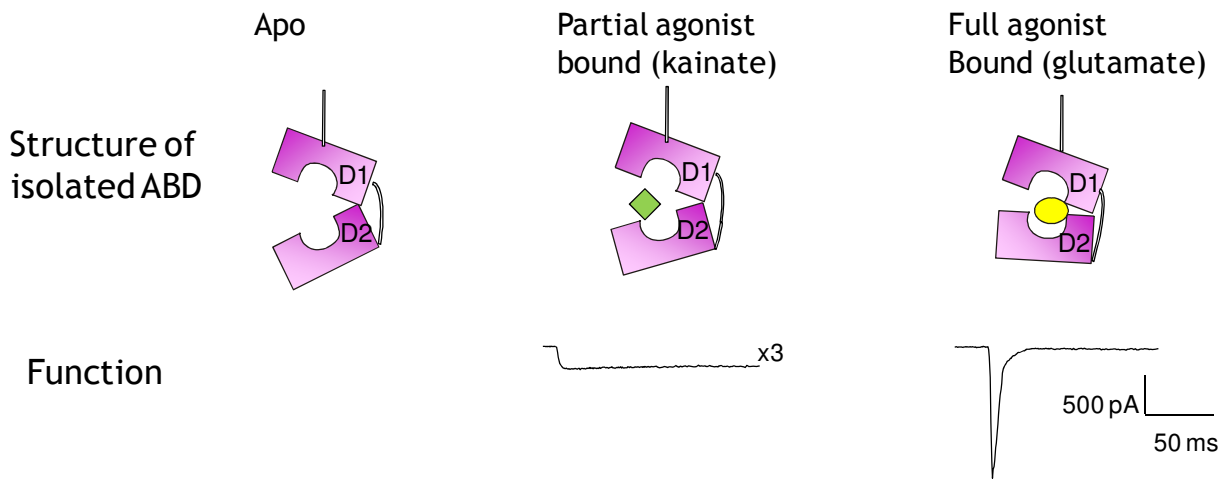


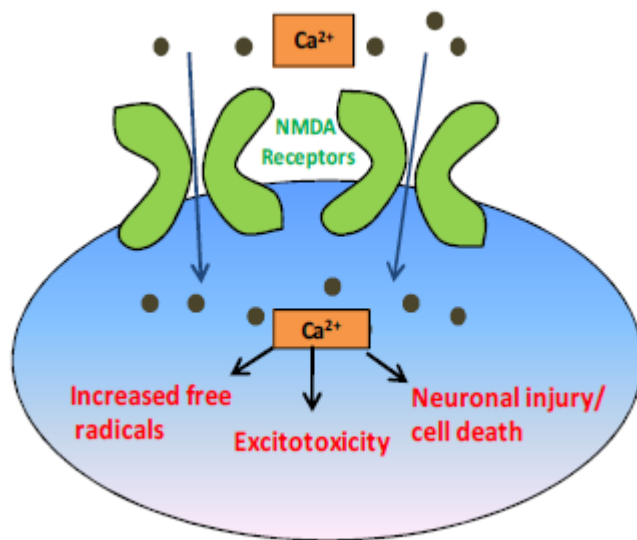
Figure 3 Cleft closure versus activation in AMPA receptors.



f. Significance

Alzheimer's disease (AD) is the most common cause of dementia and is estimated to be the fourth largest cause of death for people over 65 years of age in the US. Excitotoxicity or overstimulation of ionotropic glutamate receptors (iGluRs) is one of the key causes linked to the onset and progression of AD(55). Of particular interest is the highly Ca^{2+} permeable N-methyl-D-aspartate (NMDA) receptor, a subtype of iGluR whose excessive uncontrolled firing has been implicated in cognitive dysfunction, memory loss and other psychiatric symptoms (Figure 4). Hence major focus has been given on the development of antagonists or drugs that specifically target these receptors, thereby preventing neuronal injury and cell death. Given the undeniable importance of these receptors in mediating critical physiological processes, there is an ever-increasing need to devise effective strategies to judiciously manipulate their function in disease states (56). However, there are currently only four FDA approved medications to treat the cognitive degeneration manifested in AD patients. Memantine, an antagonist that blocks NMDA receptors, is one of those drugs and is moderately efficient in treating moderate to severe forms of AD. The major hurdle towards the development of target drugs has been the lack of a clear understanding of the molecular mechanism by which agonists/ligands mediate activation of NMDA receptors. In this dissertation, I will address this critical gap by employing an LRET (luminescence resonance energy transfer) based assay and relate the newly observed large scale conformational changes to documented functional properties.

Figure 4 The binding of ligands induces activation of NMDA receptors resulting in calcium entry into the cell. Alzheimer's disease (AD) results from uncontrolled activation of these receptors.



Chapter 2 - Fluorescence Resonance Energy Transfer (FRET)

I. Fluorescent Resonance Energy Transfer (FRET)

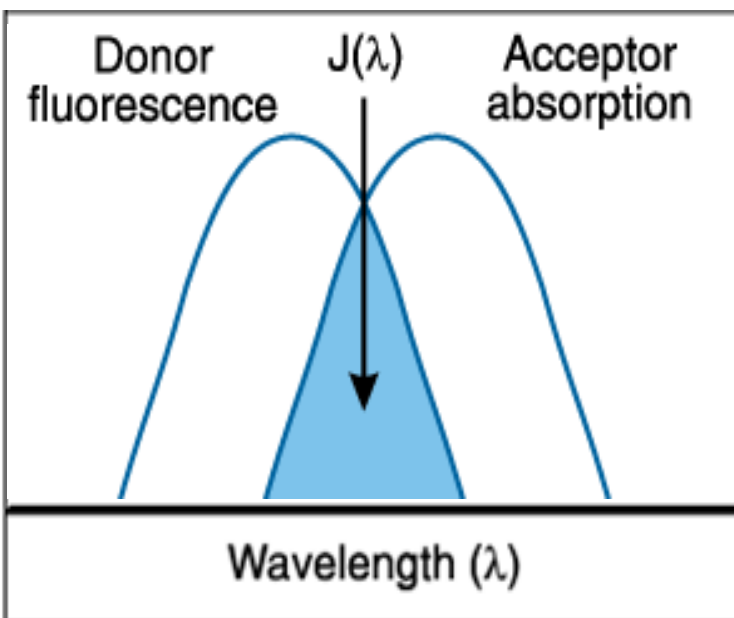
Described over 50 years ago, Fluorescence Resonance Energy Transfer (FRET) is a physical phenomenon that is now widely used in biomedical and drug research studies (57). FRET is the radiationless, distance-dependent transfer of energy from a donor to an acceptor molecule (58). It is widely used to investigate molecular interactions due to its increased sensitivity to distance. Energy is initially absorbed by a donor dye or chromophore which is then subsequently transferred to an acceptor chromophore. This transfer of energy leads to a reduction in the donor's fluorescence intensity and excited state lifetime, and an increase in the acceptor's emission intensity. In order for FRET to occur the following conditions have to be satisfied: The distance range that typically can be measured by FRET is around 10-100 Å (59). There must be an overlap between the excitation spectrum of the acceptor and the emission spectrum of the donor moiety (Figure 5). This degree of overlap is often referred to as the spectral overlap integral (J). In addition, the transition dipole orientations of the donor and acceptor must be approximately parallel. The dependence between efficiency of the process (E) and the distance between donor and acceptor is given by the Förster equation (Equation 1).

$$E = \left(1 + \left(\frac{R}{R_0}\right)^6\right)^{-1} \quad (1)$$

R_0 is the distance at which energy transfer is 50% and r is the distance between donor and acceptor. The magnitude of the R_0 is contingent on the spectral properties of the donor and the acceptor dye molecules. FRET is often referred to as a spectroscopic ruler since any process that affects energy transfer rate can be quantified. The Förster distance (R_0) given in Equation 2 is dependent on a variety of factors, including the

Figure 5 FRET occurs when the emission spectrum of the donor overlaps with the absorbance spectrum of the acceptor. Figure adapted from Selvin P.R., 1995 (59).

This research was originally published in Journal of Biological Chemistry. Gonzalez, J., Rambhadran, A., Du, M., and Jayaraman V. (2008) LRET Investigations of the Conformational Changes in the Ligand Binding Domain of a Functional AMPA Receptor. Biochemistry. 47(38):10027-32. Copyright the American Society for Biochemistry and Molecular Biology.



quantum yield of the donor (Φ_D), the refractive index of the solution (n), the dipole angular orientation of each molecule (k^2), and the spectral overlap integral of the donor and acceptor (J).

$$R_0^6 = \frac{8.785 \times 10^{-5} * \kappa^2 * \phi_D * J}{n^4}$$

$$J = \frac{\sum_i F_D(\lambda_i) * \epsilon_A(\lambda_i) * \lambda_i^4}{\sum_i F_D(\lambda_i)}$$

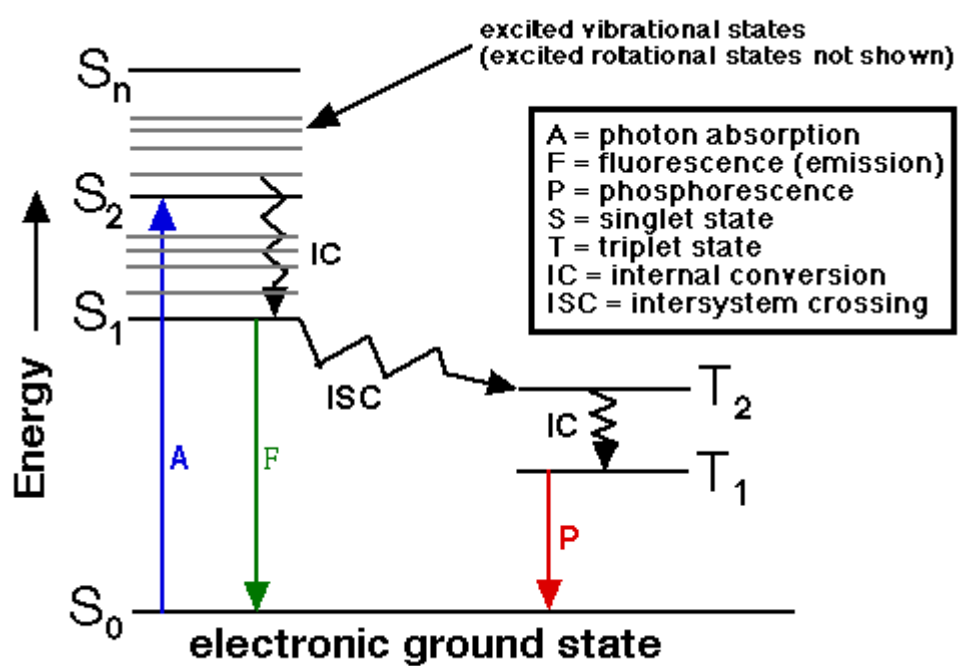
In most of the cases the donor and acceptor molecules are different, and FRET is detected by appearance of fluorescence of the acceptor or by the quenching of donor fluorescence. The donor probe is usually a fluorescent molecule, but on the other hand, a luminescent probe behaves as a fluorescent molecule in regards to its emission. When excited, electrons jump from the ground state (S_0) to a higher vibrational level. Within picoseconds, these electrons decay to the lowest vibrational levels (S_1) and eventually decay (nanosecond time scale) back to the ground state. In this process, a photon of light is emitted (57). When resonance energy transfer occurs, the photon is not emitted; instead energy is transferred to the acceptor molecule, whose electrons in turn get excited similar in manner to the donor molecule. The acceptor subsequently returns to the ground state upon emitting a photon (Figure 6).

II. Luminescence Resonance Energy Transfer (LRET)

A slightly modified version of FRET is the LRET (Luminescence Resonance Energy Transfer) technique where the donor is luminescent (60, 61). A luminescent lanthanide donor like terbium chelate is employed and upon excitation it transfers energy to a fluorescent acceptor molecule for example, ATTO465-maleimide, Fluorescein.

Figure 6 Jablonski diagram. Adapted from Lakowicz et al. 1983 (57).

This research was originally published in Journal of Biological Chemistry. Gonzalez, J., Rambhadran, A., Du, M., and Jayaraman V. (2008) LRET Investigations of the Conformational Changes in the Ligand Binding Domain of a Functional AMPA Receptor. Biochemistry. 47(38):10027-32. Copyright the American Society for Biochemistry and Molecular Biology.



LRET typically has a number of advantages to the traditional FRET method, greater distance range; temporal resolution of signals; a decrease in error in distance measurements; and finally multiple distances can be determined for a single system (62, 63).

These advantages are attributed to the inherent properties of terbium chelate, the donor used in LRET studies. Terbium chelate is isotropic, which greatly reduces the error associated with the FRET and has a high quantum yield. The four distinct emission peaks allow spectral separation of donor and acceptor fluorescence (Figure 7). This distinction offers the advantage of being able to employ a variety of acceptor pairs to give a variety of R_0 values.

The long lifetime of terbium chelate in the microsecond to millisecond timescale allows for the temporal separation of the acceptor only (which typically has a nanosecond lifetime), donor only, and LRET signal (which usually is in the microsecond scale). The donor only sample does not contribute to the LRET signal since LRET is measured at the wavelength of the acceptor; this measurement is referred to as sensitized emission. The sensitized emission is due to the acceptor gaining fluorescence from the donor. Based on lifetimes, the following equation (Equation 4) is used to calculate distances:

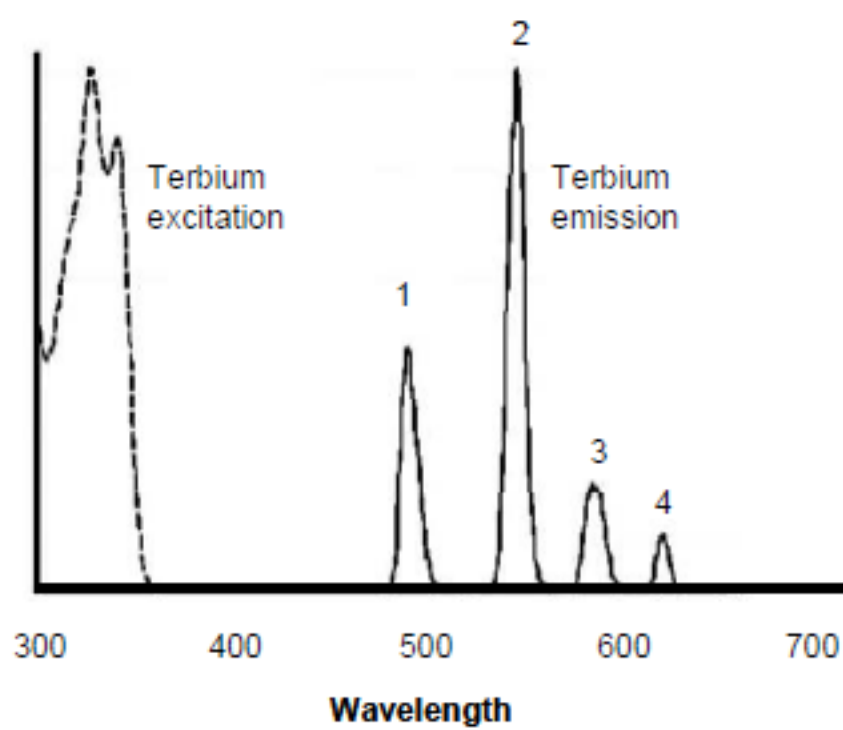
$$R = R_0 \left(\frac{\tau_{DA}}{\tau_D - \tau_{DA}} \right)^{1/6}$$

Where, τ_D is the time constant for donor fluorescence decay in the absence of the acceptor and τ_{DA} is the sensitized emission of the acceptor due to the energy transfer from the donor.

III. LRET Instrumentation

Fluorescence Spectroscopy. A cuvette based fluorescence lifetime spectrometer QuantaMaster Model QM3-SS (Photon Technology International, NJ) is used for performing fluorescence measurements. The excitation source is a high power pulsed xenon lamp. Additionally, the collected emitted light is passed through a monochromator onto a detector. Using a Peltier TE temperature controller, the sample is held at a constant 15°C temperature. Fluorescan software was used to collect data (Photon Technology International, NJ), and Origin 4.0 software is used to analyze the data (OriginLab Corp., MA) (63). Data from three to four sets of data are averaged and fitted to obtain the lifetimes. Each individual data set is examined to ensure similar trends were maintained. The donor only lifetimes were collected at 545 nm for Terbium chelate, and the sensitized emission of acceptor were measured at 510 nm for ATTO 465 and 515 nm for Fluorescein in order to obtain the LRET lifetimes. The fluorescence decay was fitted to a function that is a sum of discrete exponentials and the goodness of the exponential fit was determined from the random residual distribution with a chi-square value being close to unity.

Figure 7 Excitation and emission spectrum of Terbium chelate. Adapted from Invitrogen (Lantha Screen Thiol Reactive Terbium Chelate) product webpage.



Chapter 3—Two- Electrode Voltage Clamp (TEVC)

I. Expression system – *Xenopus Laevis* system

The *Xenopus* oocyte was initially used to express functional ion channels and receptors in 1982 and since then has become an ideal system to express and to characterize ion channels (64). Biophysical characterizations of ion channels using *Xenopus* oocytes is very simple using TEVC recordings as oocytes are large (around 1 mm in diameter). Injections of either DNA or RNA of the protein of interest are possible with oocytes. Expression can be modulated by altering the amount of DNA/RNA that is injected and the oocytes are capable of translating these nucleotides to protein (65). Proteins are trafficked and sent to their respective destination, for example, plasma membrane protein is trafficked to the plasma membrane. Although it depends on the amount and type of receptor, typically 25-50 ng of RNA is injected into each oocyte. Also, oocytes have the machinery to allow for post translational modifications of protein. *Xenopus laevis* oocytes are unfertilized eggs from the African clawed frog, and supply is easy to maintain, because frogs produce oocytes throughout the year. After surgical extraction and enzyme treatment, oocytes can be stored in saline solutions with antibiotics for over 7 days.

However, the *Xenopus laevis* oocyte expression system has several disadvantages. There are batch to batch variations in expression levels and the quality of oocytes. It is a transient expression system where expression of endogenous protein could interfere with the injected protein expression. Several important factors need to be kept in mind before selecting oocytes as an expression system: the amount of RNA to be injected, expression time and pattern, and finally the number of oocytes based on the level of expression.

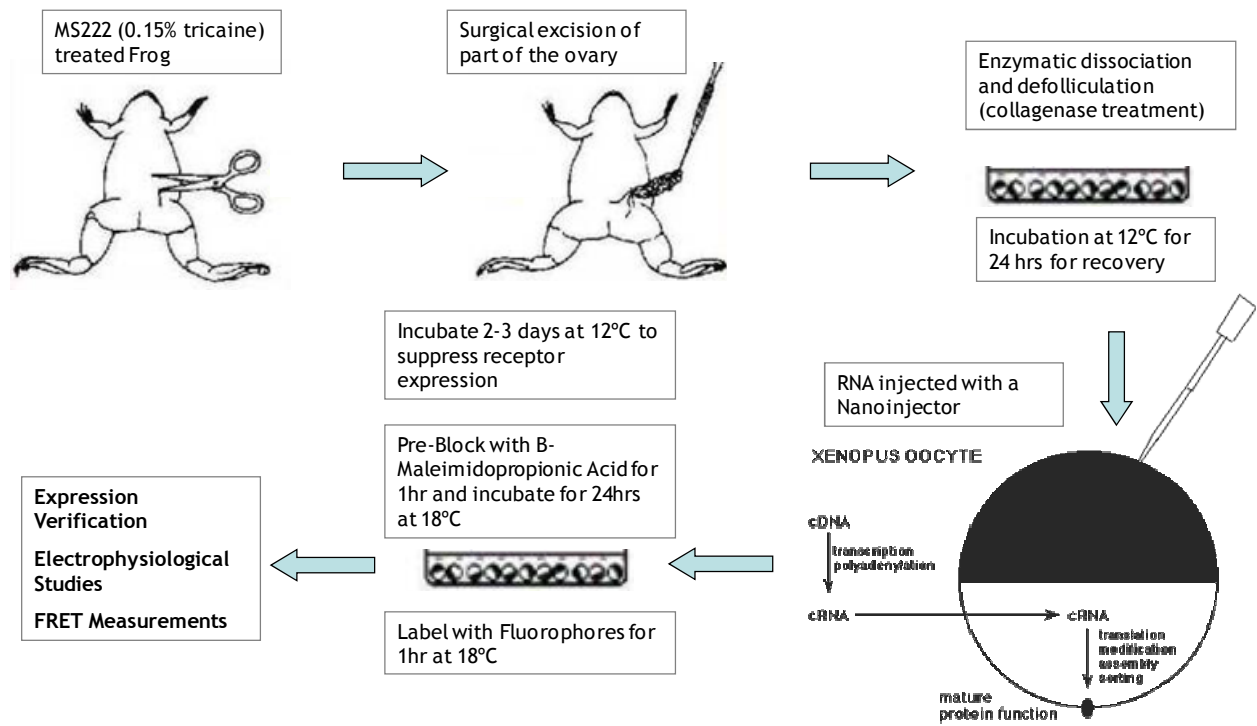
The most critical step in the utilization of oocytes for LRET experiments was the optimization of the expression system by employing a pre- blocking reagent and introducing a protease cleavage site to account for background labeling (66). For the LRET measurements, maleimide derivatives of dyes are used as donor and acceptor pairs to label the cysteine mutations introduced in the protein of interest. Thus, there was the problem of background inherent cysteines that inadvertently got labeled and hence contributed to the LRET signal. In order to avoid this issue, a pre- blocking step was introduced (a schematic of the process is shown in Figure 8). A maleimide derivative was used to block inherent cysteines prior to receptor expression (details in the appendix).

II.Two Electrode Voltage Clamp (TEVC)

The usefulness of the voltage clamp stems primarily from the fact that it allows the separation of membrane ionic and capacitive currents. Secondly, it is much easier to obtain information about channel behavior using currents measured from an area of membrane with a uniform, controlled voltage, than when the voltage is changing freely with time and between different regions of membrane. The method was initially developed by Cole in 1949 and later by Hodgkin et al. in 1952 for use with the squid giant axon (67). Since then, many variants of the technique have evolved and voltage clamp analysis has been extended to a wide range of tissues.

The membrane potential (V) is measured in volts and this is caused by the charge separation across the membrane. Current (I) is generated by the movement of ions across the membrane. Two electrodes, namely the current and voltage electrodes are inserted into the oocyte. The voltage electrode measures the membrane potential

Figure 8 A schematic of the expression system in oocytes used for LRET experiments in the NMDA receptors.



relative to the ground, while the current electrode is injecting current into the oocyte. The holding voltage is set to -60 mV and this is achieved by the voltage clamp using a negative feedback mechanism. Whenever ligand is added, the channel opens and ions flow through causing a deviation from the command voltage. The amplifier detects the difference and sends out an output signal to the current electrode. This detection and resulting signal help to maintain the holding potential. The signal equal and opposite to the current is produced and this can be measured as the current from the oocyte.

TEVC experiments were used in order to validate the functionality of the NMDA receptor and derivative mutants. The cysteine mutants used for the LRET experiments were tested for their functional properties relative to the wild type in order to establish that the mutations did not alter the biophysical properties or expression of the receptor.

Chapter 4 — Part I: LRET investigations to determine subunit arrangement in NMDA (N- Methyl- D- Aspartate) receptors

This research was originally published in Journal of Biological Chemistry. Rambhadran, A., Gonzalez, J., Jayaraman, V. 2010. Subunit arrangement in N-Methyl-D-aspartate (NMDA) receptors. *Journal of Biological Chemistry* 285(20):15296-301. Copyright the American Society for Biochemistry and Molecular Biology.

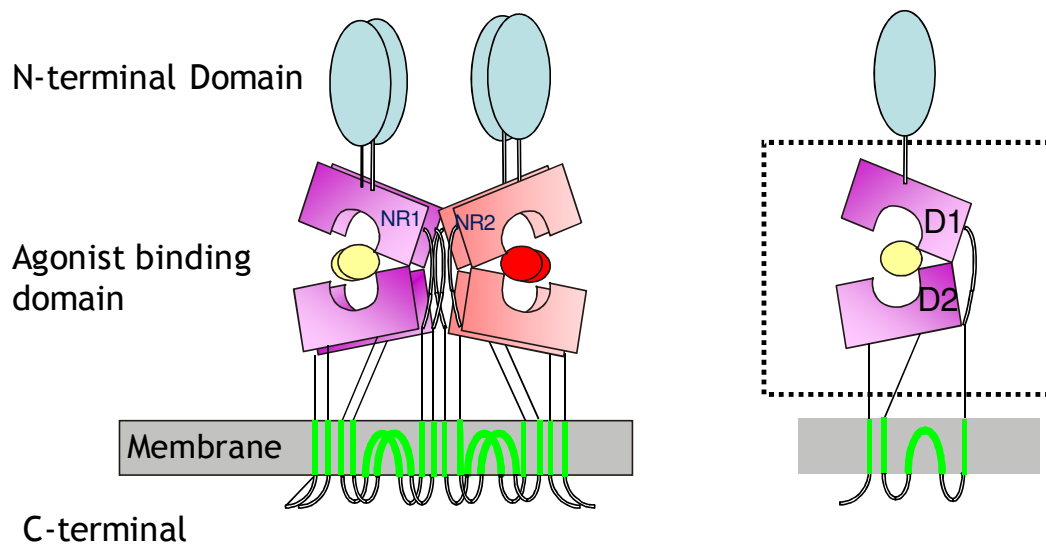
I. Architecture of N-Methyl-D-aspartate (NMDA) receptors

NMDA receptors are distinctly different from non-NMDA receptors such as AMPA and kainate receptors which can form functional homotetrameric channels activated solely by glutamate (23). The NMDA subtype is obligate heterotetramers comprised of glycine-binding GluN1 or GluN3 subunits and glutamate-binding GluN2 subunits. Depending on the cell and the developmental stage, typically one of the four GluN2 subunits (A–D) combines with a splice variant of the GluN1 subunit, yielding receptors with distinct deactivation kinetics (23). The topology of the NMDA receptor is similar to the other non- NMDA subtypes, typically the GluN1, GluN2 and GluN3, have a similar membrane topological structure, with three transmembrane domains plus a pore-loop sequence that lines the channel (Figure 9).

The extracellular portion of the receptor consists of two domains: an N-terminal domain (ATD) and the agonist binding domain (ABD). The ATD domain binds modulatory ligands like Zinc, Ifenprodil etc. but is not essential for the basic function of agonist induced channel activation and desensitization. Laube and coworkers have demonstrated that the NMDA receptors are fully functional in the absence of ATD and therefore in my proposed work to identify the stoichiometry and arrangement of the NMDA receptors I have used a modified receptor lacking the ATD that still retain the other functional components (24, 47).

While there is a structure of the full length for AMPA receptor in complex with an antagonist, there is currently no structural data available for the full length NMDA receptor (11).

Figure 9 Schematic of NMDA receptor topology. (A) NMDA receptor tetramer consisting of glycine binding NR1 subunit and glutamate binding NR2A subunit. (B) A single subunit contains an extracellular N-terminal domain, an extracellular ligand binding domain, three transmembrane segments and a re-entrant loop that form the transmembrane domain, and an intracellular C-terminus.

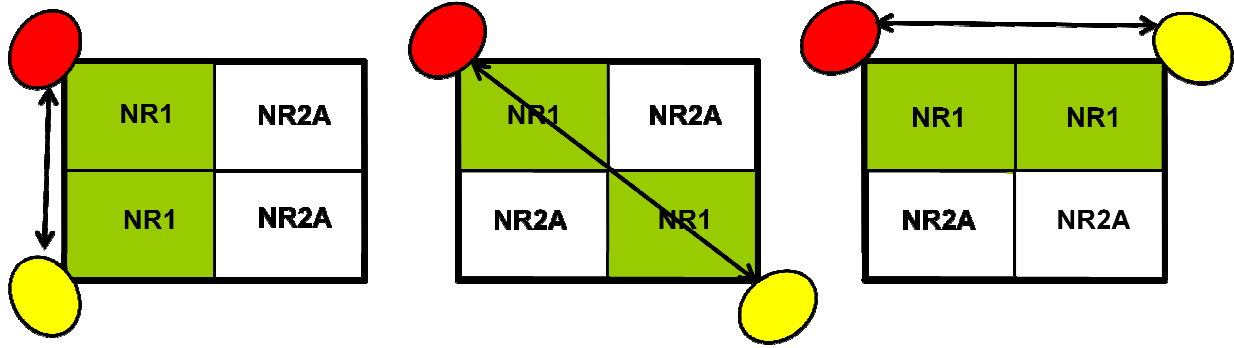


There is only one structure of the NMDA receptor GluN1-GluN2A ABD in complex with each other and this structure suggests that one of each subunit forms the dimer (13). However there is no knowledge of how the dimer assembles to form the tetramer. Additionally, even for the structure of a dimer, it should be noted that these structures were of the isolated ABD lacking the functional component of the receptor; the transmembrane segments. Hence it is still possible that in the tetramer this structure may not reflect the actual arrangement. Given the fact that several laboratories have tried to express the full length NMDA receptor and have not been successful, the proposed LRET experiments provide the best alternative, while limited in terms of not being able to provide the complete structure, to be able to provide distance constraints that will in turn be able to provide insight into the arrangement of subunits in this important class of glutamate receptors. In this chapter, the LRET technique was used in order to study the specific arrangement of subunits in a functional NMDA receptor in a physiologically relevant state.

II. Establishing the subunit arrangement of NMDA receptor

LRET is an excellent tool to probe the specific arrangement in which the subunits assemble, the advantage lies in the ability to attach donor and acceptor probes at strategic locations in the protein and by using the right pair of fluorophores to allow us to distinguish the different arrangements of the receptor (63)(Figure 10). Hence for studying the subunit arrangement of the NMDA receptor, I used modified GluN1 and GluN2A subunits of the NMDA receptor lacking the N-terminal domain. To achieve this, residues numbered 5-357 of the mature peptide were deleted for the GluN1 subunit

Figure 10 Possible subunit arrangements in the NMDA heteromeric receptor - where NR1's are either arranged in a back to back manner, across from each other or the NR1s could be arranged sideways, adjacent to each other NMDA receptors are thought to be a dimer of dimers. Crystal structures of the isolated ligand binding domain suggest that one NR1 and one NR2 subunit form the dimer.



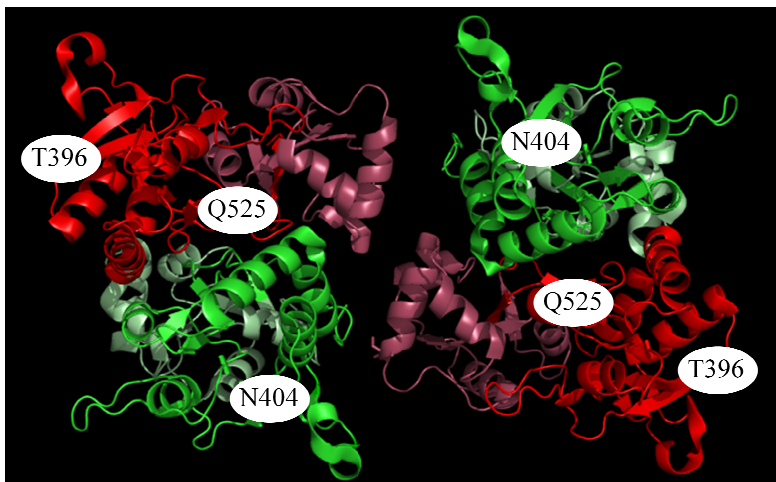
while for GluN2A residues 1-385 were deleted. Additionally, to ensure proper expression of the GluN2A subunit, a modified influenza hemagglutinin (HA) tag replaced the original signal peptide sequence (43, 47). These modifications were similar to the kind done by Laube et.al. and the expression of the modified receptor subunits were further verified by electrophysiological recordings and compared to the response from wild type receptors (47). The N-terminal domain lacking GluN1, and GluN2A subunits (Δ GluN1, Δ GluN2A) were further altered to eliminate any single non-disulphide bonded accessible cysteines. This mutagenesis approach was critical for the success of the LRET experiments since the fluorophores used were maleimide derivatives, hence to prevent background non-specific labeling it was essential to eliminate inherent non-disulphide bonded accessible cysteine. The following mutants were made; C459 in GluN1 and C399 in GluN1, C460 in GluN2A were mutated to serine. The cysteine free modified subunits (Δ GluN1* and Δ GluN2A*) served as background constructs and were used for LRET investigations by introducing either cysteines and or histidine tags that acted as donor and or acceptor sites.

In order to determine the distance between GluN1 subunits a cysteine followed by a thrombin cleavage site (C-Th) was introduced at the N-terminus of the ABD of GluN1 (Residue 396). Similarly residue 404 was chosen for the GluN2A subunit measurement (Figure 11). The thrombin cleavage site allowed us to selectively cleave the donor or acceptor fluorophore tagged to these sites. LRET lifetime is recorded before and after thrombin digestion. The final specific LRET signal was obtained upon subtracting the background non-specific lifetime. This technique was developed by the Jayaraman lab and has enabled us to overcome the background non-specific signal and thereby

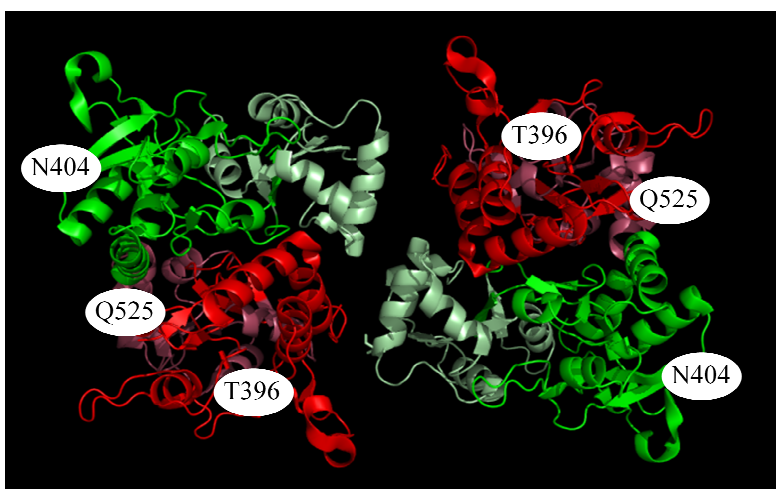
Figure 11 Possible arrangements of NR1-NR2A receptors agonist binding domains 1 and 2 based on full length AMPA receptor crystal structure. The position of the NR1 subunit on the AMPA receptor structure is colored in red for Domain 1 and in pink for Domain 2. The position of NR2A subunit on the AMPA receptor structure is colored in green for Domain 1 and pale green for Domain 2. Homologous sites tagged in the modified Δ NR1* and Δ NR2A* subunits for LRET measurements are highlighted.

This research was originally published in Journal of Biological Chemistry. Rambhadran, A., Gonzalez, J., Jayaraman, V. 2010. Subunit arrangement in N-Methyl-D-aspartate (NMDA) receptors. *Journal of Biological Chemistry* 285(20):15296-301. Copyright the American Society for Biochemistry and Molecular Biology.

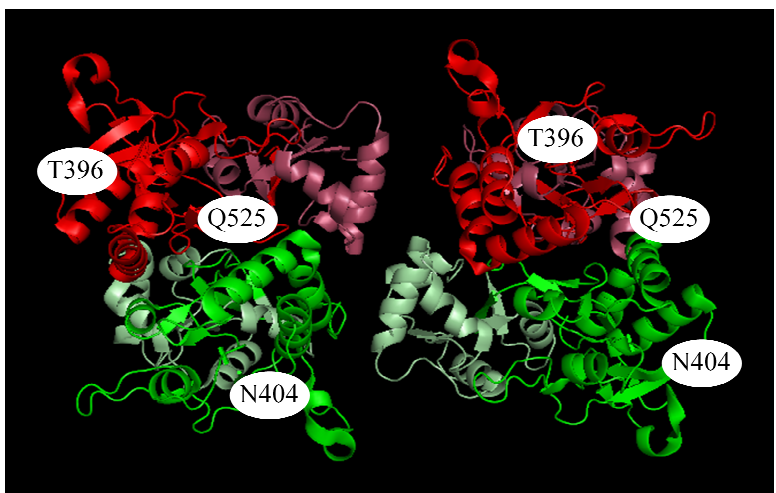
A



B



C



allowed us to work with a non- purified system in a physiological state with minimum manipulation (62)(Figure 12).

Distances within GluN1 and within GluN2A subunits: The $\Delta\text{GluN1}^*\text{T396C-Th}/\Delta\text{GluN1}^*\text{396Histag}:\Delta\text{GluN2A}^*$ labeled with terbium: $\text{Ni-(NTA)}_2\text{-Cy3}$ chelate serving as donor: acceptor pair was used to measure the distance between residue 396 on one GluN1 subunit with respect to the same residue on the second GluN1 subunit (Figure 11) (68). This combination of receptors did not give any significant LRET signal suggesting that the distance between the residue 396 on one GluN1 subunit with respect to the same residue on the second GluN1 subunit is longer than that measurable by the terbium respective donor: acceptor pair. The R_0 for this pair is 65 Å, therefore for distances >100 Å the efficiency of transfer decreases to around 6% (Figure 13). Hence it can be concluded that the distance between residues 396 on the two GluN1 subunits is > 100 Å. In a similar manner, to measure the distance between residue 404 on one GluN2A subunit and the same residue on the second GluN2A subunit, $\Delta\text{GluN1}^*:\Delta\text{GluN2A}^*\text{N404Histag}/\Delta\text{NR2A}^*\text{N404C-Th}$ construct was used and labeled with terbium: $\text{Ni-(NTA)}_2\text{-Cy3}$ chelate. The LRET lifetime for this mutant (Figure 14) could be well represented by a single exponential decay, and the corresponding distance obtained from this lifetime was 60 Å. In order to measure distances between GluN1 and GluN2A subunits, the construct $\Delta\text{GluN1}^*\text{396Histag}:\Delta\text{GluN2A}^*\text{N404C-Th}$ receptor tagged with terbium: $\text{Ni-(NTA)}_2\text{-Cy3}$ chelate was used. The LRET lifetime measured between residue 396 on GluN1 and residue 404 on GluN2A required a two exponential fit (Figure 11). The two lifetimes correspond to two distances between the

Figure 12 Strategy for control experiments in LRET investigations

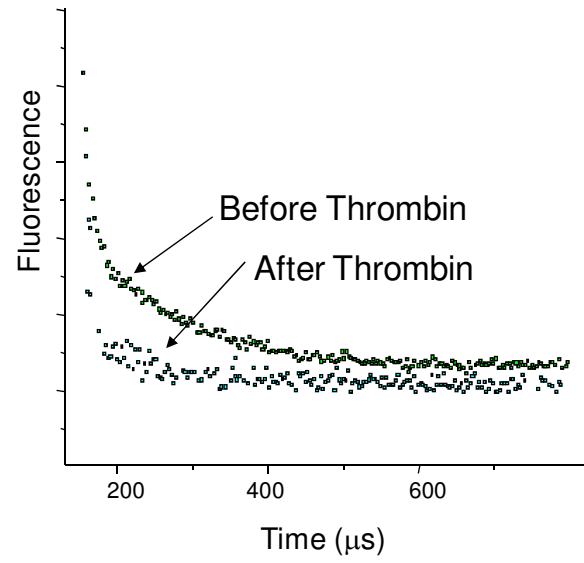
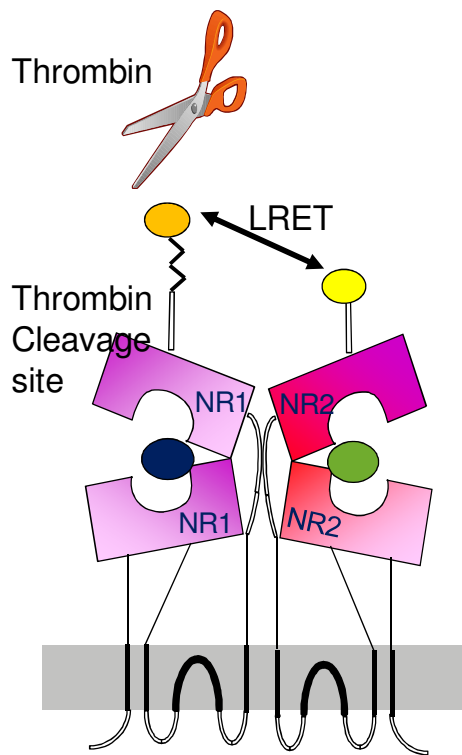


Figure 13 A plot of efficiency of FRET vs distance between fluorophores is shown for a typical donor: acceptor pair. In this case Terbium chelate: Ni-(NTA)₂-Cy3 was used.

This research was originally published in Journal of Biological Chemistry. Rambhadran, A., Gonzalez, J., Jayaraman, V. 2010. Subunit arrangement in N-Methyl-D-aspartate (NMDA) receptors. *Journal of Biological Chemistry* 285(20):15296-301. Copyright the American Society for Biochemistry and Molecular Biology.

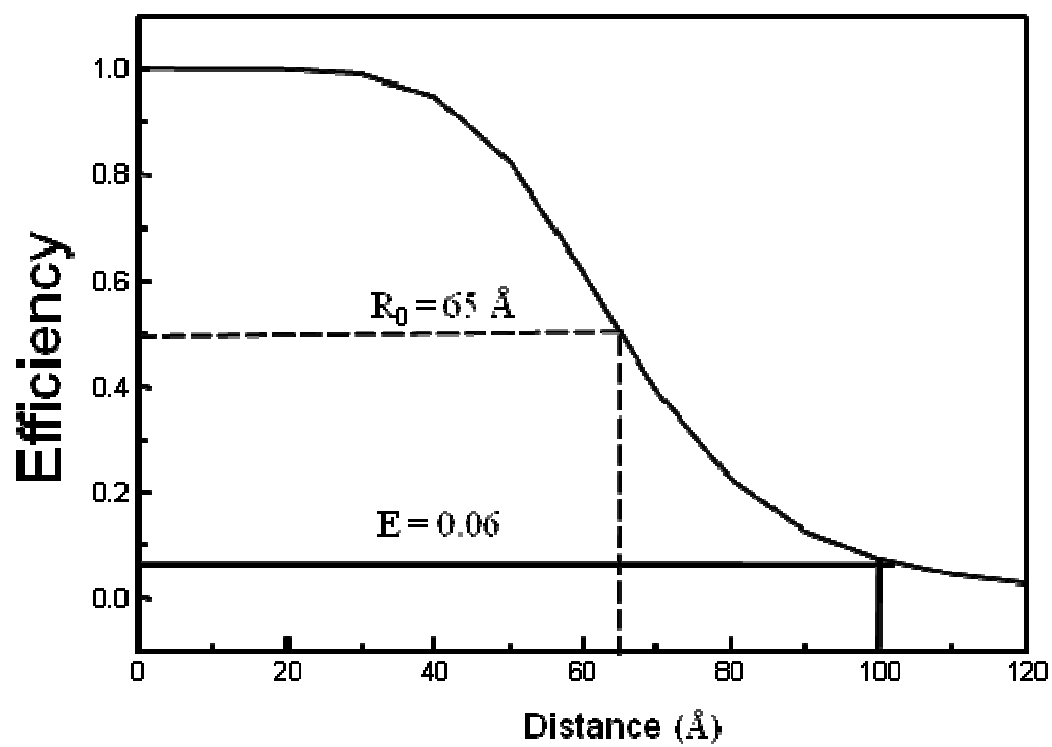
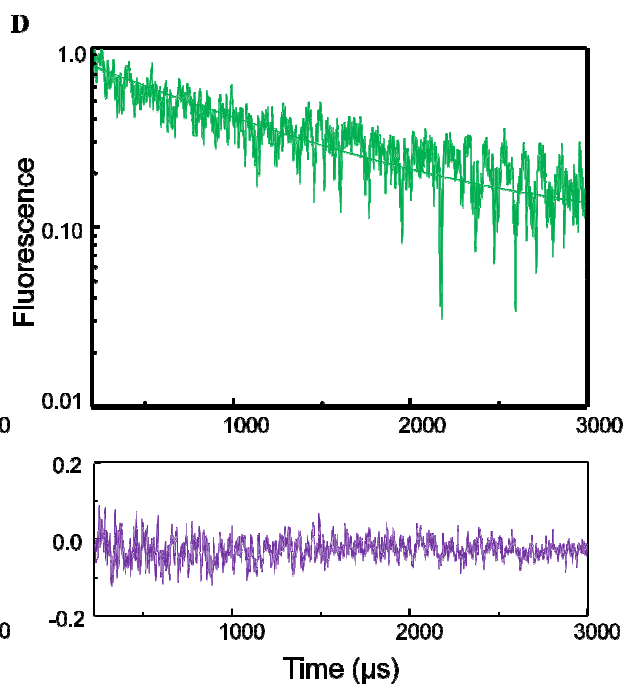
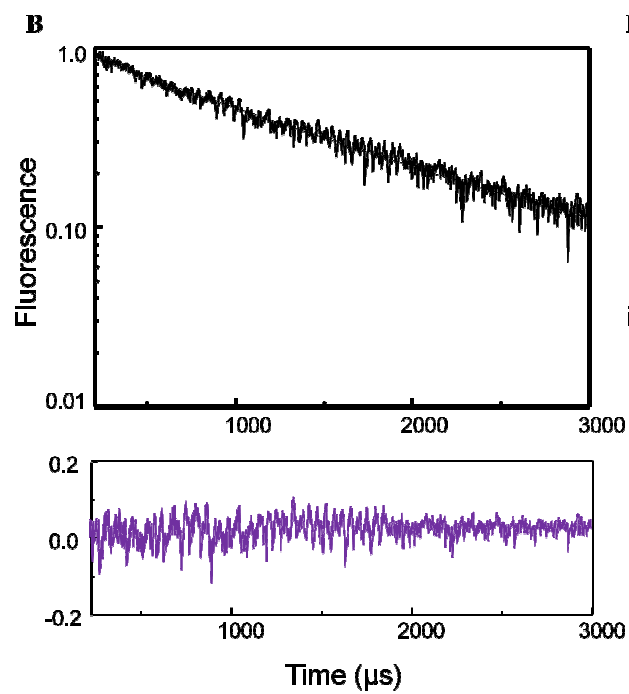
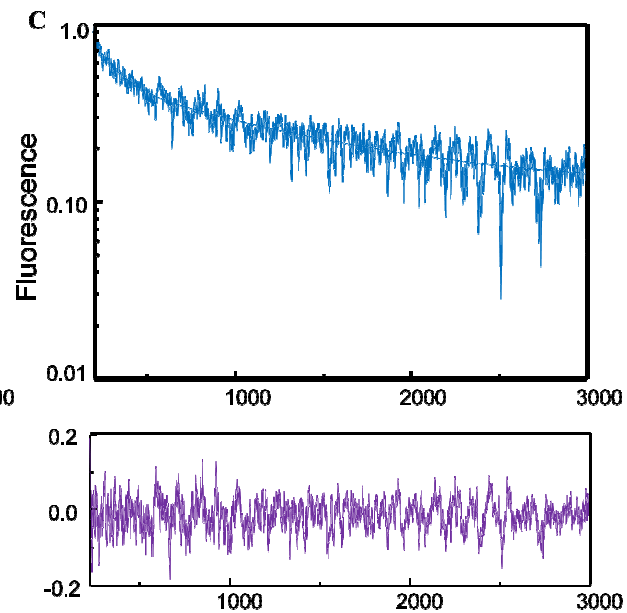
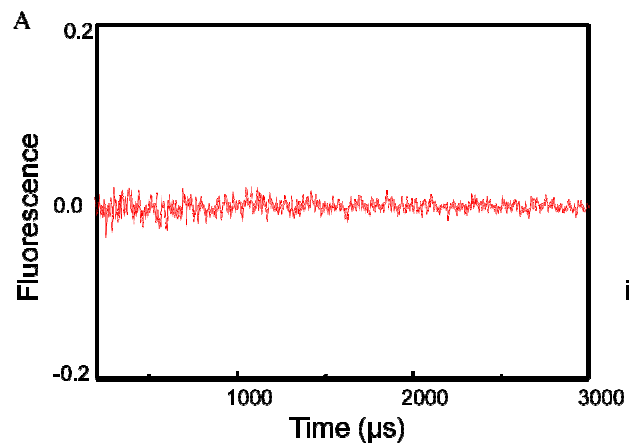


Figure 14 (A) LRET lifetimes for $\Delta NR1^*T396Histag/\Delta NR1^*T396C-Th:\Delta NR2A^*$ labeled with Terbium-chelate:(Ni-NTA)₂Cy3 as measured by the sensitized emission of acceptor at 575 nm in the presence of saturating concentrations of agonists. No LRET signal was observed. (B) LRET lifetimes for $\Delta NR1^*:\Delta NR2A^* N404Histag/\Delta NR2A^* N404C-Th$ labeled with Terbium-chelate:(Ni-NTA)₂Cy3 as measured by the sensitized emission of acceptor at 575 nm with saturating concentrations of agonists. (C) LRET lifetimes measured at 575 nm for $\Delta NR1^*T396Histag:\Delta NR2A^* N404C-Th$ labeled with Terbium chelate:(Ni-NTA)₂Cy3 under saturating concentrations of agonists.(D) LRET lifetimes measured at 515 nm for $\Delta NR1^*Th-Q525C-Th:\Delta NR2A^*$ labeled with Terbium-chelate:Fluorescein at saturating concentrations of agonists. For all mutants, the sensitized lifetime shown is the difference between the lifetimes obtained before and after thrombin digestion. The residuals for the lifetime fits are shown below each measurement with the Y-axis in linear scale.

This research was originally published in Journal of Biological Chemistry. Rambhadran, A., Gonzalez, J., Jayaraman, V. 2010. Subunit arrangement in N-Methyl-D-aspartate (NMDA) receptors. *Journal of Biological Chemistry* 285(20):15296-301. Copyright the American Society for Biochemistry and Molecular Biology.



GluN1 and GluN2A subunits. The LRET based distances obtained for the above mentioned constructs are compared to the distances for equivalent residues on the AMPA receptor full length structure for the three possible configurations in Table 1. The comparison of distances yields a final configuration that best matches Figure 15.

In order to further confirm that the NMDA receptors assembled in the configuration shown in Figure 15, we also measured the distance between residues 525 on one GluN1 subunit with respect to the same residue on the second GluN1 subunit. This particular residue was chosen because the distance changes significantly between the three possible configurations (Table 2) and therefore can be differentiated in the LRET studies. Hence for measuring this distance, Δ GluN1*Th-Q525C-Th: Δ GluN2A* construct was used and labeled with a 1:1 ratio of terbium chelate and fluorescein. The LRET lifetime for this construct could be well represented using a single exponential decay suggesting primarily a single configuration for the NMDA receptor (Figure 14). More importantly, the LRET based distance of 51 Å is closest and similar to the distance of 49 Å seen in the final proposed configuration shown in Figure 10, thus confirming that the NMDA receptors are primarily in the configuration shown in Figure 11 A. The results from the LRET studies are consistent with the crosslinking experiments performed by Eric Gouaux et.al. (Figure 20) where it has been shown that residue E699 on GluN1 subunits cross links with the corresponding residue E699 on the second GluN1 subunit (configuration 8A), however no crosslinking was observed between K641 or R645 and N675/E699 (in GluN1) and K641 or R645 (in GluN2) as would be expected for configurations in Figure 11B and Figure 11C (11) .

Figure 15 Sites that were tagged in the modified Δ NR1* and Δ NR2A* subunit for LRET measurements within the dimer are highlighted in the crystal structure of NR1-NR2A dimer (13).

This research was originally published in Journal of Biological Chemistry. Rambhadran, A., Gonzalez, J., Jayaraman, V. 2010. Subunit arrangement in N-Methyl-D-aspartate (NMDA) receptors. *Journal of Biological Chemistry* 285(20):15296-301. Copyright the American Society for Biochemistry and Molecular Biology.

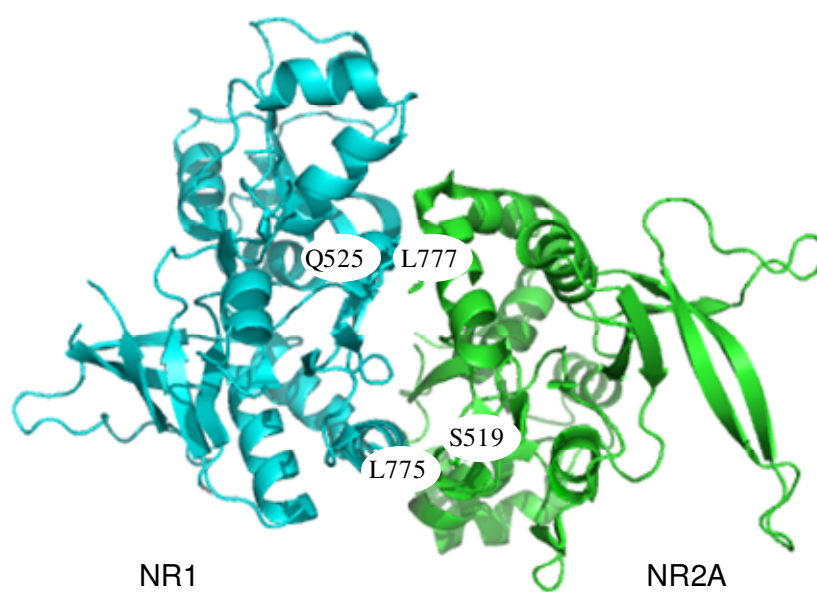


Figure 16 (A) LRET lifetimes for $\Delta\text{NR1}^*775\text{tetrahistag}:\Delta\text{NR2A}^*\text{S519C}$ labeled with Terbium-chelate before (donor) and after addition of Ni^{2+} . (B) LRET lifetimes for $\Delta\text{NR1}^*525\text{tetrahistag}:\Delta\text{NR2A}^*\text{L777C}$ labeled with Terbium-chelate before (donor) and after addition of Ni^{2+} . The residuals for the above lifetime fits are shown below each measurement, and the Y-axis is in linear scale.

This research was originally published in Journal of Biological Chemistry. Rambhadran, A., Gonzalez, J., Jayaraman, V. 2010. Subunit arrangement in N-Methyl-D-aspartate (NMDA) receptors. *Journal of Biological Chemistry* 285(20):15296-301. Copyright the American Society for Biochemistry and Molecular Biology.

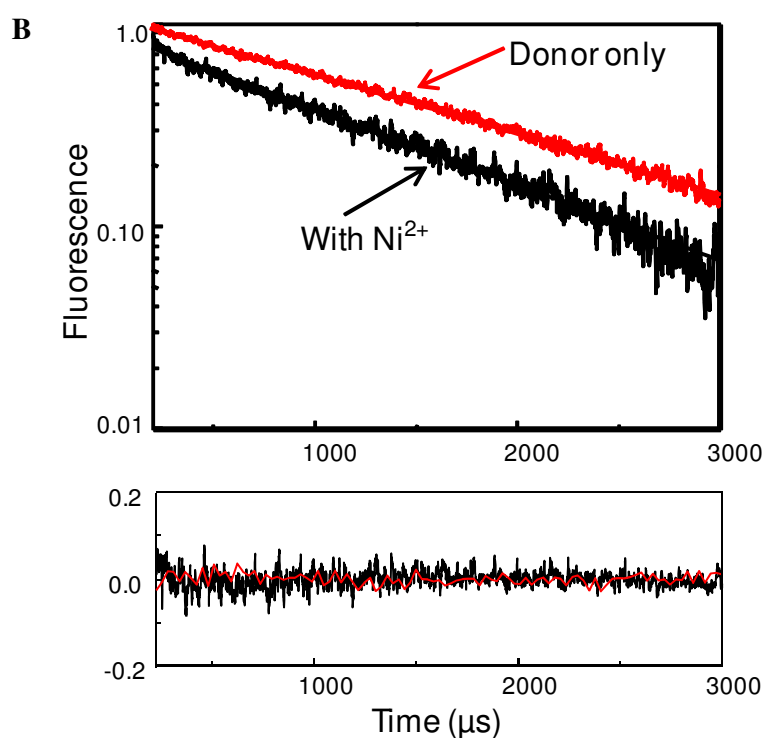
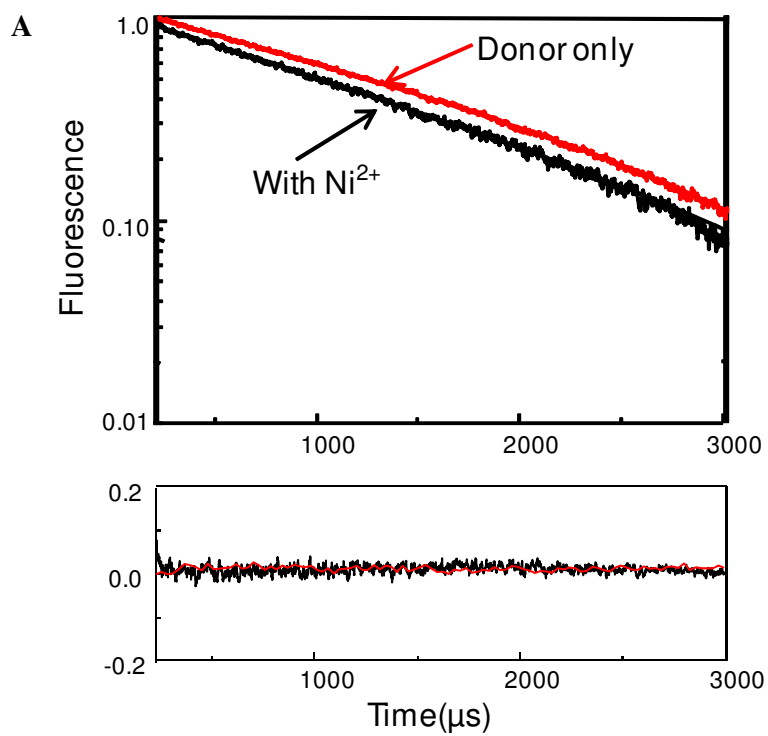


Table 1 The fluorescence lifetimes and distances for Δ NR1*: Δ NR2A* receptors.

This research was originally published in Journal of Biological Chemistry. Rambhadran, A., Gonzalez, J., Jayaraman, V. 2010. Subunit arrangement in N-Methyl-D-aspartate (NMDA) receptors. *Journal of Biological Chemistry* 285(20):15296-301. Copyright the American Society for Biochemistry and Molecular Biology.

Protein	Donor:Acceptor fluorophore pair	Donor lifetime (μ s)	Sensitized emission lifetime (μ s) Apo	Distance (\AA) Apo state	Sensitized emission lifetime (μ s) Desensitized	Distance (\AA) Desensitized state
Δ NR1*T396Histag/ Δ NR1*T396C-Th: Δ NR2A*	Terbium chelate:(Ni- NTA) ₂ Cy3	1900 \pm 1	No LRET	>100	No LRET	>100
Δ NR1*: Δ NR2A*N40 4Histag/ Δ NR2A*N404C-Th	Terbium chelate:(Ni- NTA) ₂ Cy3	1750 \pm 21	634 \pm 41	59.1 \pm 0.8	672 \pm 12	60.1 \pm 0.3
Δ NR1*T396Histag: Δ NR2A* N404C-Th	Terbium chelate:(Ni- NTA) ₂ Cy3	1904 \pm 5	1203 \pm 23/ 304 \pm 14	71.1 \pm 0.5 49.2 \pm 0.4	1254 \pm 36 318 \pm 24	72.5 \pm 0.8 49.7 \pm 0.6
Δ NR1*Th-Q525C- Th: Δ NR2A*	Terbium chelate:Fluoresc ein	1606 \pm 8	1010 \pm 28	49.1 \pm 0.5	1089 \pm 12	51 \pm 0.3
Δ NR1*525tetrahista g: Δ NR2A*L777C	Terbium chelate:Ni ²⁺	1754 \pm 5	1088 \pm 8	13.0 \pm 0.0 5	1155 \pm 42	13.3 \pm 0.2
Δ NR1*775tetrahista g: Δ NR2A*S519C	Terbium chelate: Ni ²⁺	1681 \pm 10	1290 \pm 61	14.6 \pm 0.4	1330 \pm 50	14.9 \pm 0.4
Δ NR1*T396C-Th, A715C: Δ NR2A*	Terbium chelate:ATTO46 5	1704 \pm 18	734 \pm 33	34.4 \pm 0.3	790 \pm 16	35.1 \pm 0.2

III. Mechanism of desensitization of NMDA receptor based on distance within the dimer interface

It is hypothesized that when a ligand like glutamate binds to the extracellular ABD, it causes the cleft to close, which in turn pulls apart the transmembrane segments causing the channel to open. Upon prolonged exposure to the ligand, the receptor eventually desensitizes; the channel closes owing to the stress on the transmembrane segments caused by the decoupling of the dimer interface (48). This hypothesis for desensitization is based on previous structural data obtained from the isolated ABD crystal structures of AMPA receptors that showed cyclothiazide, an allosteric modulator, and mutations in the dimer interface, like L483Y, that stabilize the dimer interface block desensitization (48). However, currently there is no structural information regarding the mechanism of desensitization of NMDA receptors. Here, we have used LRET distances of residues within the GluN1-GluN2A dimer interface to extrapolate the mechanism of desensitization of NMDA receptors.

Two sets of residues expected to be in close proximity in the dimer interface based on the X-ray structures of GluN1-GluN2A dimer were chosen for the LRET studies: The first set was residues 525 on GluN1 and 777 on GluN2A and the second pair was residues, 775 on GluN1 and 519 on GluN2A (Figure 15). In order to precisely measure the distance within the dimer and not across the dimer a cysteine mutation was introduced on one subunit while a tetrahistidine tag (HHHH) was introduced on the second subunit. Maleimide derivatives of terbium chelate served as the donor and Ni^{2+} ion (R_0 is 12 Å) acted as the acceptor. The short R_0 of 12 Å ensured that distances only within the dimer were measured and there was no transfer from the residues across the

dimer interface. In addition, the short R_0 also ensures that the non-specific labeling of cysteine residues far from the histidine tag does not contribute towards the LRET signal being measured. Therefore when short distances were measured it obviated the need to introduce a thrombin cleavage site to account for background signal. The LRET lifetimes for $\Delta\text{GluN1}^*525\text{tetrahistag}$: $\Delta\text{GluN2A}^*\text{L777C}$ and $\Delta\text{GluN1}^*775\text{tetrahistag}$: $\Delta\text{GluN2A}^*\text{S519C}$ (Figure 17) could be well represented by a single exponential fit and the respective distances are shown in Table2 and compared to the distances from the crystal structure. Saturating concentrations of the ligands glutamate and glycine were employed to make sure that the distances obtained primarily represent the desensitized state of the receptor. While the crystal structures of the isolated ABD of the GluN1-GluN2A dimer lack the transmembrane portion, the functional component of the receptor that drives the formation of the desensitized state and therefore most likely represents the structure of the dimer in the open channel form of the protein and not the desensitized form (13). The longer LRET distances in the desensitized state of the NMDA receptor relative to the distances expected for the open channel form suggests that there is a decoupling of the dimer interface in the desensitized state of the receptor. In order to confirm the accuracy of such a direct comparison of LRET distances to X-ray structures, we measured the distance within a given subunit of the receptor. For this purpose, $\Delta\text{GluN1}^*\text{T396C-Th, A715C}$: ΔGluN2A^* was used; this construct allowed us to measure the distance between residues 396 and 715 within GluN1 subunit. This construct was labeled with terbium chelate and ATTO 465 as donor and acceptor, respectively, for LRET measurements. A single exponential decay well represented the LRET lifetime and corresponded to a distance of 35.1 Å. This measurement was very

Table 2 Comparison of distances between desensitized state LRET measurements to antagonist bound crystal structure of AMPA receptor with other possible configurations.

This research was originally published in Journal of Biological Chemistry. Rambhadran, A., Gonzalez, J., Jayaraman, V. 2010. Subunit arrangement in N-Methyl-D-aspartate (NMDA) receptors. *Journal of Biological Chemistry* 285(20):15296-301. Copyright the American Society for Biochemistry and Molecular Biology.

NMDA/Homologous AMPA receptor	Distance based on LRET (Å)	AMPA receptor (PDB-3KG2)		
		Distance based on configuration A (Figure1) (Å)	Distance based on configuration B(Figure1) (Å)	Distance based on configuration C(Figure1) (Å)
NR1-396 to NR2A-404/ AMPA-393 to AMPA-393	72.5	67	67	56,102
NR1-396 to NR1-396/ AMPA-393 to AMPA-393	>100	101	56	72
NR2A-404 to NR2A-404/ AMPA-393 to AMPA-393	60	56	102	67
NR1-525 to NR1-525/ AMPA-487 to AMPA-487	51	49	82	65

similar to the observed distance of 34.3 Å in the crystal structure (Figure 17) of GluN1 subunit (14). This particular pair of residues was chosen keeping in mind that the efficiency of transfer from the second GluN1 subunit is expected to be only 0.2% for transfer between residues 396 and 396 while for transfer between residues 715-715 the transfer efficiency is 3.3% when terbium chelate and ATTO 465 are used as donor and acceptor, respectively. Therefore, these mutations do not interfere and contribute to the measured LRET signal, thus allowing us to selectively measure distance within a given subunit of GluN1. Table 3 shows a comparison of distances between the desensitized LRET measurements to the changes in distances observed for homologous residues in the desensitized like crystal structure of S729C mutant and the cyclothiazide (CTZ) bound open channel structure of the AMPA receptor (48). The distance changes between the desensitized and open channel form across the dimer for the NMDA receptors are found to be similar to AMPA receptors. This observation confirms that the dimer interface in the NMDA receptors is decoupled and provides evidence for the first time that the mechanism for desensitization in the NMDA receptors is similar to that observed in the AMPA receptors (48).

IV. Results and Discussion

Using the LRET distances determined as described above between GluN1, GluN2A and between GluN1 and GluN2A subunits, we have established the specific unique configuration in which the NMDA receptor subunits assemble to form the functional tetramer. The results show that the dimer of dimers structure is formed with the GluN1 subunits assembling diagonal to each other. The measured LRET distances are consistent with the NMDA structure predicted by Eric Gouaux based on crosslinking

Table 3 Comparison of changes in distances between desensitized and open channel states of NMDA and AMPA receptors.

This research was originally published in Journal of Biological Chemistry. Rambhadran, A., Gonzalez, J., Jayaraman, V. 2010. Subunit arrangement in N-Methyl-D-aspartate (NMDA) receptors. *Journal of Biological Chemistry* 285(20):15296-301. Copyright the American Society for Biochemistry and Molecular Biology.

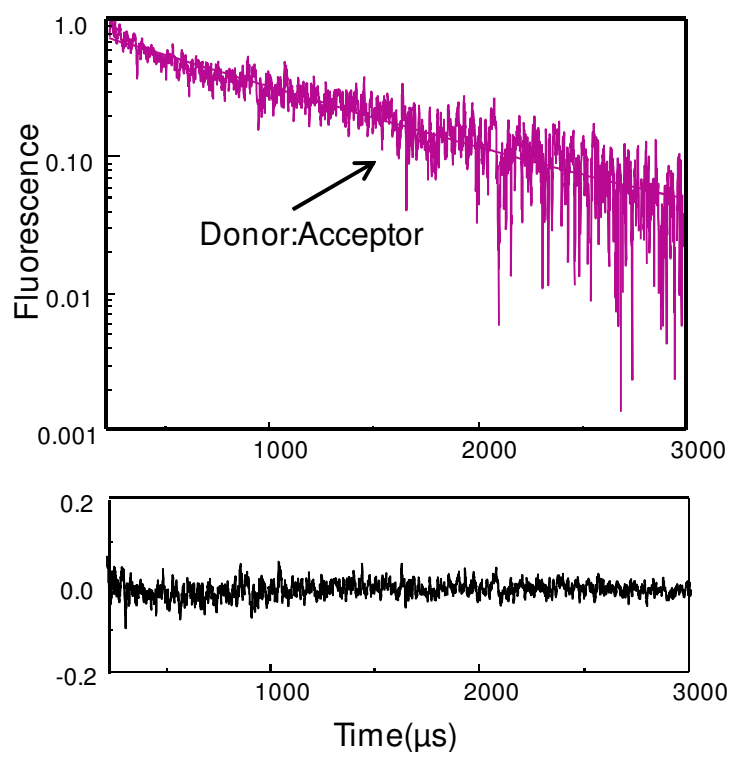
	NMDA receptor				AMPA receptor		
Protein	Distance based on LRET (Å) (A)	Distance in X-ray structure (Å) (B) (PDB-2A5T)	Difference between A and B (Å)	Protein	Distance in X-ray structure (Å) (C) (PDB-2I3W)	Distance in X-ray structure (Å) (D) (PDB-1LBC)	Difference between C and D (Å)
	Desensitized	Open			Desensitized	Open	
NR1-396 to NR2A-404	49.7	41.5	8.2	GluR2-393 to GluR2-393	54	46	8
NR1-525 to NR2A-777	13.3	7	6.3	GluR2-487 to GluR2-748	17	9	8
NR1-775 to NR2A-519	14.9	7	7.9	GluR2-484 to GluR2-748	17	8	9
NR1-396 to NR1-715	35.1	34.3	0.8	GluR2-393 to GluR2-687	35.2	34.5	0.70

experiments and also based on the structure of the AMPA receptor (GluA2) full length structure. In addition, the LRET distances measured between GluN1 and distances observed are in line with the decoupling of the dimer interface, resembling the desensitized state of the receptor. Since the isolated ABD crystallizes in the open channel state of the receptor, the longer LRET lifetime previously reported for the AMPA subtype of the glutamate receptors suggest that the mechanism for desensitization in the two subtypes of the glutamate receptor are very similar.

a. Receptor characterization by electrophysiology The modified NMDA receptor mutant proteins were expressed by injecting *Xenopus* oocytes with RNA encoding the respective modified GluN1:GluN2A subunits in a 1:2 ratio. Upon injection, the oocytes were incubated at 12 °C to allow them to recover from injection and also to minimize surface expression of the receptor. After 2 days, the oocytes are pre-blocked with β -maleimidopropionic acid for one hour at 18°C to block inherent cysteines from reacting non- specifically to the maleimide fluorophores used for LRET studies. This pre-blocking procedure was initially established in the potassium channels where blocking inherent cysteines of the oocyte increased the specificity of labeling of the receptor. The blocked oocytes continued at 18 °C for 24 hours to allow expression of the receptor. After 24 hours, the oocytes are labeled with maliemide derivatives of respective fluorophores for one hour. The excess unreacted fluorophore is then washed away with buffer. The fluorophore pairs are chosen based on the distances to be measured and the R_0 of the fluorophores. A sample for a pair with an R_0 value of 65 Å is shown in (Figure 13).

Figure 17 LRET lifetimes for Δ NR1*T396C-Th, A715C: Δ NR2A*labeled with Terbium-chelate : ATTO 465 as measured by the sensitized emission of acceptor at 510 nm under saturating concentrations of agonists. The donor: acceptor lifetime shown here is the difference between the lifetimes obtained before and after thrombin digestion. The residuals are shown below the lifetime measurement, and the Y-axis is in linear scale.

This research was originally published in Journal of Biological Chemistry. Rambhadran, A., Gonzalez, J., Jayaraman, V. 2010. Subunit arrangement in N-Methyl-D-aspartate (NMDA) receptors. *Journal of Biological Chemistry* 285(20):15296-301. Copyright the American Society for Biochemistry and Molecular Biology.



R_0 value for the following donor: acceptor pairs –Terbium: Ni -(NTA)₂-Cy3 chelate is 65 Å, Terbium chelate: Fluorescein is 45 Å, Terbium chelate:ATTO465 is 36 Å and Terbium chelate:Ni²⁺ is 12 Å. The labeled oocytes are then used for electrophysiological recordings, while for the LRET studies membrane preparations of the oocytes are used. Typically, the oocytes are lysed and solubilized in detergent like Triton X-100 (see Appendix for protocol on Membrane Preparation. (Ni-NTA)₂Cy3, is added to the membrane preparations for LRET investigations at a final concentration of 1 μM when it is used as acceptor fluorophore.

Two methodologies were used to establish the functionality of the modified NMDA receptor used for LRET studies: two-electrode voltage clamp (TEVC) and single channel measurements. Membrane fractions from oocytes expressing the modified receptor were used for the single channel recordings. These experiments were done in collaboration with Dr. Vishnu Suppiramani at Auburn University. The Po (open channel probability) for the wild type receptor was similar to the modified NMDA receptor establishing that the modifications made to the receptor did not affect channel functioning (Figure 18). For the TEVC measurements each of the modified receptors used for LRET studies to establish the configuration of the NMDA receptor was used in order to record the currents elicited and a dose response was created and compared to the typical wild type response. Currents were recorded using various concentrations of glutamate as agonist with saturating concentrations of glycine (100 μM). Peak currents were recorded and normalized to currents collected with 100 μM glutamate. The dose response curves for the mutants and wild type are shown in Figure 19. These results indicate that the mutations

Figure 18 Single channel recordings from bilayers of membrane preps of modified NMDA receptors. (Shown here is the N-Terminal deleted NMDA receptor). Single channel currents of expressed modified NMDA receptors were evoked with glutamate (2 μ M) and glycine (1 μ M) using the tip-dip bilayer method. (A) Sample trace showing upward current fluctuations voltage clamped at +60 mV. (B) Amplitude histogram with an open channel probability of 0.23 and a primary single channel conductance of ~ 25 pS. Calibration 1.5 pA, 100 ms. These results suggest that the membrane preparations used for the LRET investigations have functional NMDA receptors and the manipulations for the LRET data collection do not have a significant effect on the receptor function.

open

close

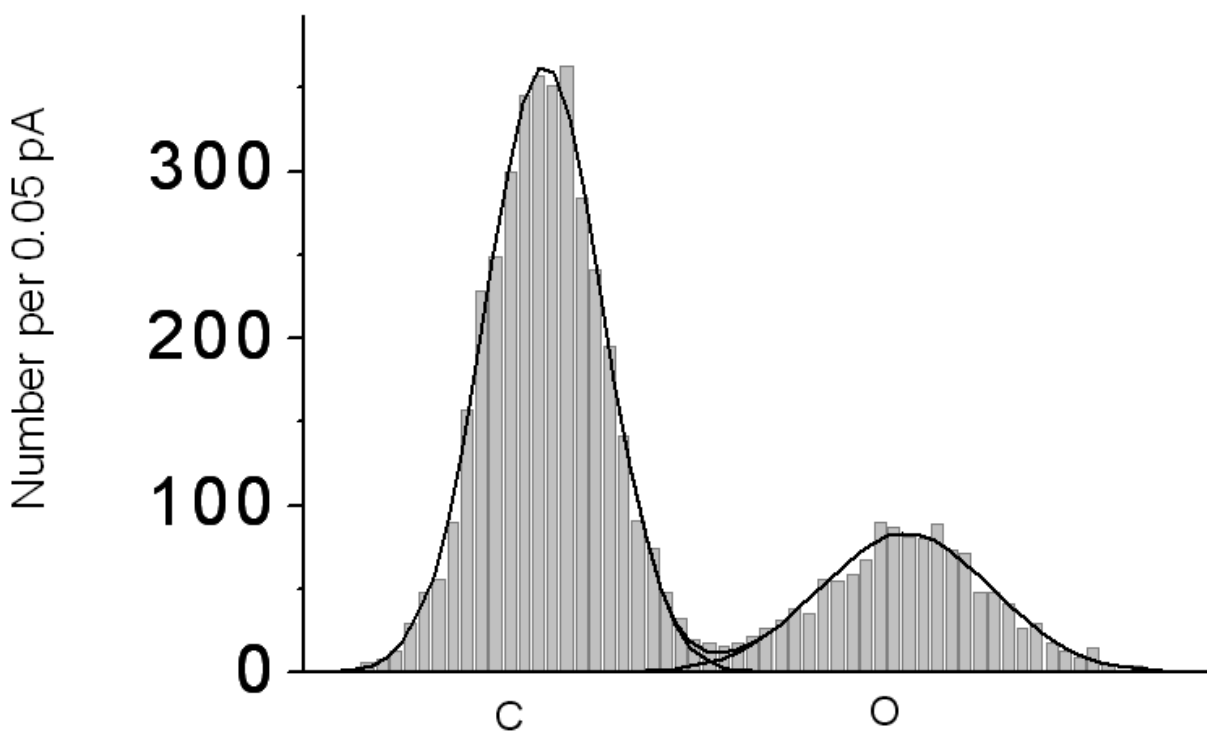
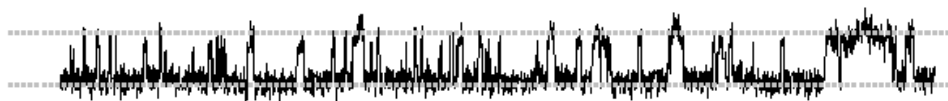
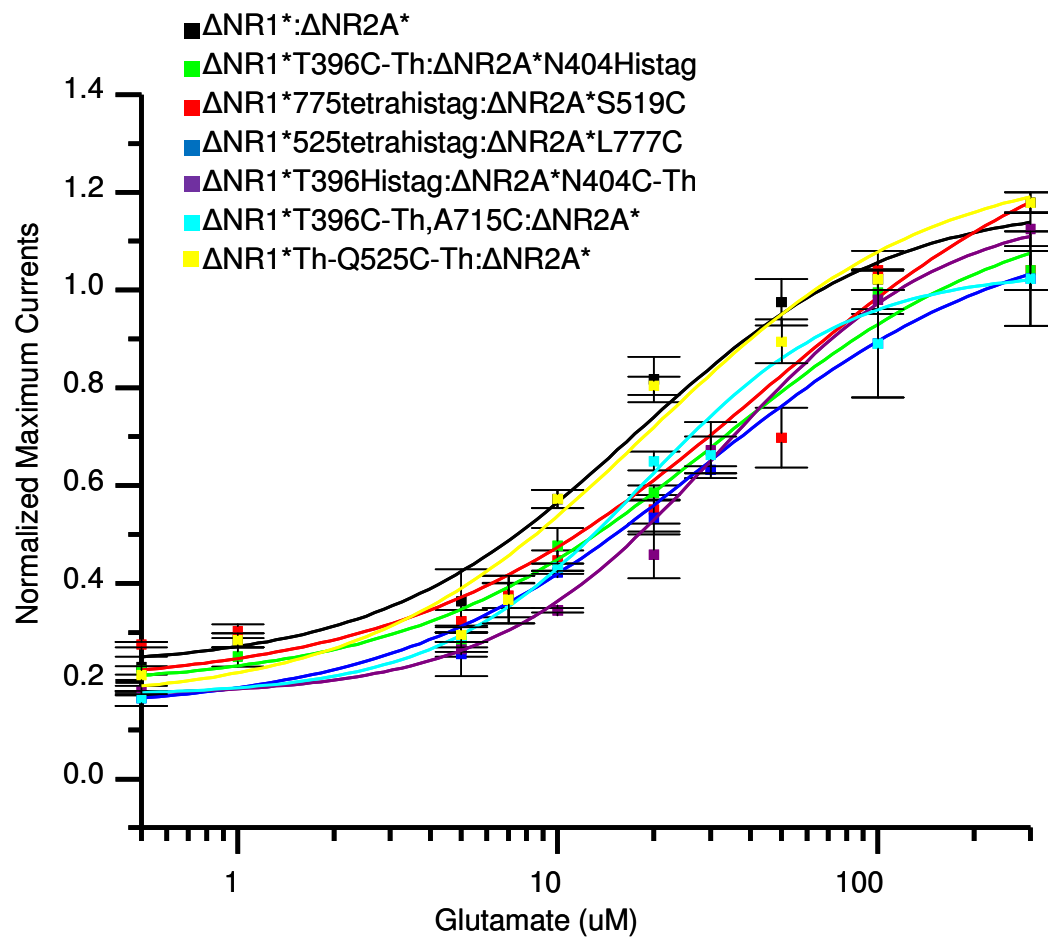


Figure 19 Dose response curves showing maximum current as a function of glutamate concentration for the Δ NR1*: Δ NR2* and mutant NMDA receptors labeled with donor:acceptor fluorescent tags using two electrode voltage clamp measurements. All currents were recorded in the presence of saturating concentrations of glycine (100 μ M). Currents were normalized to reading taken with 100 μ M glutamate.

This research was originally published in Journal of Biological Chemistry. Rambhadran, A., Gonzalez, J., Jayaraman, V. 2010. Subunit arrangement in N-Methyl-D-aspartate (NMDA) receptors. *Journal of Biological Chemistry* 285(20):15296-301. Copyright the American Society for Biochemistry and Molecular Biology.



and fluorophores introduced for the LRET investigation do not perturb the functionality of the receptor.

b. Validation of the results based on comparison to full length AMPA structure and cross linking investigations

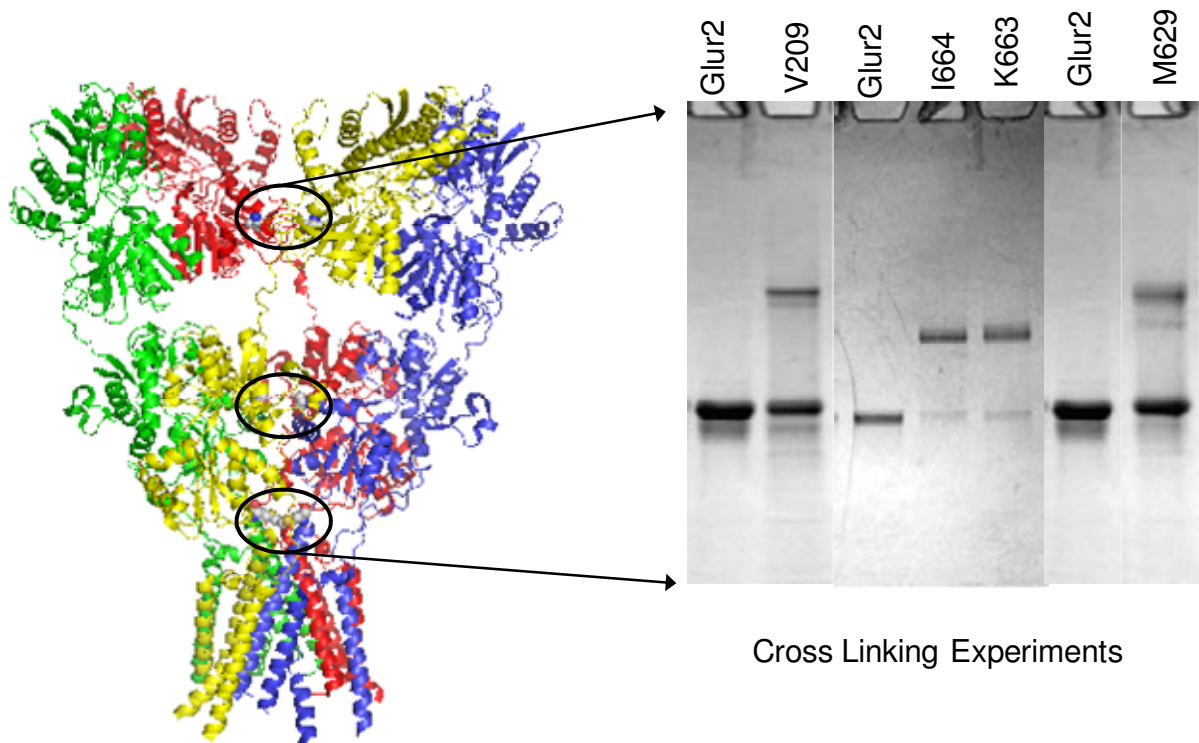
The LRET based configuration obtained was similar to the specific tetrameric arrangement predicted for the ABD of GluN1-GluN2A using cysteine cross- linking studies. Specifically it was shown that residues N 675 and E699 of GluN1 subunits spontaneously formed disulphide bonds when mutated to cysteines (Figure 20) (11). This finding along with the structure of the full length GluA2 subunit of AMPA receptor is in close agreement with the arrangement proposed by using LRET studies.

V. Future Experiments

While the configuration of the NMDA receptor subunits at the level of ABD has been established, the arrangement with respect to the ATD is yet to be determined. Determination of this arrangement is critical especially for the NMDA subtype since this domain has been shown to modulate the properties of the channel. The current hypothesis based on biochemical and functional investigations is that allosteric inhibitors such as Zn^{2+} and ifenprodil mediate their inhibitory mechanism by inducing a cleft closure conformational change upon binding to the N-terminal domain (40, 42). Currently, there is just two crystal structures of the ATD of GluN2B subunit, one in complex with Zn^{2+} and of the other of GluN1-GluN2B dimer (40, 42). Hence establishing the configuration of the full length receptor (including the ATD) using LRET will help in elucidating the mechanism of modulation of the NMDA receptors. Also, this study will

further confirm the validity of the arrangement established by LRET in the full length receptor.

Figure 20 The full length GluA2 subunit crystal structure along with sites that were chosen for cross linking studies is highlighted. Adapted from Sobolevsky, A.I. et.al., 2009 (11).



Chapter 5 — Part II: Probing the conformational changes in the agonist binding domain that controls receptor activation in NMDA (N- Methyl- D- Aspartate) receptors

This research was originally published in Journal of Biological Chemistry. Rambhadran, A., Gonzalez, J., Jayaraman, V. 2011. Conformational changes in the agonist binding domain of NMDA receptors. *Journal of Biological Chemistry* 286(19):16953-7. Copyright the American Society for Biochemistry and Molecular Biology.

I. Testing the activation hypothesis

The structures of the ABD of the GluN1 subunit bound to full agonist glycine and partial agonists such as D-cycloserine, and ACPC showed no significant differences in the extent of cleft closure (13, 14). Based on these structures it has been hypothesized that the NMDA receptors could follow a two state model, where the cleft exists in either an open or closed form. Activation of the channel could be due to a shift in the equilibrium between these two states. However, this conclusion has not been tested and is based only on a limited number of structures. Additionally, if there is a shift in the equilibrium then at least some of the partial agonist bound structures should be in an open state. But this trend is not observed in any of the structures solved for the various partial agonists. Additionally, to draw comparisons between the different subtypes of the glutamate receptor, it is important to compare subunits that bind glutamate and not the glycine (inherently different from glutamate) binding site of the GluN1 subunit to glutamate binding sites of the AMPA receptors. At present there is only one structure available for the isolated ABD of the GluN2A subunit bound to glutamate (13). Therefore, it is still not known if the GluN2 subunit exhibits a graded cleft closure as seen for the AMPA and kainate subtypes (69-71). The hypothesis is that in the tetrameric form of the receptor, the GluN2 subunit that binds the glutamate would behave in a similar manner to the other glutamate binding subunits of the other subtypes of receptor with the extent of cleft closure being the primary mechanism by which the agonist mediates channel activation (70). In this chapter, I present the use of LRET is used to measure the amount of cleft closure both in the GluN1 and GluN2A subunits of NMDA receptor using agonist of varying efficacies.

II. LRET to measure the extent of cleft closure at the ABD of GluN2A subunit of the NMDA receptor

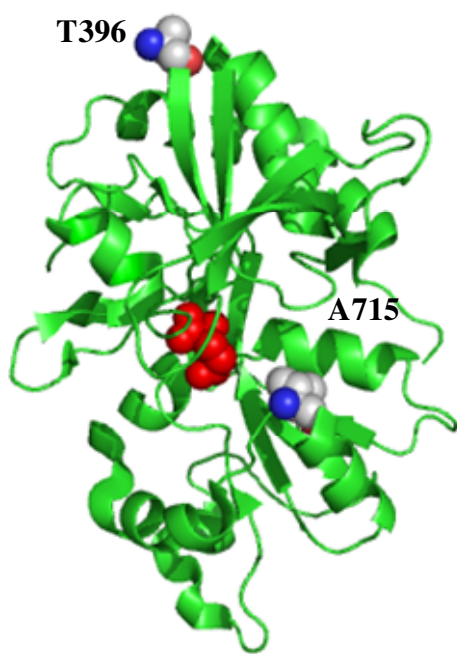
In order to study the conformational changes at the ABD of GluN2A subunit, wide range of activations with different agonists was employed and the LRET based cleft closure conformational changes were correlated to the differences in efficacies of the agonists using TEVC recordings.

For the LRET experiments, cysteine mutations were introduced at residue 404 located at the N-terminus in domain 1 and residue 713 present in domain 2 of the ABD of GluN2A (Figure 21). This pair of residues was chosen based on the previously established subunit arrangement of the NMDA receptors such that a direct read out of cleft closure within the dimer can be obtained and measurement of distances across the dimer was avoided (72). Since maleimide derivative of fluorophores were employed, background LRET signal was minimized by introducing a Thrombin (Th) cleavage site adjacent to the cysteine at position 404(N404C-Th). Thus, the LRET specific to the GluN2A subunit was obtained upon cleavage with thrombin which selectively cleaves the donor or acceptor fluorophore labeled at that site (62). The LRET lifetime recorded after thrombin digestion represents the background non-specific signal, this lifetime was later subtracted from the original LRET signal to get the final specific LRET signal for the GluN2A*N404C-Th, V713C mutant (Figure 23).

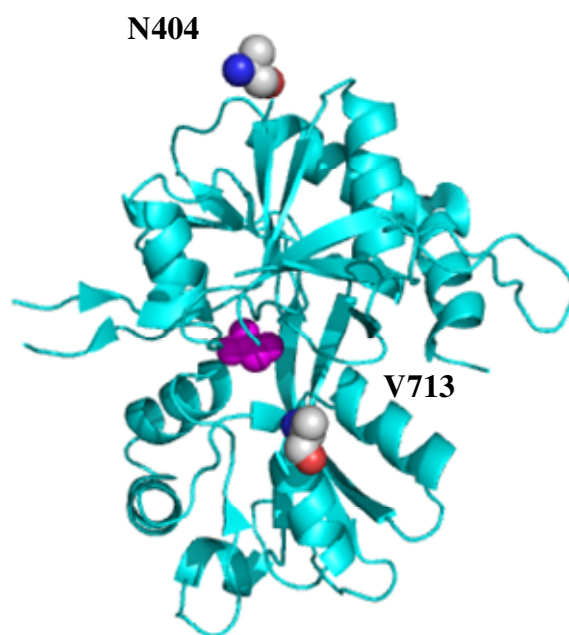
Maleimide derivatives of Terbium chelate and Fluorescein served as donor and acceptor fluorophores respectively, for the LRET experiments. Distances were recorded between residues 404 and 713 under no ligand (apo), antagonist (DLAPV), partial agonist (Homoquinolinic acid, HQ), and full agonist (Glutamate) bound state for

Figure 21 Sites that were tagged in the GluN1* and GluN2A* subunit to probe for cleft closure conformational changes using LRET measurements are highlighted in the crystal structure of the ABD of GluN1 bound to glycine and GluN2A bound to glutamate(12-14) .

This research was originally published in Journal of Biological Chemistry. Rambhadran, A., Gonzalez, J., Jayaraman, V. 2011. Conformational changes in the agonist binding domain of NMDA receptors. *Journal of Biological Chemistry* 286(19):16953-7. Copyright the American Society for Biochemistry and Molecular Biology.



GluN1 ABD



GluN2A sites ABD

Figure 22 Dose response curves showing maximum current as a function of glutamate concentration for the GluN1*: GluN2A* and mutant NMDA receptors labeled with donor:acceptor fluorescent tag using two electrode voltage clamp measurements. All currents were recorded in the presence of saturating concentrations of glycine (100 μ M). Currents were normalized to reading taken with 1mM glutamate.

This research was originally published in Journal of Biological Chemistry. Rambhadran, A., Gonzalez, J., Jayaraman, V. 2011. Conformational changes in the agonist binding domain of NMDA receptors. *Journal of Biological Chemistry* 286(19):16953-7. Copyright the American Society for Biochemistry and Molecular Biology.

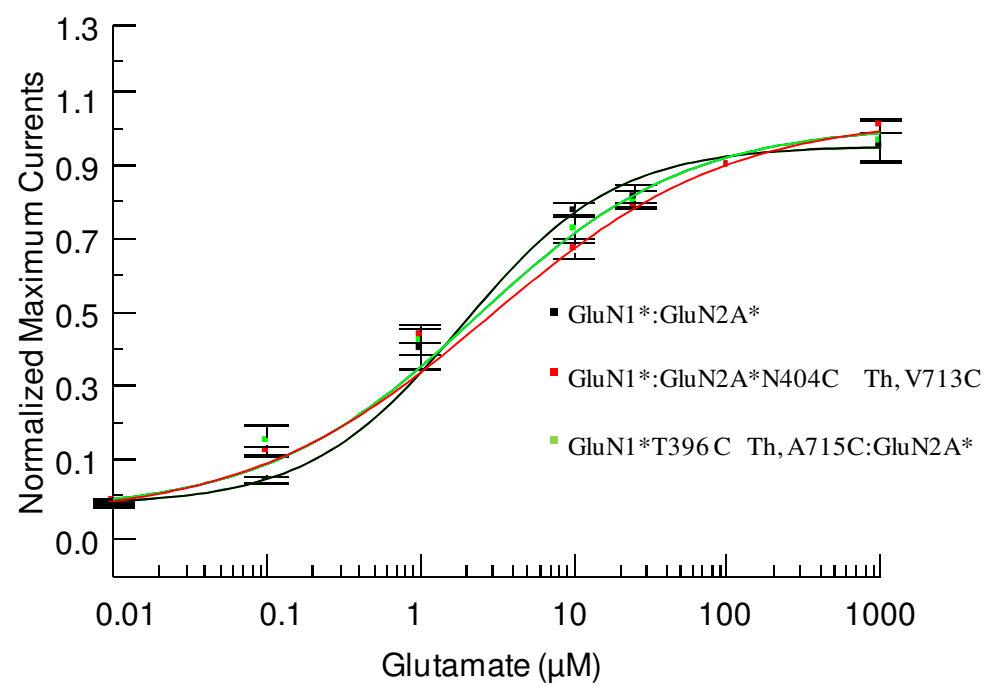
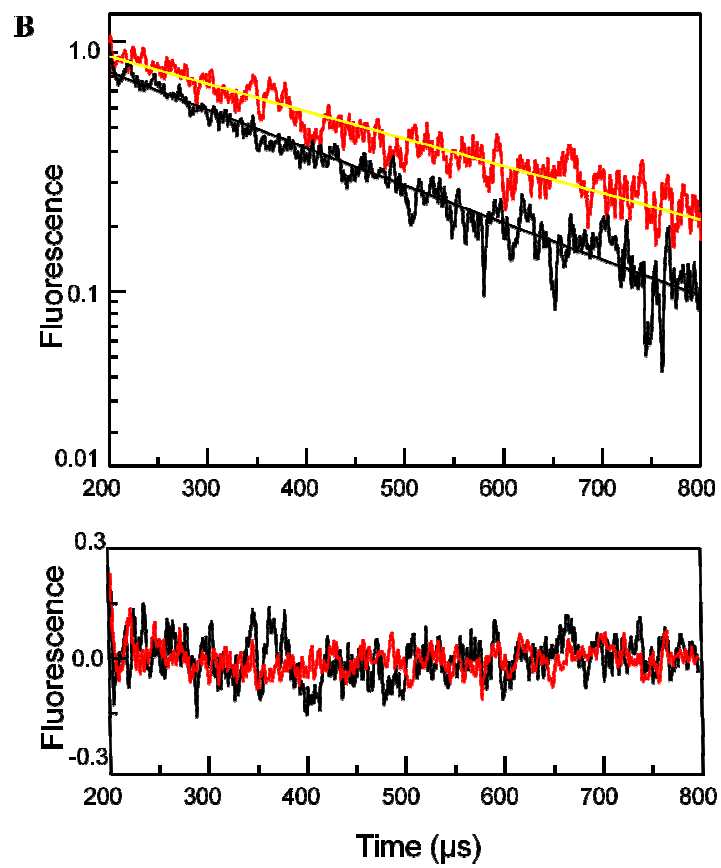
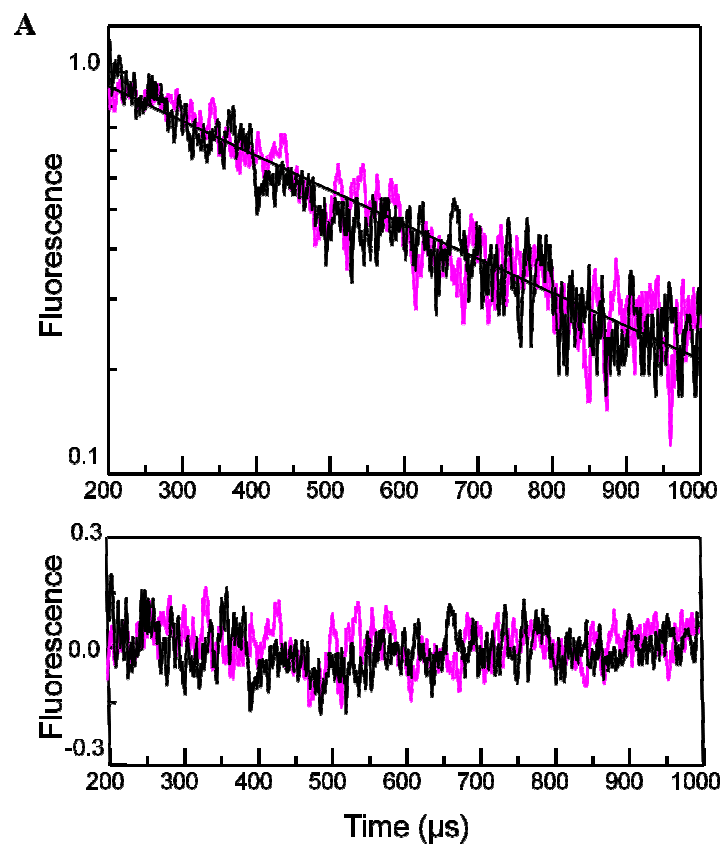


Figure 23 Cleft closure in the ABD of GluN2A* subunit: (A) Apo (black) and Antagonist (DLAPV in magenta) bound LRET lifetimes for GluN1*:GluN2A*N404C-Th, V713C labeled with Terbium chelate: Fluorescein as measured by the sensitized emission of acceptor at 515 nm. The residuals for the above lifetime fits are shown below each measurement, and the Y-axis is in linear scale.

(B) LRET lifetimes for GluN1*: GluN2A*N404C-Th, V713C labeled with Terbium chelate: Fluorescein as measured by the sensitized emission of acceptor at 515 nm under saturating concentrations of full agonist (Glutamate in black) and partial agonist (HQ in red). The residuals for the above lifetime fits are shown below each measurement the Y-axis in linear scale.

This research was originally published in Journal of Biological Chemistry. Rambhadran, A., Gonzalez, J., Jayaraman, V. 2011. Conformational changes in the agonist binding domain of NMDA receptors. *Journal of Biological Chemistry* 286(19):16953-7. Copyright the American Society for Biochemistry and Molecular Biology.



the GluN2A subunit. In all conditions saturating concentrations of agonists were used. The concentration of the agonists used was determined based on the dose response curves created using different concentrations of the agonists. Shown is a typical dose response curve using glutamate as an agonist (Figure 22), while for other agonists, data from previous literature was used. The final specific LRET lifetimes obtained upon subtracting the non – specific background thrombin digested lifetime could be well represented by single lifetime decay for all the ligands. The lifetimes and the corresponding distances are given in Table 4.

III. LRET to measure the extent of cleft closure at the ABD of GluN1 subunit of the NMDA receptor

To fully understand the conformational changes accompanying agonist binding to NMDA receptors it is critical that changes associated with the glycine binding GluN1 subunit of NMDA receptors also be examined. The crystal structures of GluN1 ABD with agonists of different efficacies have been solved and they indicate that there are no changes in the amount of cleft closure between agonists of varying activation (12, 14). It is still unclear whether this lack of correlation between extent of cleft closure and activation is due to crystallographic limitations and the absence of the functional transmembrane component of the receptor. Hence, to resolve this enigma, an LRET based approach similar to the kind described in the previous section for GluN2A receptors was used. Conformational changes at the ABD of the GluN1 subunit were measured using agonists of varying activations in the full length NMDA receptor. For these experiments, residues 396 at the N-terminus in domain 1 and 715 present in domain 2 of GluN1 subunit were chosen to give a direct cleft closure read out.

Figure 24 Cleft closure in the ABD of GluN1* subunit: LRET lifetimes for GluN1*T396 C-Th, A715C: GluN2A* labeled with Terbium chelate: ATTO 465 as measured by the sensitized emission of acceptor at 510 nm under saturating concentrations of full agonist (Glycine in black) and partial agonists (DCS in green, ACPC in red). The residuals for the above lifetime fits are shown below each measurement, and the Y-axis is in linear scale.

This research was originally published in Journal of Biological Chemistry. Rambhadran, A., Gonzalez, J., Jayaraman, V. 2011. Conformational changes in the agonist binding domain of NMDA receptors. *Journal of Biological Chemistry* 286(19):16953-7. Copyright the American Society for Biochemistry and Molecular Biology.

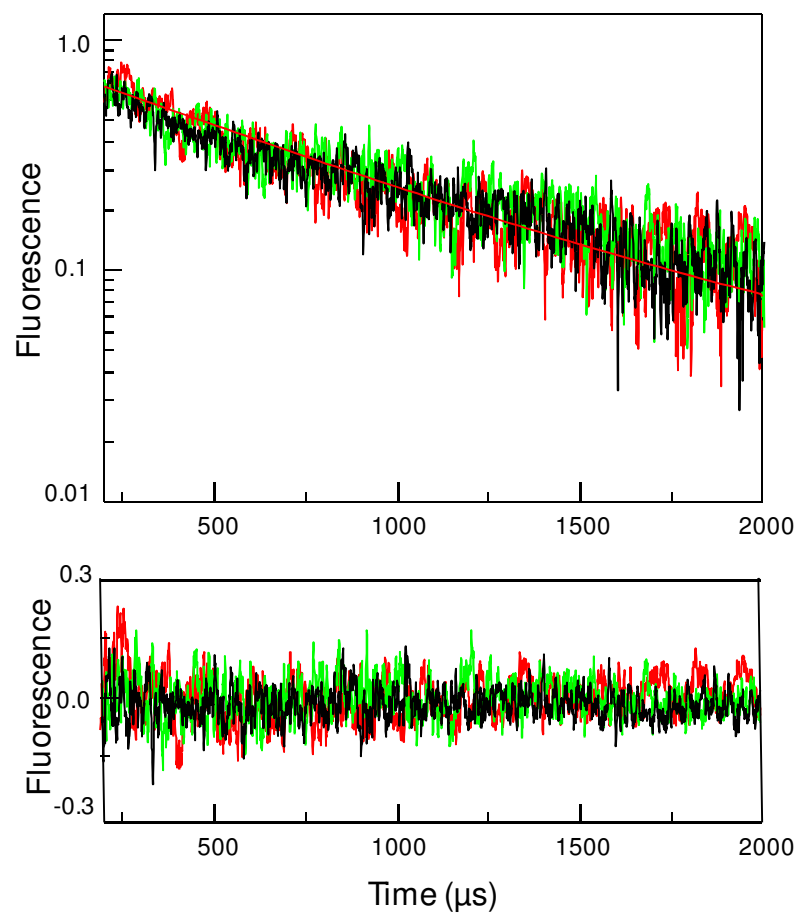


Table 4 The Fluorescence Lifetimes and Distances for GluN1*:GluN2A* Receptors.

This research was originally published in Journal of Biological Chemistry. Rambhadran, A., Gonzalez, J., Jayaraman, V. 2011. Conformational changes in the agonist binding domain of NMDA receptors. *Journal of Biological Chemistry* 286(19):16953-7. Copyright the American Society for Biochemistry and Molecular Biology.

Protein	Donor: Acceptor fluorophore pair	Ligated state	Donor lifetime (μ s)	Sensitized emission lifetime (μ s)	Distance (\AA)
GluN1*:GluN2A*N404C-Th, V713C	Tb: FI	Apo	1680 \pm 40	520 \pm 44	39.4 \pm 0.6
GluN1*:GluN2A*N404C-Th, V713C	Tb: FI	Antagonist (DLAPV)	1694 \pm 21	498 \pm 26	38.9 \pm 0.4
GluN1*:GluN2A* N404C-Th, V713C	Tb: FI	Homoquinolinic acid (HQ)	1628 \pm 12	390 \pm 25	37.1 \pm 0.4
GluN1*:GluN2A* N404C-Th, V713C	Tb: FI	Glutamate	1608 \pm 8	295 \pm 41	35.1 \pm 0.8
GluN1*T396 C-Th, A715C:GluN2A*	Tb: ATTO 465	Glycine	1681 \pm 10	788 \pm 22	35.0 \pm 0.1
GluN1*T396 C-Th, A715C:GluN2A*	Tb: ATTO 465	1- aminocycloprop ane-1-carboxylic acid (ACPC)	1754 \pm 5	766 \pm 22	34.6 \pm 0.2
GluN1*T396 C-Th, A715C:GluN2A*	Tb: ATTO 465	D- cycloserine (DCS)	1704 \pm 15	720 \pm 12	34.8 \pm 0.1

This mutant GluN1*^{T396C-Th}, A715C: GluN2A* was expressed in *Xenopus oocytes* and labeled using maleimide derivatives of Terbium chelate: ATTO 465. LRET was measured using saturating concentrations of full agonist (Glycine) and two partial agonists (D-cycloserine, DCS and 1- aminocyclopropane-1-carboxylic acid, ACPC) that showed varying amounts of activation. The final specific LRET lifetime is given in Table 4; this data was obtained upon subtracting the background thrombin digested lifetime.

IV. Results and Discussion

a. Modifications introduced to the full length NMDA receptor for LRET studies: The full length NMDA receptors were used to study the mechanism of cleft closure. Both the GluN1 and GluN2A subunits of the NMDA receptor were modified in order to eliminate any single non-disulphide bonded accessible cysteines. Residues C2 and C459 in GluN1 and C204, C399 and C460 in GluN2A were mutated to serine. These modified subunits were referred to as GluN1* and GluN2A* and were in turn used for LRET studies by introducing cysteines that enabled labeling using a maleimide derivative of donor and acceptor fluorophores. The integrity of the plasmid after mutagenesis was verified by sequencing and the mutants were characterized using TEVC to ensure their functionality.

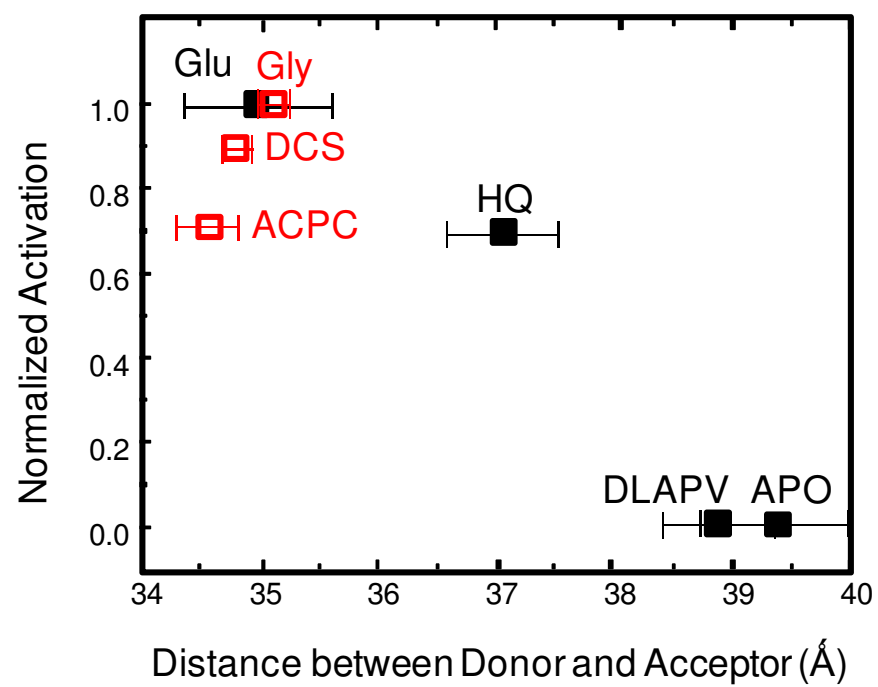
b. Mechanism of activation at GluN2A subunit of NMDA receptor : The observed LRET lifetime and distance for GluN1*:GluN2A*^{N404C-Th}, V713C mutant decreased from 39.4 ± 0.6 Å for the Apo state to 35.1 ± 0.8 Å for the full agonist glutamate-bound form indicating that the cleft closes around 4 Å upon binding of full agonist. While the lifetime and corresponding distance for the partial agonist (HQ) was 37.1 ± 0.4 Å, this distance is

indicative of a partially stabilized cleft with a difference of 2 Å between apo and HQ bound form. Interestingly, the antagonist (DLAPV) stabilized conformation with a distance of 38.9 ± 0.4 was very similar to the open cleft seen for the unligated apo state of the receptor. Therefore, based on the LRET distances it can be concluded that there is a negative correlation between the extent of cleft closure and the extent of activation with full agonists bound receptors having a shorter distance and partial agonist bound receptors having longer distances. These results support the cleft closure hypothesis that is also observed for AMPA and kainate subtype of glutamate receptors where the extent of cleft closure acts as the major coupling mechanism by which agonists mediate activation (70, 71).

c. Mechanism of activation at GluN1 subunit of NMDA receptor: Based on the crystal structures, it was previously proposed that the GluN1 subunit could follow a two-state model with a shift in equilibrium between the closed and open cleft states. However, the LRET lifetimes do not support this model since the lifetimes do not require two exponentials and can be fit using a single exponential decay (Table 4). However, if there is a large overlap between the states the protein probes in the apo and other ligated states, then differentiation of the two forms becomes unfeasible using LRET. Also, even in the AMPA subtype of glutamate receptors there are several mutants that show a deviation from the cleft closure hypothesis. NMR and single molecule FRET experiments on these mutants have been performed and they do not support the two-state model and instead indicate other mechanisms such as the dynamics of the protein, and differences in specific interactions such as hydrogen bonds to likely play a

Figure 25 Dependence of cleft closure versus extent of activation for the ABD of GluN1* (open red squares) and GluN2A* (closed squares) subunits.

This research was originally published in Journal of Biological Chemistry. Rambhadran, A., Gonzalez, J., Jayaraman, V. 2011. Conformational changes in the agonist binding domain of NMDA receptors. *Journal of Biological Chemistry* 286(19):16953-7. Copyright the American Society for Biochemistry and Molecular Biology.



role in the differences in activation by different ligands (54, 73-76). Likewise, although we observe a correlation between the average extent of cleft closure and activation for the GluN2A subunit, the dynamics and specific interactions at the level of side chains may also play a role in activation for this subunit (75).

d. Statistical evidence regarding significance of differences in the calculated LRET distances: A two-tailed t-test was performed for statistical analysis of differences in the measured LRET distances and a p value of ≤ 0.05 was considered significant. For the GluN2A subunit, the measured LRET distance decreased from 39.4 ± 0.6 Å for the Apo form to 35.1 ± 0.8 Å for the glutamate-bound state. The two-tailed test yielded $p=0.0017$ thus indicating a statistically significant 4 Å decrease in cleft closure between the Apo and full agonist bound form. Likewise, the LRET distance for the partial agonist (HQ) was 37.1 ± 0.4 Å with a statistically significant difference of 2 Å between apo and HQ bound form. The two-tailed test p value was 0.0052. On the other hand for the GluN1 subunit, the two- tailed test p value for difference in LRET distances measured between the full agonist (glycine) and partial agonists (DCS/ACPC) bound forms is greater than 0.05 and hence considered to be statistically insignificant.

V. Future Experiments

The results based on the LRET investigations on the full length NMDA receptors suggest that the extent of cleft closure could be the major coupling mechanism for activation specifically for the glutamate binding GluN2A subunit of NMDA receptor; it is still unclear what contribution the glycine binding GluN1 subunit makes. Also since the LRET based distances are ensemble measurements there is still a possibility that other

factors like dynamics of the protein and side chain interactions could play a promising role. Hence, to further examine the specific mechanism of activation detailed structural investigations like single molecule FRET (smFRET) should be performed on both the GluN1 and GluN2A subunits using the spectrum of agonists similar to the ones employed earlier in the section.

Chapter 6— Part III: Examining the conformations explored by the agonist binding domain of AMPA (α -amino-3-hydroxy-5-methyl-4-isoxazole propionate) subtype of glutamate receptors.

Reproduced in part with permission from Landes, C.F., Rambhadran, A., Taylor, J.N., Salatan, F., and Jayaraman, V. 2011. Structural landscape of the isolated ligand binding domain of single AMPA receptors. *Nature Chemical Biology*, 7(3):168-173. Copyright 2011 Nature Publishing Group.

I. Mechanism of activation in AMPA receptors

The mechanism by which the agonist induces activation and eventually desensitization still remains an elusive question for the glutamate receptor family although different mechanisms have been proposed. The initial crystal structures of the soluble ABD of the GluA2 subunit of AMPA receptors displayed a graded bilobed cleft upon binding agonists of varying efficacy (49, 53, 54, 70, 77). In the Apo state, the cleft is fully open and there is no current associated with this state. Current measurements were recorded using the full length receptor expressed in HEK- 293 cells and electrophysiological recordings were performed in the absence and presence of partial and full agonists. In the partial agonist bound state, the cleft is partially closed (12 degree more closed than in the apo form) and the currents associated with this state are intermediary. Finally, when a full agonist like glutamate is bound, the cleft is closed the greatest (20 degrees more closed than the apo state) and the corresponding current is maximum eliciting the greatest activation. Antagonists, stabilize the cleft in an open form similar to the apo state thus keeping the channel closed. Based on these structural and other functional electrophysiological studies it has been proposed that the amount of cleft closure is the primary mechanism by which activation occurs in these receptors (77).

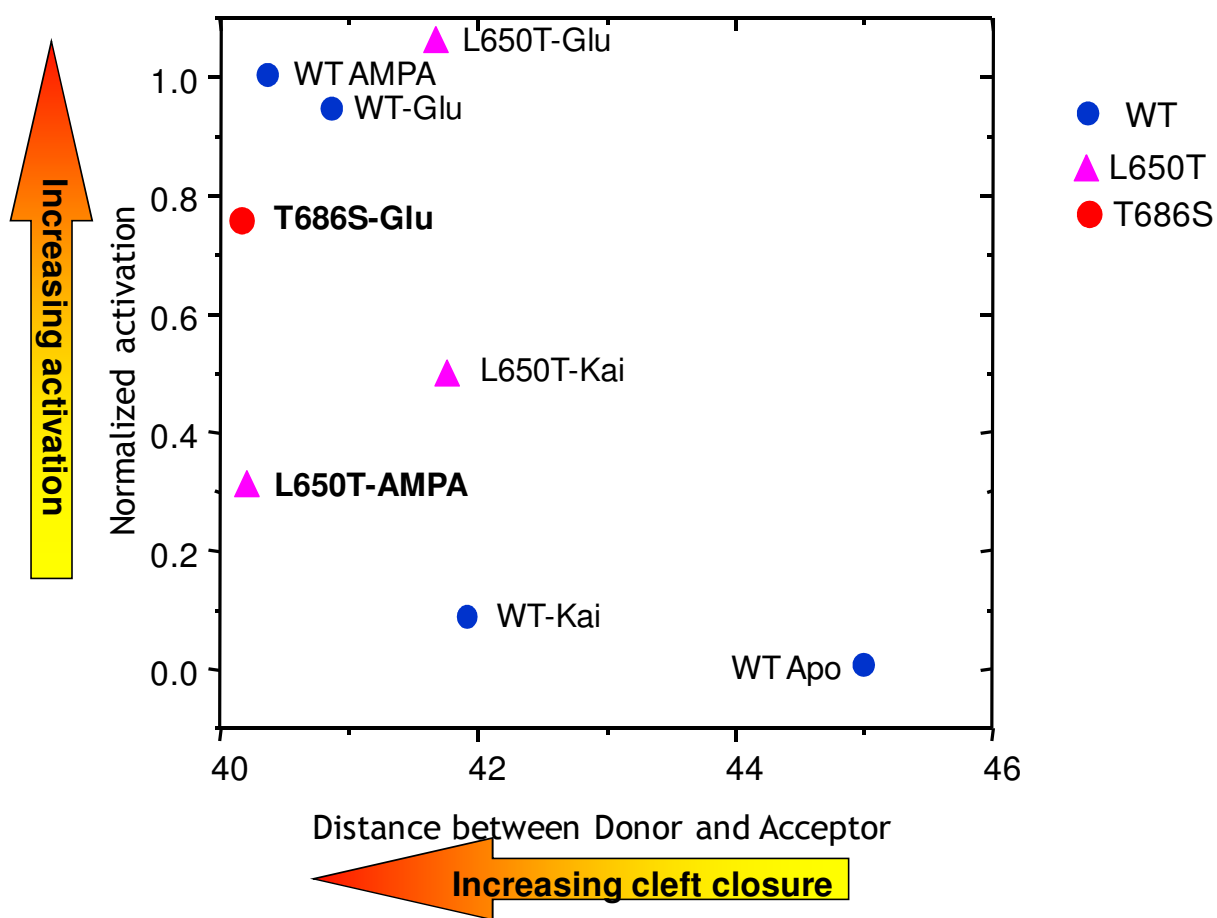
However, there are several exceptions to the cleft closure hypothesis. According to the crystal structures, kainate acts as partial agonist since it gets sterically hindered at the ABD between residues L650 and Y450 (63, 78). Mutations at these residues, especially to those amino acids that are smaller and flexible are therefore expected to make the cleft more flexible, thereby allowing kainate to lodge deeper in the cleft and cause greater activation compared to the wild type. Specifically, the L650T (Leucine 650 to

Threonine) mutation has a profound effect on the AMPA receptor activity. For this mutant, as expected, kainate induced activation is higher but ironically AMPA activation is lower (similar to that of a partial agonist) even though the cleft is closed to the same extent as when glutamate is bound which causes greater activation in the wild type. Likewise, for the full agonist glutamate bound T686S mutant, the activation is only partial for the same degree of cleft closure similar to the wild type. In addition, solution based NMR studies on the different halogen substituted willardiines showed no significant differences in the extent of cleft closure even with different degrees of activation (76).

There are several limitations to the current approaches taken to study protein. While crystal structures provide an initial insight into the lowest energy state structure of the protein, ensemble LRET investigations measurements only yield the average of the various states explored by the protein (63). Therefore, to gain a more complete understanding it is vital to determine the range of states that the protein visits. In this chapter we have used smFRET (single molecule fluorescence resonance energy transfer) to directly measure all the configurations that the protein explores in the GluA2 agonist binding domain (GluA2- ABD) both in the apo and glutamate bound state for the wild type protein and T686S mutant protein.

The T686 is involved in stabilizing the cleft via cross cleft hydrogen bonding, thus when the threonine residue is mutated to a serine, it causes destabilization of the cleft. The result is a floppy and unstable dynamic protein (78). Previous investigations of the ABD with the T686 mutants have revealed that this mutant deviates from the cleft closure

Figure 26 Extent of cleft closure in the ABD of glutamate receptor plotted as a function of activation for wild type and mutants (T686S and L650T) that deviate from the cleft closure hypothesis. Adapted from Ramanoudjame, G. et.al., 2006 (63, 79).



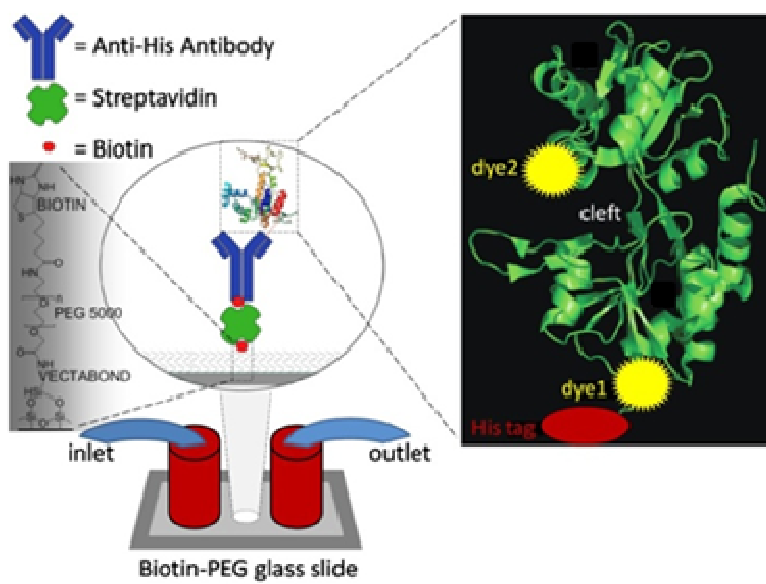
hypothesis since the protein is more flexible and thus explores configurations that are futile in terms of being able to mediate channel opening even though the crystal structures point to a closed cleft. These findings correlate well with electrophysiological measurements performed on this mutant protein where even in the presence of the full agonist glutamate the activation resembles that of a partial agonist (78).

II. Experimental set- up for the smFRET experiments

The purified Histidine tagged GluA2-ABD protein was immobilized on a PEGylated glass coverslip surface via biotin-streptavidin-antiHIS-HIS chemical interaction (Figure 27). This interaction was achieved using a Biotin conjugated Anti- His antibody coupled to the GluA2 protein which was later allowed to react with streptavidin-biotin PEGylated cover slip surface. Streptavidin acted as the linker connecting the biotin-PEG slide and the biotin-Anti-His Ab – GluR2-ABD. This procedure maximizes both the conformational freedom of the two domains while minimizing nonspecific protein/dye chemistry reactions. Maleimide derivatives of Alexa555 and Alexa647 were employed to label the GluR2- ABD protein via two Cysteine mutations that replaced T394 and S652 amino acids respectively. This particular mutant was chosen based on previous work performed by the Jayaraman lab where ensemble LRET measurements were performed (63, 80). Also, the mutations introduced were confirmed by whole cell recordings to not interfere with channel functioning in the full length GluA2 receptor. The immobilized, dye-labeled GluA2-ABD protein was then placed on a micro-reaction chamber through which buffer solutions with and without the ligand was perfused via syringe pumps.

Figure 27 Set- up for immobilization of labeled GluA2-ABD for smFRET experiments.

Reproduced in part with permission from Landes, C.F., Rambhadran, A., Taylor, J.N., Salatan, F., and Jayaraman, V. 2011. Structural landscape of the isolated ligand binding domain of single AMPA receptors. *Nature Chemical Biology*, 7(3):168-173. Copyright 2011 Nature Publishing Group.



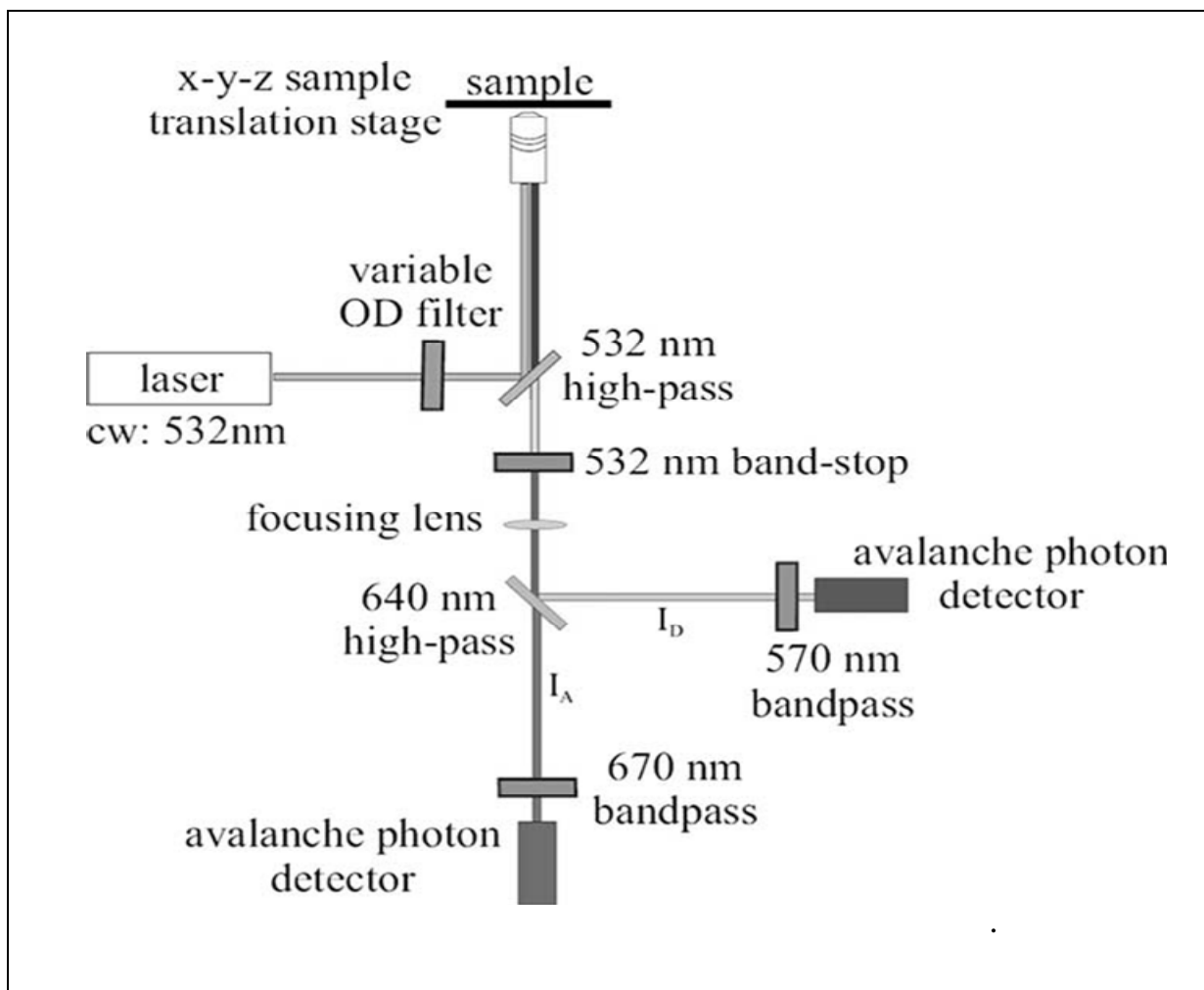
The micro- reaction chamber was constructed by placing a coverslip with two ports on top of the biotin-PEG glass slide. The two ports served as inlet and outlet ports for the flow system. In order to minimize dye photobleaching an oxygen scavenging system was employed. This solution was composed of 3% β -D-(+)-glucose (Sigma), 0.1 mg of glucose oxidase per ml of solution, 0.02 mg of catalase per ml of solution, 2 mM MgCl_2 , and saturated solution of Trolox powder (6-hydroxy-2,5,7,8-tetramethylchroman-2-carboxylic acid). The buffering solutions used for the experiments comprised of phosphate buffered saline solution with 1 mM glutamate in the case of the glutamate experiments.

FRET Instrumentation

A schematic of the scanning confocal smFRET instrumentation is shown in Figure 28. The micro chamber holding the sample is perched on top of a closed-loop x-y-z piezo stage with 100 x 100 x 20 μm travel range and 1-nm specificity. An incident light of 532-nm generated using solid state laser light was used to excite the sample. The power of the laser light was in turn adjusted using neutral density filters. The excitation light has a Gaussian profile beam at the sample juncture. This was achieved by expanding the excitation light to overfill the back aperture of a FLUAR 100x 1.3 NA oil immersion microscope objective. Fluorescence was collected by the objective and a dichroic mirror separated the incident excitation light. The signal was later passed through a second dichroic mirror (640-nm high-pass filter) to separate the donor and the acceptor emission. The resulting donor and the acceptor fluorescence signals were collected by two avalanche photodiode detectors respectively.

Figure 28 Scanning confocal smFRET instrument set- up.

Reproduced in part with permission from Landes, C.F., Rambhadran, A., Taylor, J.N., Salatan, F., and Jayaraman, V. 2011. Structural landscape of the isolated ligand binding domain of single AMPA receptors. *Nature Chemical Biology*, 7(3):168-173. Copyright 2011 Nature Publishing Group.



Data Collection and Analysis

The emission intensity trajectories were collected at a 1-ms resolution and later binned up to 10 ms to enhance the S/N ratio. The fluorescence signals of the donor (I_D) and the acceptor (I_A) were collected until the fluorophores were photobleached. The apparent FRET efficiency (E_A) was calculated using the following equation:

$$E_A = \left(\frac{I_A}{I_A + I_D} \right) \quad (1)$$

The distance between the two fluorophores was calculated with the following equation:

$$E = \left(1 + \left(\frac{R}{R_0} \right)^6 \right)^{-1} \quad (2)$$

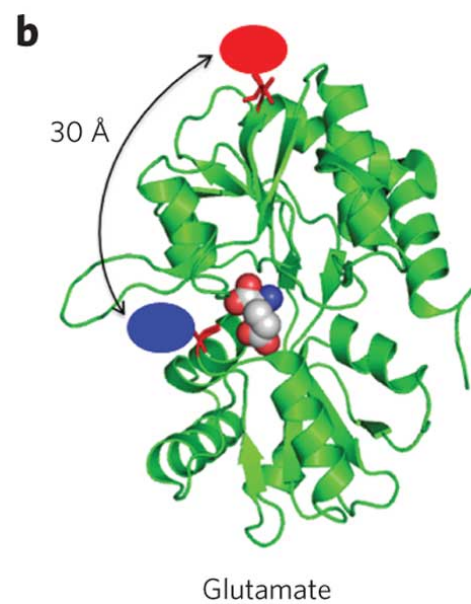
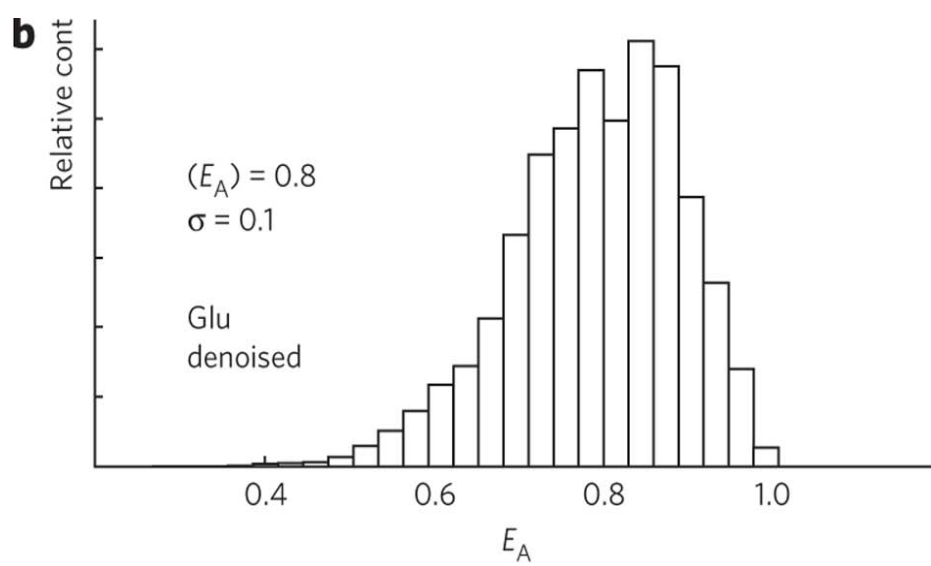
Where: R = is the inter-dye distance, and R_0 = is the Förster radius, which, for the Alexa 555-Alexa 647 pair, is approximately 5.1 nm.

III. Structural landscape of the GluA2- glutamate bound form

The ensemble histogram for the GluA2 in the glutamate bound form is compiled using many single molecule measurements for statistical analysis (Figure 29). The average FRET efficiency for the glutamate bound form is 0.80 and this corresponds to an inter-dye distance of 40.5 Å. Since the protein construct containing the T394C and S652C mutations is similar to the protein that the Jayaraman lab had used for performing ensemble FRET studies using maleimide derivatives of Terbium chelate and Fluorescein, it becomes feasible to compare the average distance obtained using smFRET technique to the ensemble LRET distance measured previously. The average distance matches almost exactly to that estimated in the ensemble FRET measurements, of 40.8 Å (63).

Figure 29 Denoised histogram for the glutamate bound GluA2-Wild type protein along with the crystal structure of GluA2-ABD protein highlighting the distance between the two cysteine residues tagged with fluorophores.

Reproduced in part with permission from Landes, C.F., Rambhadran, A., Taylor, J.N., Salatan, F., and Jayaraman, V. 2011. Structural landscape of the isolated ligand binding domain of single AMPA receptors. *Nature Chemical Biology*, 7(3):168-173. Copyright 2011 Nature Publishing Group.



This comparison is important since it provides evidence that the labeling technique and immobilization process did not affect either the cleft closure read out or the dye chemistry. The comparison further underscores the fact that the distances from the ensemble measurements on GluA2 protein are similar to the average smFRET values. The smFRET histogram compiled from individual protein molecules allows for the identification of the broad distribution and the range of states the protein probes even when bound to glutamate (81, 82). The analysis indicated that there are primarily four states that the protein explores each centered at apparent FRET values of $0.59 \pm 5.8\%$, $0.72 \pm 4.8\%$, $0.81 \pm 4.2\%$, and $0.90 \pm 3.8\%$. This data is the first experimental evidence that has been performed on single GluA2 protein molecules that provides support to the complex free energy landscape predicted by Benoit and co-workers (83). The distances between the attached fluorophores are provided in terms of FRET efficiencies of these states. However, the source of the distance changes could not be ascribed to a particular attribute; it could arise due to side chain rearrangements, hydrogen bond changes causing alterations in the backbone orientations etc (54, 75, 80). Hence, the precise nature of the conformational change associated with these distances changes cannot be determined using these measurements.

The trajectories of the single FRET molecules are collected in 1 ms time bins and further binned to 10 ms for data analysis, so that the fastest events that can be measured are at least 10 ms in lifetime. Under such conditions, glutamate unbinding or binding which typically occurs 1-2 orders of magnitude faster than the time scale of our experiments cannot be measured, and we can consider glutamate to be in its equilibrium bound state during the time scale of our measurements. The rates thus

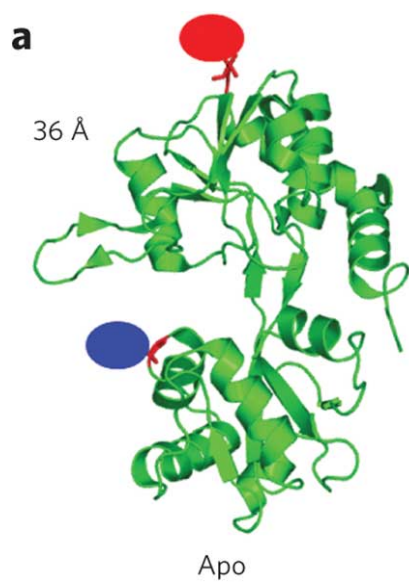
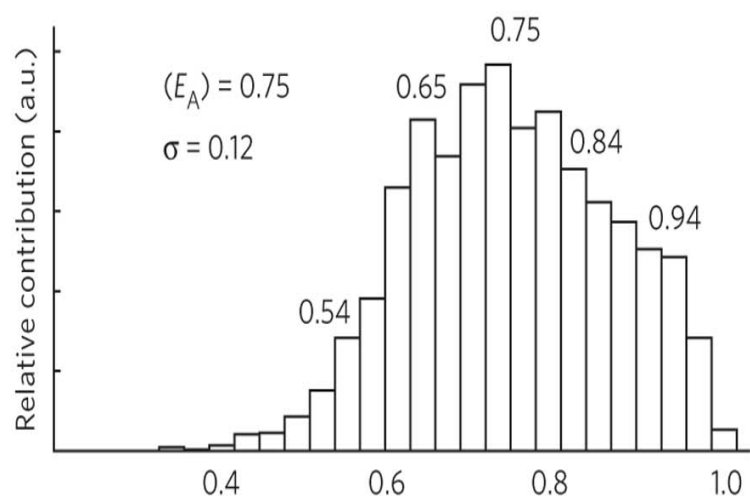
extracted here can be compared to NMR experiments performed on the same protein that focused on similar phenomena (54, 73, 84). The NMR experiments found that stabilization of the ABD occurred on time scales that are of the order of ms or longer. These time scales therefore cannot be compared to those obtained, for example, via channel conductance experiments that typically measure channel opening /closing dynamics of full length membrane proteins. These measurements explore the dynamics after ligand binding and initial cleft closure caused by agonist binding. To obtain a more rigorous analysis of the rate constants associated with conformational exchange would require a combination of more data points and increased time resolution of the experiments.

IV. Structural landscape of the GluA2 in the Apo state

In a manner similar to the glutamate bound experiments described in the previous section, data was collected for the apo GluA2 -ABD protein. As expected from crystallographic and ensemble FRET experiments, the overall structure of the protein in the apo state is more open (63, 70, 85). This conformation is evident from an observed decrease in the average smFRET value for the apo GluR2-ABD, as shown in Figure 29. Also the overall spread in the data, expressed in terms of standard deviation, indicates that the protein explores a broader potential landscape than when bound to glutamate. These observations have been previously predicted by simulations performed by Benoit and co workers (83). Five-states were required to appropriately depict the data, as shown in Figure 29. These states were found to be centered at apparent FRET values of $0.54 \pm 7.3\%$, $0.65 \pm 6.1\%$, $0.75 \pm 5.2\%$, $0.84 \pm 4.7\%$, and $0.94 \pm 4.2\%$.

Figure 30 Denoised histogram for the Apo GluA2-Wild type protein along with crystal structure of GluA2-ABD apo protein highlighting the distance between the two cysteine residues tagged with fluorophores.

Reproduced in part with permission from Landes, C.F., Rambhadran, A., Taylor, J.N., Salatan, F., and Jayaraman, V. 2011. Structural landscape of the isolated ligand binding domain of single AMPA receptors. *Nature Chemical Biology*, 7(3):168-173. Copyright 2011 Nature Publishing Group.



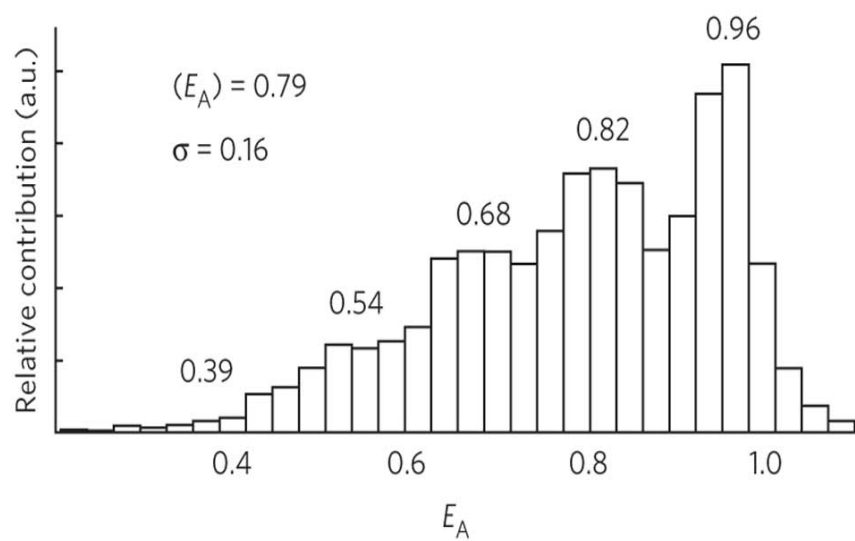
There are two possible reasons for the identification of 5 states for the apo GluA2-ABD protein. The first comes from an examination of the 1-dimensional free energy plot explained by Benoit and co-workers (83). Although the curve for the Apo protein contains four inflection points that indicate local free energy minima, there are additional points where the curve flattens without actually inflecting. Changes in temperature or ionic conditions could shift the equilibrium enough to stabilize additional local minima states. Additionally, the order parameters used in the theoretical examination were chosen for, among other qualities, their efficacy in extracting equilibrium distributions, as opposed to dynamics (86). Different order parameters might lead to additional local minima that comprise conformational intermediates. The predicted energy landscape for the apo GluR2-ABD using smFRET is considerably broader than that of glutamate bound protein indicating that the apo protein probes more states than the glutamate bound protein.

V. Structural landscape of the GluA2- T686S mutant protein

The T686S mutant of GluR2-ABD lacks the hydrogen bonding that stabilizes the inter cleft bonding, and hence serves as a good candidate to study the dynamics of the protein using smFRET (78). As shown in Figure 31, the average smFRET value for the mutant is 0.79 and the broad distribution of the states support the fact that the mutant is more open overall even in the presence of glutamate. The distribution could be best fit with a five-state model. The states identified are $0.39 \pm 12\%$, $0.54 \pm 8.7\%$, $0.68 \pm 6.9\%$, $0.82 \pm 5.7\%$, and $0.96 \pm 4.9\%$.

Figure 31 Denoised histogram for the T686S mutant GluA2- protein.

Reproduced in part with permission from Landes, C.F., Rambhadran, A., Taylor, J.N., Salatan, F., and Jayaraman, V. 2011. Structural landscape of the isolated ligand binding domain of single AMPA receptors. *Nature Chemical Biology*, 7(3):168-173. Copyright 2011 Nature Publishing Group.



VI. Results and Discussion

The data obtained from the smFRET experiments for the average FRET efficiency and the corresponding distances match very well with the previous ensemble FRET investigations performed on the apo and Glutamate bound GluA2-ABD protein (63). This correlation provides sufficient validity of the smFRET data. In Table 5, a comparison is drawn between the *average* FRET/ distances with most probable state FRET / distances obtained from the smFRET investigations. While for the Apo GluA2-ABD protein the overall dynamics reveal that the 0.65 state is the most probable state. This conformation is in stark contrast to the glutamate-bound GluA2-ABD protein, where the closed form is favored resulting in 0.81 state being most prevalent.

From the table it can also be understood that the most probable conformation can differ from the average conformation (70). Further, these observations are correlated to changes seen in the crystal structure of GluA2-ABD between the Apo and Glutamate bound protein. As seen from the table, the most probable state is in good agreement with the crystal structure distances. This striking correlation further strengthens the analysis and also addresses the differences seen between the smaller changes reported earlier using ensemble FRET data to those observed in the crystal structures.

An interesting aspect of the smFRET histograms is that they provide the overall spread of the various states of the protein. This spread indicates that even in the glutamate bound state, the protein is not rigidly locked as expected according to the crystal structure. In addition, the smFRET data also demonstrate that the protein in the

Table 5 A comparison of distances obtained via the smFRET experiments, traditional ensemble FRET investigations and X-ray structures.

Reproduced in part with permission from Landes, C.F., Rambhadran, A., Taylor, J.N., Salatan, F., and Jayaraman, V. 2011. Structural landscape of the isolated ligand binding domain of single AMPA receptors. *Nature Chemical Biology*, 7(3):168-173. Copyright 2011 Nature Publishing Group.

Method	Points of Measurement between residues 394 and 652	Apo GluR2- ABD (Å)	Glutamate bound GluR2- LBD (Å)	Difference in distance (Å)
X-Ray ^{7,36}	C α to C α	36	30	6
Ensemble FRET ¹⁴	Average distance between Donor :Acceptor	45	41	4
smFRET	Distance between Donor :Acceptor for most probable conformation	46	40	6
smFRET	Distance between Donor :Acceptor for average conformation	43	40	3

lack of an agonist that is in the apo form explores a broader landscape. Such broad distribution of smFRET values observed is consistent with the landscape predicted by simulations (83). For the glutamate bound form of the T686S mutant, the closed form is nearly the same as that of the wild type glutamate-bound protein. This result is in agreement with the crystal structure of glutamate bound T686S, where a closed cleft similar to that observed for the wild type glutamate bound protein is seen.

However, what is observed from the T686S GluA2-ABD histogram is that the mutant populates a broader range of distance distributions and more importantly accesses states that are more open than the glutamate bound wild type protein GluA2-ABD. These results indicate that the dynamics and the landscape that the protein probes play a vital role in translating conformational changes to efficacy. Also based on the simulations study, it was suggested that although the overall agonist-bound closed form is destabilized in the T686S protein relative to the wild type, the mutation also decreases steric hindrance in the cleft closure step(86)(85)(84)(83). This difference results in a structure that is less rigid, and capable of exploring a wider range of both open and closed cleft states, this structure is what is observed in the smFRET investigations.

In conclusion, the smFRET analysis of GluA2-ABD determined that the glutamate-bound form is not a rigid, locked conformation, but instead is comprised of multiple conformations of varying efficiencies. In addition, comparison of the apo and T686S mutant form allowed the hypothesis that there is an optimal protein flexibility that informs the functions of the seemingly disparate processes of activation and desensitization of the protein. In essence, the investigations illustrate that activation is

dependent not on a rigid closed cleft, but instead on the probability that a given subunit will occupy a closed cleft conformation, which in turn is not only determined by the lowest energy state but by the range of states that the protein explores.

VII. Future Experiments

The establishment of the smFRET experimental set –up has provided an ideal platform to probe the dynamics of the range of states the protein explores and thereby draw conclusions on the mechanism of activation of these receptors. Similar investigations on the NMDA subtype of glutamate receptors, that is the GluN1- ABD and GluN2A- ABD will be highly resourceful in establishing why the glycine binding GluN1 subunit behaves differently and doesn't follow the cleft closure hypothesis. By probing the range of states the GluN1-ABD protein explores in the presence of full and partial agonists we can determine the mechanism of activation in this subunit and directly draw a comparison to correlate the glutamate binding GluN2A –ABD role. Based on the previously established LRET results for the cleft closure in NMDA receptors, we hypothesize that the spread for the GluN1-ABD will be much broader similar to the distribution observed for the T686S mutant of GluA2-ABD. While on the other hand, the GluN2A-ABD will have a much narrower spread. Likewise, studies can be extended to examine the role of accessory proteins like Trans- membrane AMPA receptor regulatory proteins (TARPS) to determine their role in AMPA receptor trafficking and activation.

Overall Conclusions

Remembering the house you grew up in as a child, the friends you had in high school or the name of your first dog is all possible due to a family of proteins called glutamate receptors that are constantly at work in the human brain. The primary function of this protein is to enable neurons (or nerve cells) in our body to communicate with one another. It is this communication that makes it possible for us to learn, remember, memorize and recall events and happenings in our everyday life. There are many occasions when the relaying of information breaks down due to excessive uncontrolled firing of the nerve cells. This leads to a plethora of problems including dementia, depression, learning and memory loss to name a few. Studies have implicated the glutamate family of proteins, specifically the NMDA (N-methyl D-aspartate) receptor subtype, as a key player in various neuronal disorders such as Alzheimer's, Huntington's or ALS (Amyotrophic lateral sclerosis) that manifest due to degeneration of neuronal cells. In fact Alzheimer's disease (AD) is the most common form of dementia and is estimated to be the fourth largest cause of death for people over 65 years of age in the US. There are 5.3 million Americans who suffer from this progressive and fatal disease. AD destroys brain cells resulting in memory loss and problems with thinking and behavior that drastically affect the quality of life. However, there are currently only four FDA approved medications to treat the cognitive degeneration manifested in AD patients. Memantine, an antagonist that blocks one subtype of glutamate receptors is one of those drugs and is only moderately efficient in treating moderate to severe forms of AD.

Hence there is a pressing need to develop antagonists or drugs that specifically target these receptors thereby preventing neuronal injury and cell death. A major hurdle towards the development of target drugs has been the lack of a clear understanding of the mechanism by which NMDA receptors are activated.

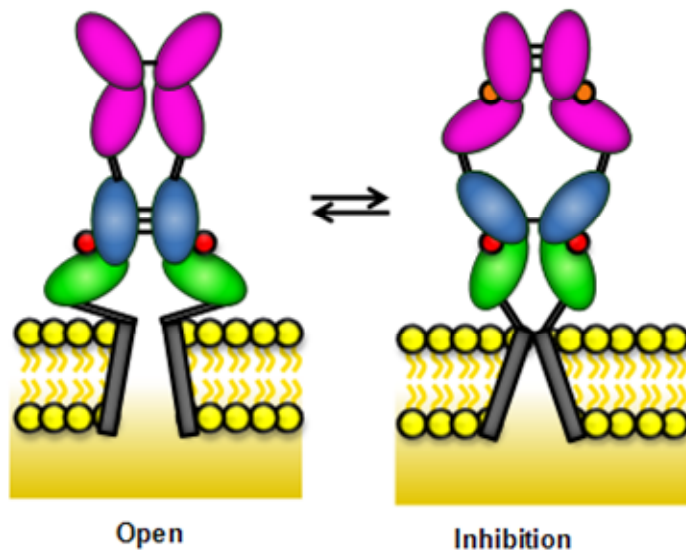
NMDA receptors are tetrameric with two glycine binding (GluN1) and two glutamate binding (GluN2A-D) subunits arranged as a dimer of dimers. Glycine and glutamate binding to an extracellular agonist binding domain initiates a series of conformational changes resulting in the formation of a central cation selective transmembrane channel. This process of channel opening can be inhibited and modulated allosterically by the binding of small molecules to the extracellular N-terminal domain adjacent to the agonist binding domain. In this dissertation, I have addressed the question of the specific arrangement of subunits in the NMDA receptor and how agonists activate the receptor using LRET as a molecular ruler.

Luminescence resonance energy transfer (LRET) is a widely used technique to measure large scale conformational changes in proteins. Using a combination of agonists with varying efficacies, mutant, and wild type proteins, I have determined that the GluN1 subunits are arranged across from each other in a diagonal manner in a functional NMDA receptor. In addition, I have confirmed that the mechanism of activation is conserved among the different subtypes of glutamate receptors.

The LRET investigations were complemented by biochemical and electrophysiological investigations and thus allow us to draw direct correlations between structure and function in this important protein.

The results from the structural studies combined with the functional data have yielded invaluable information on the mechanism of NMDA receptor activation. A schematic of the proposed mechanism of activation and inhibition in NMDA receptors is shown in Figure 32. The proposed subunit arrangement and distance constraints using LRET can be used as a model for the NMDA receptor structure and model compounds can be screened for their potential to either activate or inhibit the receptors using conventional docking methods. Further, cleft closure has been shown as the primary mechanism of activation using LRET measurements; this can be used as a powerful tool to screen various modulators/candidate drugs to determine their efficacy on the NMDA receptors. By understanding the molecular mechanism of channel function, we will thus be able to aid in future drug design with the potential to inhibit the protein in the case of stroke or activate this important class of receptors in cases where we want to enhance memory.

Figure 32 Mechanism of inhibition in NMDA receptors: The binding of agonist to the ABD causes cleft closure which in turn places a stress on the linker connecting the transmembrane domain, this causes channel opening (activation). The binding of modulators/inhibitors to the ATD causes cleft closure of the ATD, this leads to a separation of the linker region connecting ATD and ABD, causing the decoupling of ABD dimer interface eventually causing the channel to close (inhibition). This inhibition is stabilized by dimer interactions at the ATD.



Appendix

This research was originally published in Journal of Biological Chemistry. Rambhadran, A., Gonzalez, J., Jayaraman, V. 2010. Subunit arrangement in N-Methyl-D-aspartate (NMDA) receptors. *Journal of Biological Chemistry* 285(20):15296-301. Copyright the American Society for Biochemistry and Molecular Biology.

This research was originally published in Journal of Biological Chemistry. Rambhadran, A., Gonzalez, J., Jayaraman, V. 2011. Conformational changes in the agonist binding domain of NMDA receptors. *Journal of Biological Chemistry* 286(19):16953-7. Copyright the American Society for Biochemistry and Molecular Biology.

I. Molecular Biology

a. ΔN^* - NMDA Receptor

The plasmid for the GluN1 and GluN2A full length receptor was provided by Dr. Nakanishi. This plasmid was modified by deleting the Amino Terminal domain (ATD), residues 5-357 for GluN1 and 1-385 for GluN2A. A non- disulphide bonded accessible cysteines were mutated to serine residues. Residues C459 in GluN1 and C399 and, C460 on the extracellular side of GluN2A were changed to serines, producing modified Δ GluN1* and Δ GluN2A* receptors. Mutations in the plasmids were introduced using the Stratagene QuikChange site-directed mutagenesis kit (Stratagene, CA). All constructs were cloned in pcDNA3.1 (+) or pGEM vector and the integrity of the plasmid was confirmed by sequencing.

b. GluN1*: GluN2A* Receptor

For cleft closure experiments, the full length GluN1 and, GluN2A were used and modified such that there are no external non- disulphide cysteines accessible. To achieve this, C2 and C459 in GluN1 and C204, C399 and C460 in GluN2A were mutated to serines. The background modified construct was referred as GluN1*: GluN2A* receptor and was cloned in pGEM vector.

c. RNA synthesis for oocyte injection

The mMessage mMachine Kit (Ambion) was used in the *in vitro* synthesis of capped RNA. In brief, for one reaction (20 μ L), 1 μ g of linearized mutant DNA is used. Upon linearizing, the DNA is cleaned via gel-extraction kit to remove impurities and the linear DNA is eluted in nuclease-free water. Further, 10 μ L of 2X NTP/CAP, 2 μ L of 10X sample reaction buffer, 2 μ L of the respective enzyme(T7 RNA polymerase) along with

necessary volume of nuclease-free water to make up the final volume to 20 μ l. This reaction mix is incubated at 37 °C for 2 hours. Then, 1 μ L of TURBO DNase is added to remove any template DNA contamination and further incubated at 37 °C for 15-30 minutes. Lithium chloride was used to precipitate the RNA. Typically, 30 μ L of lithium chloride is added and allowed to chill overnight at -20 °C for a minimum of 5 hours. The RNA is later precipitated by centrifuging at max speed to isolate the pellet, washed with 70% ethanol, and finally resuspended in nuclease-free water to desired concentration. The RNA is later quantified, run on an agarose gel to ensure quality and size, and stored in aliquots at -70 °C until further use.

II. *Xenopus* oocyte extraction and preparation

African clawed frogs were used as the source of oocytes. Frogs are anesthetized using 1-2 g/L of tricaine methane sulfonate (MS222) powder that is dissolved in deionized autoclaved water, buffered to pH of 7.5 using 5mM Hepes (1.192 g/L) and sodium bicarbonate. This solution of MS222 is always prepared fresh and is filter-sterilized and autoclaved prior to use. The frog is bathed in this solution to enable anesthetization.

To perform non-survival frog surgery and oocyte harvest, aseptic techniques are used in a special area designated for frog procedures. In brief, the frog is placed in a container with anesthesia (tricaine methane sulfonate) in water. After about 15 minutes, the frog is kept on a tray covered with ice and saran wrap. This induces hypothermia and thus prolongs the analgesic effect. The anesthetized frogs are verified by disturbance either by pinching their toes and gently inverting them. The surgical procedure begins by making a small incision (usually around 0.5cm) in the lower left or right abdomen. The abdominal region is then opened and ovaries containing approximately 200-300 oocytes are removed with the help of forceps. To finally euthanize the frog, the frog is decapitated and pithed while under the anesthetic effect or is given an anesthetic overdose (>2.5 g/L).

To perform survival surgery on the frogs, strict aseptic procedures are employed. Surgical gloves, and sterile/autoclaved instruments are used. All surgical procedures are performed in areas designated for surgery and they were maintained under aseptic conditions. Pre-surgery preparations included sterilizing surgical instruments with 70% ethanol and flaming. The frog is anesthetized by immersion in MS222 solution for 15 to

30 minutes and is verified by frog's response to disturbance. Anesthesia will persist for a minimum of 20 minutes. Frog is placed on tray with ice covered with saran wrap to induce hypothermia and prolong the analgesic effect. Pre-wet paper towels are placed in direct contact with the frog's skin to keep them moist. For the surgery, a small incision (about 0.5cm) is made in the lower portion of the abdomen either to the left or right. A similar incision is made through the frog's abdominal muscle. Strand of eggs or ovaries containing approximately 200-250 oocytes is removed with the help of forceps. Following this removal, the incision is closed with absorbable suture after ensuring that no air is trapped under the skin. The frog is then bathed in plain water 2-3 times and placed head- up in a bucket without anesthetic to ensure their revival. The activity of the frog is then monitored until it is actively swimming in the bucket. After a return to normal activity, the frog placed in a separate tank to monitor its health for a few days. No additional antibiotic treatments are necessary owing to a natural antibiotic in *Xenopus* skin. A maximum of two survival surgeries is performed on a frog, one on each side of the abdomen. If for some reason the frog is distressed, the veterinarians will be informed and upon their recommendation the future course of action is determined. Typical problems include a lack of vigorous swimming when disturbed, poor appetite, or mild skin rash. In extreme cases, when no appropriate treatment is available, the frog is euthanized. Also on occasions when a frog is unable to produce quality oocytes, it is euthanized. Usually, there are few complications associated with surgery, but if there is any sign of a problem, like uncontrolled bleeding, the frog is decapitated and pithed under anesthetics or given an anesthetic overdose.

Preparation of oocytes: Oocytes are defolliculated by incubation with 1-1.5 mg/ml collagenase. The collagenase is dissolved in Ca^{2+} -free solution containing (in mM): 83 NaCl, 2 KCl, 1 MgCl_2 , 5 HEPES, pH 7.5. The collagenase treatment is allowed to proceed for 90-120 minutes. The preparation is then thoroughly rinsed with Barths storage solution containing (in mM): 88 NaCl, 2.5 NaHCO_3 , 1.1 KCl, 0.4 CaCl_2 , 0.3 $\text{Ca}(\text{NO}_3)_2$, 0.8 MgCl_2 , 2.5 mM sodium pyruvate, 10 HEPES, pH 7.3, and 5 $\mu\text{g/ml}$ gentamicin; and stored overnight. Typically, stage V–VI oocytes are individually sorted and injected with RNA of the modified receptor.

III. Pre-blocking and Expression

The oocytes are incubated for 2-3 days at 12 °C after injection, and then pre-labeled with a maleimide derivative to block the inherent cysteines. β -maleimidopropionic acid made in Barths storage solution is used at a final concentration of 100 μ M for 1 hour at 18 °C. The oocytes are then washed extensively to get rid of the blocking reagent using Barths solution. The pre-blocked oocytes are later allowed to express at 18 °C for 24 to 36 hours. At the end of 24-36 hours, the oocytes are labeled (described in the next section).

IV. Labeling oocytes

For subunit arrangement measurements using $\Delta\text{GluN1}^*:\Delta\text{GluN2A}^*$ and mutants, 1 μM terbium chelate was used for donor only experiments. While for donor: acceptor LRET studies, either 1 μM ATTO465 or Fluorescein in a 1:1 ratio is added simultaneously along with donor for 1 hour to label the oocytes in Barth's storage solution. While for longer and shorter distance measurements 1 μM $(\text{Ni-NTA})_2\text{Cy3}$ or Ni^{2+} , respectively, is added separately to the cuvette. The membrane preparations obtained upon lysing the oocytes were used for single channel recordings and LRET experiments. Background LRET was measured 1-3 hours after the addition of Thrombin (1-3 U, from Calbiochem, CA) to the cuvette and subtracted from the total LRET signal to get the final specific signal from the receptors.

For the cleft closure experiments with $\text{GluN1}^*:\text{GluN2A}^*$, 1 μM terbium chelate is used for donor-only experiments. Membrane lysates for LRET experiments are prepared as explained in the next section. The acceptor fluorophore used is either 1 μM maleimide derivative of ATTO 465 or Fluorescein. The acceptor is added along with terbium chelate for donor:acceptor experiments in a 1:1 ratio. Background LRET was measured 1-3 hours after the addition of Thrombin (1-3 U, from Calbiochem, CA) to the cuvette and subtracted from the total LRET signal to get the final specific signal from the receptors.

V. Membrane Preparation

For LRET studies, approximately 300-500 labeled oocytes expressing modified NMDA receptors are lysed by gently douncing in 1.5 mL of lysis buffer. The lysis buffer consists of 20 mM Tris, pH 7.6, 200 mM NaCl, 1% Triton X-100, and EDTA-free Complete Protease Inhibitor Cocktail (Roche). The lysed oocytes are then spun at 5000 rpm for 20-30 minutes to get rid of the cell debris and nuclear components, followed by a 13,000-15,000 rpm for 30 minutes at 4°C to collect the supernatant. The membrane suspensions are resuspended in Barth's storage solution to achieve final desired volume.

VI. Electrophysiology

Two-electrode voltage-clamp (TEVC) recordings were performed using the NPI TEC amplifier (ALA Scientific, NY). Typically, the microelectrodes were filled with 3M KCl and had resistances of 1-3 MOhms. A narrow flow-through recording chamber with a volume of 75 μ l was used to minimize the solution exchange time (ALA Scientific, NY). The extracellular solution contained (in mM): 100 NaCl, 1 KCl, 0.7 BaCl₂, 0.8 MgCl₂, and 5 HEPES, pH 7.5 with NaOH. Currents were recorded with Cell Works software (ALA Scientific, NY), exported and analyzed using Origin 4.0 (OriginLab, MA). Whole-cell current recordings were performed as previously described (87).

VII. Expression and labeling of the isolated ABD of GluA2

The GluA2-ABD plasmid was provided by Dr Eric Gouaux (Oregon Health and Science University, Portland, OR). S652C, T394C and T686S mutations were introduced using Quick Change Site- Directed Mutagenesis Kit (Stratagene). The GluA2-ABD and mutant T686S –GluA2 ABD protein were expressed and purified as described by Armstrong et al (53). In brief, the wild type and mutant protein were expressed in *Escherichia Coli* Origami–B (DE3) cells and the Histidine tag containing proteins were subjected to purification using Ni-NTA Hi Trap column (GE Healthcare). 0.1-0.5 μ M protein in phosphate buffer with 1mM glutamate was used for labeling. Thiol- reactive maleimide derivatives of Alexa 555 and 647 (Invitrogen) served as donor and acceptor probes. The Alexa fluorophores are directly linked to the thiol group of the cysteines in the proteins and no additional linkers are present between the fluorophores and the protein. Unreacted excess dyes were removed by dialyzing extensively in either phosphate buffer only for Apo experiments or in phosphate buffer containing 10mM glutamate for glutamate bound single molecule experiments. Preparation of samples for the single molecule experiments were performed as described by Hanson et al and is explained in the next section.

VIII. Sample preparation for smFRET experiments

Glass slides used for smFRET experiments are plasma cleaned to remove impurities from the surface. Vectabond (Vector Labs), a proprietary aminosilane, was used to amine functionalize the surface. The amine group of the Vectabond reacted with the NHS ester group of O-[2-(N-Succinimidylloxycarbonyl)-ethyl]-O'-methylpolyethylene glycol 5000 (NHS-PEG-5000 – Fluka)) and NHS-PEG-5000-Biotin (biotin-PEG – NOF Corporation). The sample chamber was assembled by placing a coverslip with two ports on top of the biotin-PEG glass slide(88, 89)(87, 88)(86, 87)(85, 86). The two ports were used as inlet and outlet ports for the flow system. The GluA2-ABD was attached to a biotin-conjugated anti-histidine monoclonal antibody (biotin-Anti-His Ab, Rockland). The biotin-PEG slide was incubated with streptavidin (SA) solution. The SA served as the linker between the biotin-PEG slide and the biotin-Anti-His Ab – GluA2-ABD.

An oxygen scavenging flow solution was prepared by following an established protocol. The flow solution was composed of 3% (wt/vol) β -D-(+)-glucose (Sigma), 0.1 mg of glucose oxidase (Roche Applied Science) per ml of solution, 0.02 mg of catalase (Roche Applied Science) per ml of solution, 2 mM MgCl_2 , and saturated solution of Trolox powder (6-hydroxy-2,5,7,8-tetramethylchroman-2-carboxylic acid; Fluka). The Trolox powder was dissolved in PBS, and then subsequently filtered (90, 91). The final flow solutions contained 10 mM glutamate in phosphate buffered saline solution in the case of the glutamate-bound experiments.

Bibliography

1. Hille, B. 2001. Ion channels of excitable membranes. Sinauer, Sunderland, Mass.
2. Hille, B. 1992. Ionic channels of excitable membranes. Sinauer Associates, Sunderland, Mass.
3. Dingledine, R., K. Borges, D. Bowie, and S. F. Traynelis. 1999. The glutamate receptor ion channels. *Pharmacological Reviews* 51:7-61.
4. Madden, D. R. 2002. The structure and function of glutamate receptor ion channels. *Nat Rev Neurosci* 3:91-101.
5. Brauner-Osborne, H., J. Egebjerg, E. O. Nielsen, U. Madsen, and P. Krogsgaard-Larsen. 2000. Ligands for glutamate receptors: design and therapeutic prospects. *J Med Chem* 43:2609-2645.
6. Gouaux, E., and R. Mackinnon. 2005. Principles of selective ion transport in channels and pumps. *Science* 310:1461-1465.
7. Mayer, M. L., and N. Armstrong. 2004. Structure and function of glutamate receptor ion channels. *Annu Rev Physiol* 66:161-181.
8. Mayer, M. L. 2005. Glutamate receptor ion channels. *Curr Opin Neurobiol* 15:282-288.
9. Keinänen, K., W. Wisden, B. Sommer, P. Werner, A. Herb, T. A. Verdoorn, B. Sakmann, and P. H. Seeburg. 1990. A family of AMPA-selective glutamate receptors. *Science* 249:556-560.
10. Doyle, D. A., J. M. Cabral, R. A. Pfuetzner, A. Kuo, J. M. Gulbis, S. L. Cohen, B. T. Chait, and R. MacKinnon. 1998. The structure of the potassium channel: molecular basis of K⁺ conduction and selectivity. *Science* 280:69-77.

11. Sobolevsky, A. I., M. P. Rosconi, and E. Gouaux. 2009. X-ray structure, symmetry and mechanism of an AMPA-subtype glutamate receptor. *Nature* 462:745-756.
12. Furukawa, H., and E. Gouaux. 2003. Mechanisms of activation, inhibition and specificity: crystal structures of the NMDA receptor NR1 ligand-binding core. *The EMBO journal* 22:2873-2885.
13. Furukawa, H., S. K. Singh, R. Mancusso, and E. Gouaux. 2005. Subunit arrangement and function in NMDA receptors. *Nature* 438:185-192.
14. Inanobe, A., H. Furukawa, and E. Gouaux. 2005. Mechanism of partial agonist action at the NR1 subunit of NMDA receptors. *Neuron* 47:71-84.
15. Bräuner-Osborne, H., J. Egebjerg, E. O. Nielsen, U. Madsen, and P. Krogsgaard-Larsen. 2000. Ligands for glutamate receptors: design and therapeutic prospects. *Journal of Medicinal Chemistry* 43:2609-2645.
16. Kwak, S., and J. H. Weiss. 2006. Calcium-permeable AMPA channels in neurodegenerative disease and ischemia. *Curr Opin Neurobiol* 16:281-287.
17. Moriyoshi, K., M. Masu, T. Ishii, R. Shigemoto, N. Mizuno, and S. Nakanishi. 1991. Molecular cloning and characterization of the rat NMDA receptor. *Nature* 354:31-37.
18. Lerma, J., A. V. Paternain, A. Rodriguez-Moreno, and J. C. Lopez-Garcia. 2001. Molecular physiology of kainate receptors. *Physiological Reviews* 81:971-998.
19. Mayer, M. L. 2005. Crystal structures of the GluR5 and GluR6 ligand binding cores: molecular mechanisms underlying kainate receptor selectivity. *Neuron* 45:539-552.

20. Mayer, M. L., A. Ghosal, N. P. Dolman, and D. E. Jane. 2006. Crystal structures of the kainate receptor GluR5 ligand binding core dimer with novel GluR5-selective antagonists. *J Neurosci* 26:2852-2861.
21. Hollmann, M., and S. Heinemann. 1994. Cloned glutamate receptors. *Annual Review of Neuroscience* 17:31-108.
22. Nakanishi, S., and M. Masu. 1994. Molecular diversity and functions of glutamate receptors. *Annual Reviews in Biophysical and Biomolecular Structure* 23:329-348.
23. Paoletti, P., and J. Neyton. 2007. NMDA receptor subunits: function and pharmacology. *Current opinion in pharmacology* 7:39-47.
24. Madry, C., I. Mesic, I. Bartholomaeus, A. Nicke, H. Betz, and B. Laube. 2007. Principal role of NR3 subunits in NR1/NR3 excitatory glycine receptor function. *Biochemical and biophysical research communications* 354:102-108.
25. Wisden, W., and P. H. Seeburg. 1993. Mammalian ionotropic glutamate receptors. *Current Opinion in Neurobiology* 3:291-298.
26. Johnson, J. W., and P. Ascher. 1987. Glycine potentiates the NMDA response in cultured mouse brain neurons. *Nature* 325:529-531.
27. Bergink, V., H. J. van Megen, and H. G. Westenberg. 2004. Glutamate and anxiety. *Eur Neuropsychopharmacol* 14:175-183.
28. Bettler, B., and C. Mulle. 1995. Review: neurotransmitter receptors. II. AMPA and kainate receptors. *Neuropharmacology* 34:123-139.
29. Choi, D. W. 1988. Glutamate neurotoxicity and diseases of the nervous system. *Neuron* 1:623-634.

30. Waxman, E. A., and D. R. Lynch. 2005. N-methyl-D-aspartate receptor subtypes: multiple roles in excitotoxicity and neurological disease. *Neuroscientist* 11:37-49.
31. Dingledine, R., and P. J. Conn. 2000. Peripheral glutamate receptors: molecular biology and role in taste sensation. *J Nutr* 130:1039S-1042S.
32. Hinoi, E., T. Takarada, T. Ueshima, Y. Tsuchihashi, and Y. Yoneda. 2004. Glutamate signaling in peripheral tissues. *Eur J Biochem* 271:1-13.
33. Salter, M. W. 1998. Src, *N*-Methyl-D-aspartate (NMDA) receptors, and synaptic plasticity. *Biochemical Pharmacology* 56:789-798.
34. Wollmuth, L. P., T. Kuner, P. H. Seeburg, and B. Sakmann. 1996. The NR1- and NR2A- subunits contribute differentially to the selectivity filter of NMDA receptor channels. *Journal of Physiology* 491:779-797.
35. Salter, M. W. 1999. A pinch of salt for NMDA receptors. *Molecular Psychiatry* 4:209-211.
36. Schoepfer, R., H. Monyer, B. Sommer, W. Wisden, R. Sprengel, T. Kuner, H. Lomeli, A. Herb, M. Köhler, N. Burnashev, W. Günther, P. Ruppersberg, and P. Seeburg. 1994. Molecular biology of glutamate receptors. *Progress in Neurobiology* 42:353-357.
37. Turecek, R., V. Vlachova, and L. Vyklicky. 1997. Spontaneous openings of NMDA receptor channels in cultured rat hippocampal neurons. *European Journal of Neuroscience* 9:1999-2008.
38. Zhang, W., J. R. Howe, and G. K. Popescu. 2008. Distinct gating modes determine the biphasic relaxation of NMDA receptor currents. *Nature neuroscience* 11:1373-1375.

39. Watanabe, M., Y. Inoue, K. Sakimura, and M. Mishina. 1992. Developmental changes in distribution of NMDA receptor channel subunit mRNAs. *Neuroreport* 3:1138-1140.
40. Karakas, E., N. Simorowski, and H. Furukawa. 2011. Subunit arrangement and phenylethanolamine binding in GluN1/GluN2B NMDA receptors. *Nature* 475:249-253.
41. Paoletti, P., F. Perin-Dureau, A. Fayyazuddin, A. Le Goff, I. Callebaut, and J. Neyton. 2000. Molecular organization of a zinc binding n-terminal modulatory domain in a NMDA receptor subunit. *Neuron* 28:911-925.
42. Karakas, E., N. Simorowski, and H. Furukawa. 2009. Structure of the zinc-bound amino-terminal domain of the NMDA receptor NR2B subunit. *The EMBO journal* 28:3910-3920.
43. Rachline, J., F. Perin-Dureau, A. Le Goff, J. Neyton, and P. Paoletti. 2005. The micromolar zinc-binding domain on the NMDA receptor subunit NR2B. *J Neurosci* 25:308-317.
44. Paoletti, P., A. M. Vergnano, B. Barbour, and M. Casado. 2009. Zinc at glutamatergic synapses. *Neuroscience* 158:126-136.
45. Masuko, T., K. Kashiwagi, T. Kuno, N. Nguyen, A. J. Pahk, J. Fukuchi, K. Igarashi, and K. Williams. 1999. A regulatory domain (R1-R2) in the amino terminus of the *N*-methyl-D-aspartate receptor: effects of spermine, protons, and ifenprodil, and structural similarity to bacterial leucine/isoleucine/valine binding protein. *Molecular Pharmacology* 55:957-969.

46. Ayalon, G., E. Segev, S. Elgavish, and Y. Stern-Bach. 2005. Two regions in the N-terminal domain of ionotropic glutamate receptor 3 form the subunit oligomerization interfaces that control subtype-specific receptor assembly. *J Biol Chem* 280:15053-15060.
47. Madry, C., I. Mesic, H. Betz, and B. Laube. 2007. The N-terminal domains of both NR1 and NR2 subunits determine allosteric Zn²⁺ inhibition and glycine affinity of N-methyl-D-aspartate receptors. *Mol Pharmacol* 72:1535-1544.
48. Armstrong, N., J. Jasti, M. Beich-Frandsen, and E. Gouaux. 2006. Measurement of conformational changes accompanying desensitization in an ionotropic glutamate receptor. *Cell* 127:85-97.
49. Armstrong, N., Y. Sun, G. Q. Chen, and E. Gouaux. 1998. Structure of a glutamate-receptor ligand-binding core in complex with kainate. *Nature* 395:913-917.
50. Cheng, Q., and V. Jayaraman. 2004. Chemistry and conformation of the ligand-binding domain of GluR2 subtype of glutamate receptors. *The Journal of biological chemistry* 279:26346-26350.
51. Mayer, M. L. 2006. Glutamate receptors at atomic resolution. *Nature* 440:456-462.
52. Armstrong, N. A., and E. Gouaux. 2000. Mechanisms for activation and antagonism of an AMPA-sensitive glutamate receptor: crystal structures of the GluR2 ligand binding core. *Neuron* 28:165-181.

53. Armstrong, N., M. Mayer, and E. Gouaux. 2003. Tuning activation of the AMPA-sensitive GluR2 ion channel by genetic adjustment of agonist-induced conformational changes. *Proc Natl Acad Sci U S A* 100:5736-5741.
54. Ahmed, A. H., A. P. Loh, D. E. Jane, and R. E. Oswald. 2007. Dynamics of the S1S2 glutamate binding domain of GluR2 measured using ¹⁹F NMR spectroscopy. *The Journal of biological chemistry* 282:12773-12784.
55. Van Den Bosch, L., P. Van Damme, E. Bogaert, and W. Robberecht. 2006. The role of excitotoxicity in the pathogenesis of amyotrophic lateral sclerosis. *Biochim Biophys Acta* 1762:1068-1082.
56. Cull-Candy, S., S. Brickley, and M. Farrant. 2001. NMDA receptor subunits: diversity, development and disease. *Curr Opin Neurobiol* 11:327-335.
57. Lakowicz, J. R. 1983. *Principles of Fluorescence Spectroscopy*. Plenum Press, New York.
58. Selvin, P. R. 2000. The renaissance of fluorescence resonance energy transfer. *Nat Struct Biol* 7:730-734.
59. Selvin, P. R. 1995. Fluorescence resonance energy transfer. *Methods Enzymol* 246:300-334.
60. Selvin, P. R. 2002. Principles and biophysical applications of lanthanide-based probes. *Annu Rev Biophys Biomol Struct* 31:275-302.
61. Selvin, P. R., and J. E. Hearst. 1994. Luminescence energy transfer using a terbium chelate: improvements on fluorescence energy transfer. *Proc Natl Acad Sci U S A* 91:10024-10028.

62. Gonzalez, J., A. Rambhadran, M. Du, and V. Jayaraman. 2008. LRET investigations of conformational changes in the ligand binding domain of a functional AMPA receptor. *Biochemistry* 47:10027-10032.
63. Ramanoudjame, G., M. Du, K. A. Mankiewicz, and V. Jayaraman. 2006. Allosteric mechanism in AMPA receptors: A FRET-based investigation of conformational changes. *Proc Natl Acad Sci U S A* 103:10473-10478.
64. Miledi, R., I. Parker, and K. Sumikawa. 1982. Synthesis of chick brain GABA receptors by frog oocytes. *Proceedings of the Royal Society of London. Series B, Containing papers of a Biological character* 216:509-515.
65. Gurdon, J. B., C. D. Lane, H. R. Woodland, and G. Marbaix. 1971. Use of frog eggs and oocytes for the study of messenger RNA and its translation in living cells. *Nature* 233:177-182.
66. Cha, A., G. E. Snyder, P. R. Selvin, and F. Bezanilla. 1999. Atomic scale movement of the voltage-sensing region in a potassium channel measured via spectroscopy. *Nature* 402:809-813.
67. Huxley, A. 2002. From overshoot to voltage clamp. *Trends Neurosci* 25:553-558.
68. Kapanidis, A. N., Y. W. Ebright, and R. H. Ebright. 2001. Site-specific incorporation of fluorescent probes into protein: hexahistidine-tag-mediated fluorescent labeling with (Ni(2+):nitrilotriacetic Acid (n)-fluorochrome conjugates. *J Am Chem Soc* 123:12123-12125.
69. Du, M., A. Rambhadran, and V. Jayaraman. 2009. Vibrational spectroscopic investigation of the ligand binding domain of kainate receptors. *Protein Sci* 18:1585-1591.

70. Armstrong, N., and E. Gouaux. 2000. Mechanisms for activation and antagonism of an AMPA-sensitive glutamate receptor: crystal structures of the GluR2 ligand binding core. *Neuron* 28:165-181.
71. Du, M., A. Rambhadran, and V. Jayaraman. 2008. Luminescence resonance energy transfer investigation of conformational changes in the ligand binding domain of a kainate receptor. *The Journal of biological chemistry* 283:27074-27078.
72. Rambhadran, A., J. Gonzalez, and V. Jayaraman. 2010. Subunit arrangement in N-methyl-D-aspartate (NMDA) receptors. *The Journal of biological chemistry* 285:15296-15301.
73. McFeeters, R. L., and R. E. Oswald. 2002. Structural mobility of the extracellular ligand-binding core of an ionotropic glutamate receptor. Analysis of NMR relaxation dynamics. *Biochemistry* 41:10472-10481.
74. Landes, C. F., A. Rambhadran, J. N. Taylor, F. Salatan, and V. Jayaraman. 2011. Structural landscape of isolated agonist-binding domains from single AMPA receptors. *Nature chemical biology* 7:168-173.
75. Maltsev, A. S., and R. E. Oswald. 2010. Hydrophobic side chain dynamics of a glutamate receptor ligand binding domain. *The Journal of biological chemistry* 285:10154-10162.
76. Maltsev, A. S., A. H. Ahmed, M. K. Fenwick, D. E. Jane, and R. E. Oswald. 2008. Mechanism of partial agonism at the GluR2 AMPA receptor: Measurements of lobe orientation in solution. *Biochemistry* 47:10600-10610.

77. Gouaux, E. 2004. Structure and function of AMPA receptors. *The Journal of physiology* 554:249-253.
78. Robert, A., N. Armstrong, J. E. Gouaux, and J. R. Howe. 2005. AMPA receptor binding cleft mutations that alter affinity, efficacy, and recovery from desensitization. *J Neurosci* 25:3752-3762.
79. Mankiewicz, K. A., A. Rambhadran, L. Wathen, and V. Jayaraman. 2008. Chemical interplay in the mechanism of partial agonist activation in alpha-amino-3-hydroxy-5-methyl-4-isoxazolepropionic acid receptors. *Biochemistry* 47:398-404.
80. Mankiewicz, K. A., A. Rambhadran, M. Du, G. Ramanoudjame, and V. Jayaraman. 2007. Role of the chemical interactions of the agonist in controlling alpha-amino-3-hydroxy-5-methyl-4-isoxazolepropionic acid receptor activation. *Biochemistry* 46:1343-1349.
81. Taylor, J. N., and C. F. Landes. 2011. Improved resolution of complex single-molecule FRET systems via wavelet shrinkage. *The journal of physical chemistry* 115:1105-1114.
82. Taylor, J. N., D. E. Makarov, and C. F. Landes. 2011. Denoising single-molecule FRET trajectories with wavelets and Bayesian inference. *Biophysical journal* 98:164-173.
83. Lau, A. Y., and B. Roux. 2007. The free energy landscapes governing conformational changes in a glutamate receptor ligand-binding domain. *Structure* 15:1203-1214.

84. Fenwick, M. K., and R. E. Oswald. 2010. On the mechanisms of alpha-amino-3-hydroxy-5-methylisoxazole-4-propionic acid (AMPA) receptor binding to glutamate and kainate. *The Journal of biological chemistry* 285:12334-12343.
85. Madden, D. R., N. Armstrong, D. Svergun, J. Perez, and P. Vachette. 2005. Solution X-ray scattering evidence for agonist- and antagonist-induced modulation of cleft closure in a glutamate receptor ligand-binding domain. *The Journal of biological chemistry* 280:23637-23642.
86. Lau, A. Y., and B. Roux. 2007. The Free Energy Landscapes Governing Conformational Changes in a Glutamate Receptor Ligand-Binding Domain. *Structure (Cambridge, MA, United States)* 15:1203-1214.
87. Du, M., S. A. Reid, and V. Jayaraman. 2005. Conformational changes in the ligand-binding domain of a functional ionotropic glutamate receptor. *J Biol Chem* 280:8633-8636.
88. Zeng, Y., H.-W. Liu, C. F. Landes, Y. J. Kim, X. Ma, Y. Zhu, K. Musier-Forsyth, and P. F. Barbara. 2007. Probing nucleation, reverse annealing, and chaperone function along the reaction path of HIV-1 single-strand transfer. *Proc. Natl. Acad. Sci. USA* 104:12651-12656.
89. Landes, C. F., Y. Zeng, H. W. Liu, K. Musier-Forsyth, and P. F. Barbara. 2007. Single-Molecule study of the Inhibition of HIV-1 transactivation response region DNA/DNA annealing by argininamide. *Journal of the American Chemical Society* 129:10181-10188.

90. Cordes, T., J. Vogelsang, and P. Tinnefeld. 2009. On the Mechanism of Trolox as Antiblinking and Antibleaching Reagent. *Journal of the American Chemical Society* 131:5018-5019.
91. Rasnik, I., S. A. McKinney, and T. Ha. 2006. Nonblinking and long-lasting single-molecule fluorescence imaging. *Nature Meth.* 3:891-893.

Vitae

Anu Rambhadran was born on August 8, 1981 in Chennai, India. She attended University of Madras located in Chennai, India beginning in 1998. Anu received the University Merit Rank for excellence in undergraduate degree program and graduated with a B.Tech in Chemical Engineering in 2002. She continued her education in Biotechnology at Birla Institute of Technology and Science, Pilani India and graduated with honors in the year 2004. In 2006, she joined Dr. Vasanthi Jayaraman's laboratory at University of Texas Health Science Center, Houston as a Research Technician and later continued in the same lab as a graduate student after enrolling into the Graduate School of Biomedical Sciences. She has gained the interdisciplinary experience in Biochemistry, Physical Chemistry, and Molecular Biology that are critical in addressing important questions concerning structure and function in proteins. Anu has traveled to University of California and Yale in order to be trained in smFRET and single channel recordings techniques in the laboratory. Anu received numerous awards for outstanding work while being a graduate student, like the President's Research Scholarship award, Dean's Research award from UT-Houston Medical School Graduate Student Education Committee, Mc Govern award for presentation skills and other awards for poster presentation. Anu has presented her work at several prestigious conferences including the Biophysical Society Meeting in 2007, 2008 and 2011 in addition to the Gordon Research Conference-Ion Channels in 2010. She was granted a Ph.D. in Biochemistry and Biophysics in October of 2011. Her publications include:

- Rambhadran A**, Gonzalez J, and Jayaraman V. Conformational changes at the Agonist Binding Domain of the NMDA Receptors. *J. Biol. Chem.* 2011. May 13; 286(19):16953-7.
- Landes CF, **Rambhadran A**, Taylor JN, Salatan F, and Jayaraman V. Structural landscape of isolated Ligand Binding Domain of single AMPA receptors. *Nature Chemical Biology.* 2011. March 7 (3):168-73.
- Rambhadran A**, Gonzalez J, and Jayaraman V. LRET Investigations of Subunit Arrangement in NMDA Receptors. *J. Biol. Chem.* 2010. May 14;285(20):15296-301.
- Du M, **Rambhadran A** and Jayaraman V. Vibrational spectroscopic investigation of the ligand binding domain of kainite receptors. *Protein Science* 2009; 18(8):1585-91.
- Rambhadran A**, Mankiewicz K, Wathen L, and Jayaraman V. Chemical interplay in the mechanism of partial agonist activation in alpha-amino-3-hydroxy-5-methyl-4-isoxazolepropionic acid receptors. *Biochemistry* 2008; 47(1):398-404.
- Gonzalez J, **Rambhadran A**, Du M, and Jayaraman V. LRET Investigations of Conformational Changes in the Ligand Binding Domain of a Functional AMPA Receptor. *Biochemistry* 2008.Sep 23;47(38):10027-32.
- Du M, **Rambhadran A** and Jayaraman V. Luminescence resonance energy transfer investigation of Conformational changes in the ligand binding domain of a kainate receptor. *J Biological chemistry* 2008; 283(40):27074-8.
- Mankiewicz K, **Rambhadran A**, Du M, Ramanoudjame G, and Jayaraman V. Role of chemical interactions of the agonist in controlling alpha-amino-3-hydroxy-5-

methyl-4-isoxazolepropionic acid receptor activation. *Biochemistry* 2007;
46(5):1343-09.